Thermax

1 Fundamentals

2 Design

3 Research

Excel

2

Thermodynamic Analyses and Optimisation of Energy-Conversion Systems using Excel

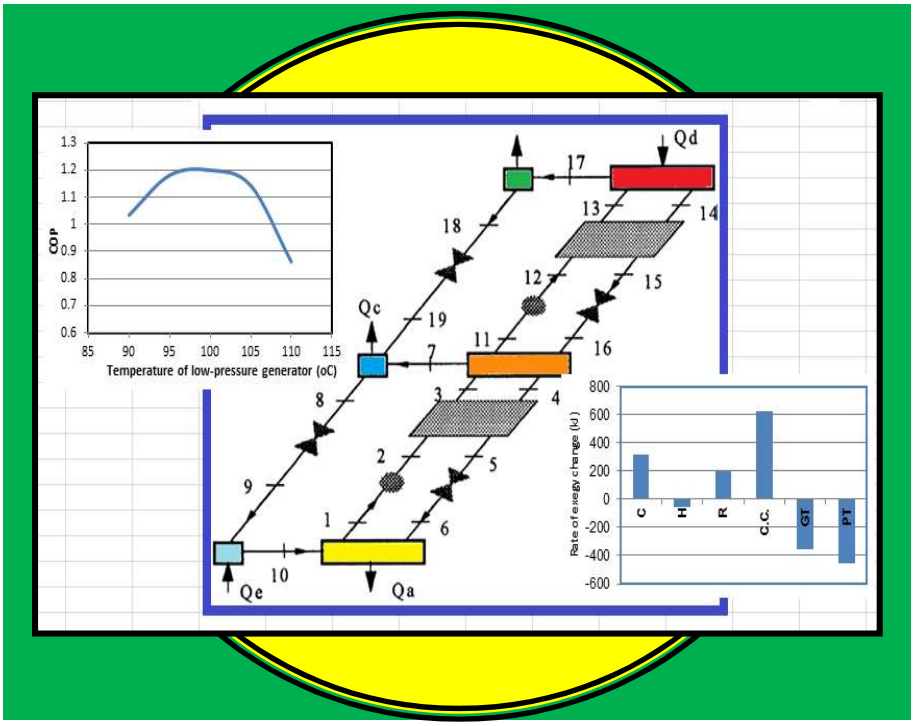

Mohamed M. El-Awad

Thermodynamic Analyses and Optimisation of Energy-Conversion Systems using Excel

Thermodynamic Analyses and Optimisation of Energy-Conversion Systems using Excel

Mohamed M. El-Awad

July, 2025

Preface

The design methodologies of energy-conversion and utilisation systems are mainly based on applying the principles of engineering thermodynamics. These principles must be properly understood by engineering students considering the devastating effects of large-scale energy utilisation that make proper design and operation of the systems more critical than ever before. However, thermodynamics is usually seen as a difficult subject mainly because thermodynamic analyses require the physical properties of the fluids involved to be determined at different phases, temperatures, and pressures. Although the traditional method of using property tables and charts is important for introducing the basic concepts of the subject, tables and charts are not suitable for conducting parametric sensitivity analyses that help the students to understand these concepts better. Tables and charts are also not suitable for design optimisation analyses of complex energy-conversion systems that aim to maximise their economic feasibility and minimise their environmental impact. In this respect, computer-aided methods can improve the learning process by helping the students to easily conduct such analyses and by making the relevant thermodynamic models more realistic compared to the traditional models that usually adopt many idealisations and simplifying assumptions.

There are a number commercial computer applications originally developed for industrial and research analyses that can also be used for educational purposes. However, they are not the ideal method because of their cost and complexity and because they don't allow white-box modelling of the systems to be analysed. On the other hand, developing the required thermodynamic models using standard computer programming requires good programming skills and takes a long time. A perfect solution to this problem is offered by the general-purpose spreadsheet applications such as Microsoft Excel. Compared to the dedicated commercial software, Excel has the advantages of being widely available on personal computers and simple to use. As a modelling platform for engineering analyses, Excel provides a rich library of mathematical functions and powerful graphic tools for data visualisation. Although it does not provide functions for determining fluid properties which are necessary for thermodynamic analyse, such functions can be developed as custom functions with the Visual Basic for Applications (VBA) programming language that comes with Microsoft Applications. While the property functions enable the students to deal with time-consuming parametric studies and iterative solutions, the Solver add-in that comes with Excel enables them to perform constrained and multi-variable optimisation analyses of energy-conversion systems.

This book presents an Excel add-in called Thermax that provides property functions for numerous working fluids that are used in energy-conversion systems that include twenty-nine ideal gases, water and superheated steam, twenty-eight synthetic and natural refrigerants, two aqua solutions for vapour-absorption refrigeration, humid air for psychrometric analyses, and atmospheric air at various temperatures. The book shows how Excel with Thermax functions can be used to deal with thermodynamic analyses of the basic gas and vapour power cycles and the combined cycle, the simple, multi-stage

compression and cascade vapour-compression refrigeration cycles, and the single-effect and two-effect vapour-absorption refrigeration cycles. Two chapters of book show how the functions can be used for psychrometric analyses of air-conditioning systems and processes and for the development of a general sheet for combustion analyses. Three chapters of the book deal with thermoeconomic optimisation analyses of energy-conversion systems by considering three examples which are the air-bottoming cycle, the gas-turbine cycle with inlet-air cooling, and the combined Brayton-Rankine cycle. The last chapter demonstrates the use of the functions for thermodynamic evaluation of a new cycle for low-temperature heat-recovery that combines the ORC and the TFC cycles.

Most of the examples considered in the book have been adopted from popular textbooks and published work so that the results obtained by Thermax functions can be verified. While relevant exercises are provided at the end of Chapters 2 to 5, more challenging exercises and mini projects are given in the last appendix of the book. This book is the second book in a set of four books that deal with computer-aided thermofluid analyses by using the Excel-based modelling platform. The books have been written for educational purposes, but it is hoped that they can also be useful for practicing engineers and researchers.

Acknowledgements
The development of Thermax and the writing of this set of books would not have been possible without benefitting from the efforts of many colleagues who have made their publications, data, and software available in the open literature or on their websites. A special gratitude goes to the Mechanical Engineering Department at the University of Alabama (USA) whose initiative "*Excel for Mechanical Engineering*" both inspired and helped me to develop Thermax. I am also indebted to Universiti Putra Malaysia and Universiti Tenaga Nasional (Malaysia), the University of Khartoum (Sudan), and the University of Technology and Applied Sciences (Oman) for their generous support at different periods of my academic career and hope that they find the books a worthy token of appreciation and gratitude. Last, but not least, I am grateful to my beloved family for the unfailing support I needed desperately to complete this work at a a time of conspiracy, betrayal, and war.

CONTENTS

Chapter 1

Introduction

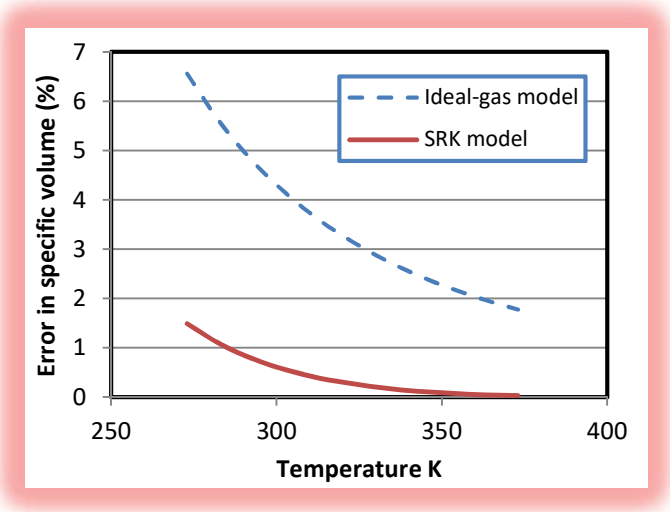

Thermodynamic analyses of the energy-conversion cycles that involve phase changes of the working fluid, like the Rankine cycle, require the determination of fluid properties at different phases of the fluid. For these analyses computer-aided methods are more convenient than traditional methods that use property tables and charts. For the cycles that involve gases and do not involve phase changes computer-aided methods are also advantageous because they allow the application of the variable specific-heat method of analysis instead of the approximate constant specific-heat method which is less accurate. This chapter reviews the principles of thermodynamic analyses of energy-conversion systems and discusses the advantages of computer-aided methods for such analyses. The chapter also highlights the capabilities of Microsoft Excel as a modelling platform for thermodynamic analyses and thermoeconomic optimisation of energy-conversion systems and introduces Thermax, the Excel add-in that is used to conduct the various analyses presented in this book.

1.1. A brief review of thermodynamics

The principles of engineering thermodynamics help us to evaluate and optimise the performance of the various energy-conversion systems. To evaluate the energy transfer between an energy-conversion system and its surroundings and account for the various losses that usually occur in any energy-conversion or energy-transfer process, the three basic thermodynamic principles are the conservation of mass, the conservation of energy (the first-law of thermodynamics), and the second-law of thermodynamics. For illustration, consider the air-compression system shown on Figure 1.1 that has two stages of compression separated by an intercooler.

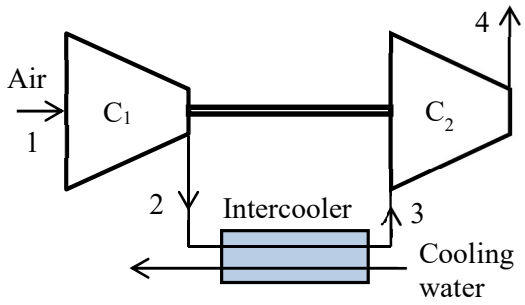

Figure 1.1. Schematic diagram of a two-stage air compressor with inter-stage intercooling

Air enters the system at a temperature T_1 and pressure P_1. The first-stage compressor, C_1, compresses the air adiabatically to state 2, after which it enters the intercooler where its temperature is reduced to T_3. The second-stage compressor, C_2, then increases the air pressure to P_4 and temperature to T_4. Figure 1.2 shows the compression process on a temperature-entropy diagram. The required compression work is divided between the two compressor stages depending on their compression ratios and there is a certain value of the intermediate pressure (P_i) that minimises the total work. The principles of thermodynamics help us to determine this optimum intermediate pressure.

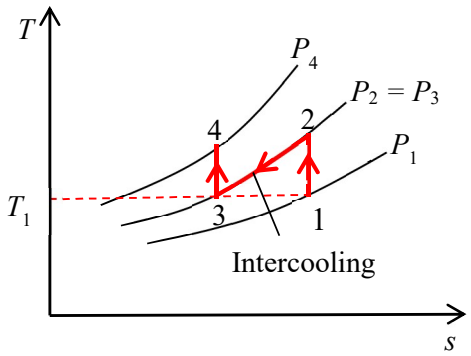

Figure 1.2. *T-s* diagram of a two-stage air compressor with inter-stage intercooling

Treating the two compression stages as steady-flow processes, and neglecting changes in kinetic and potential energy, the first-law of thermodynamics leads to [1]:

$$q - w = (h_{out} - h_{in}) \tag{1.1}$$

Where q and w are the amounts of heat transfer and work transfer per unit mass flow rate of air, respectively, and ($h_{out} - h_{in}$) is the resulting enthalpy change in the stage. Equation (1.1) adopts the usual sign convention that heat into the system is positive, while work into the system is negative. Assuming the compression processes in both stages to be adiabatic (q=0) and reversible means that the processes are isentropic as shown on Figure 1.2. Using an average value of the specific heat for air at constant pressure (c_p), the compression work per unit mass flow rate of air in stage 1 (w_1) and in stage 2 (w_2) can be determined from Equation (1.1) as follows:

$$w_1 = -(h_2 - h_1) = -c_p(T_2 - T_1) \tag{1.2}$$

$$w_2 = -(h_4 - h_3) = -c_p(T_4 - T_3) \tag{1.3}$$

Therefore, the total compression work in both stages (w_{total}) is given by:

$$w_{total} = w_1 + w_2 = -c_p[(T_2 - T_1) + (T_4 - T_3)] \tag{1.4}$$

Assuming perfect intercooling, i.e., $T_3 = T_1$, and rearranging Equation (1.4):

$$w_{total} = c_p T_1 \left[\left(1 - \frac{T_2}{T_1}\right) + \left(1 - \frac{T_4}{T_3}\right) \right] = c_p T_1 \left[2 - \left(\frac{T_2}{T_1}\right) - \left(\frac{T_4}{T_3}\right) \right] \tag{1.5}$$

Since the two compression processes are assumed to be isentropic and the specific heat c_p for air to be constant, for an ideal gas the temperature ratios in Equation (1.5) can be converted into pressure ratios by using the second law of thermodynamics as follows:

$$\frac{T_2}{T_1} = \left(\frac{P_2}{P_1}\right)^{\frac{k-1}{k}} \tag{1.6}$$

$$\frac{T_4}{T_3} = \left(\frac{P_4}{P_3}\right)^{\frac{k-1}{k}} \tag{1.7}$$

Where k is the ratio of specific heats ($k=c_p/c_v$); c_v is the specific heat for air at constant volume. Assuming that there is no pressure loss in the intercooler, i.e., $P_3 = P_2 = P_i$, substitution from Equations (1.6) and (1.7) into Equation (1.5) gives:

$$w_{total} = c_p T_1 \left[2 - \left(\frac{P_i}{P_1}\right)^{\frac{k-1}{k}} - \left(\frac{P_4}{p_i}\right)^{\frac{k-1}{k}} \right] \tag{1.8}$$

To see how the total compression work varies with the intermediate pressure P_i, let us consider the specific case in which T_1= 300K, P_1=100 kPa, and P_4 = 900 kPa. Using Equation (1.8), the total compression work in the system was calculated for different values of P_i and the result is shown on Figure 1.3. The figure shows that the value of P_i at which the total compression work is minimal is around 300 kPa. Increasing or decreasing P_i from this value will increase the compression work.

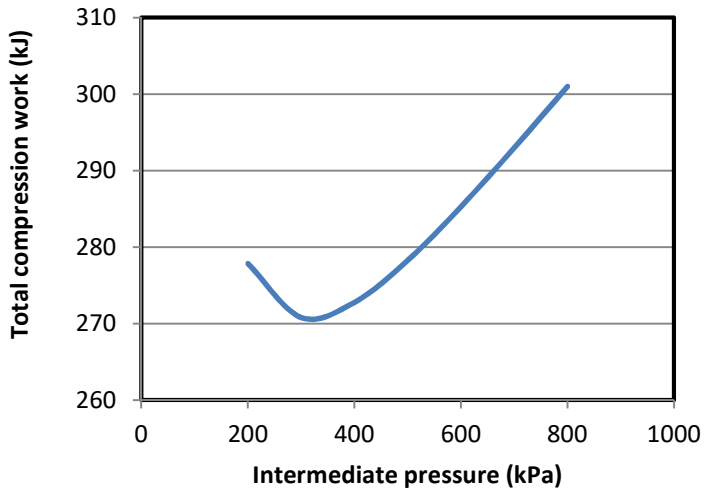

Figure 1.3. Variation of the total compression work with the intermediate pressure

The principles of thermodynamics are also useful for performance evaluation and optimisation of the more complicated power and refrigeration systems. For example, consider the regenerative steam-turbine power plant shown on Figure 1.4.

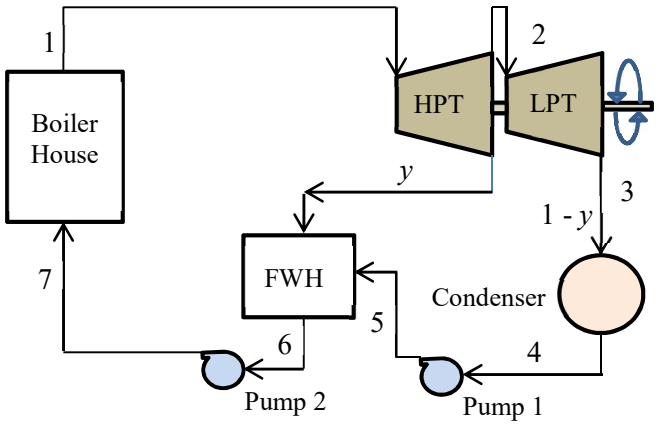

Figure 1.4. Schematic diagram of a regenerative steam-turbine power plant

This plant consists of a boiler house for producing superheated steam, a high-pressure steam turbine (HPT), a low-pressure steam turbine (LPT), a condenser, an open feed-water heater (FWH) and two feed-water pumps. A fraction of the steam (y) is extracted after the HPT for preheating the feed-water before going back to the boiler house. The extracted steam reduces the work output from plant, but it also reduces the amount of heat added in the boiler and its net effect is to increase the thermal efficiency of the plant. There is also a certain extraction pressure for the steam at which the plant's thermal efficiency attains a maximum value. As shown below, the principles of thermodynamics can be used to determine this optimum steam-extraction pressure.

The net specific work output from the plant (w_{net}) is given by:

$$w_{net} = w_{out} - w_{in} \tag{1.9}$$

Where w_{out} is the total specific work output from the two turbines and w_{in} is the total work input to the two pumps which are given by:

$$w_{out} = w_{HPT} + w_{LPT} \tag{1.10}$$

$$w_{in} = w_{P1} + w_{P2} \tag{1.11}$$

Where w_{HPT} and w_{LPT} are the specific work output from the high-pressure turbine and the low-pressure turbine, respectively, and w_{P1} and w_{P2} are the specific work input in pump

1 and pump 2, respectively. Assuming the two turbines and the two pumps to be adiabatic and neglecting the changes in kinetic and potential energies, the work output or input for each device can be determined from the enthalpy difference across the device. Per each kg of steam generated in the boiler, these are given by:

$$w_{HPT} = (h_1 - h_2) \tag{1.12}$$

$$w_{LPT} = (1-y)(h_2 - h_3) \tag{1.13}$$

$$w_{P1} = (1-y)(h_5 - h_4) \tag{1.14}$$

$$w_{P2} = (h_7 - h_6) \tag{1.15}$$

Mass and energy balance over the open feed-water heater gives:

$$yh_2 + (1-y)h_5 = 1 \times h_6 \tag{1.16}$$

The specific heat input to the boiler (q_{in}) is determined by the relevant enthalpy change as follows:

$$q_{in} = (h_1 - h_7) \tag{1.17}$$

Therefore, the thermal efficiency of the plant (η) can be calculated from:

$$\eta = w_{net} / q_{in} \tag{1.18}$$

Both w_{net} and η depend on the fraction of steam extracted for regeneration (y); which in turn depends on the extraction pressure (P_2). Figure 1.5 shows the variation of y and η with P_2 for an ideal cycle in which P_1 = 15 MPa, T_1 = 600°C, and P_4 = 10 kPa. The figure shows that the cycle's efficiency attains a maximum value of 45.55% when P_2 is about 1000 kPa.

It should be mentioned that the working fluid in the above power plant changes its phase from subcooled liquid water to superheated steam in the boiler, becomes a saturated mixture of water and steam in the low-pressure turbine, and returns to subcooled water in the condenser. Therefore, appropriate property relationships, tables, or charts are needed in order to determine the working fluid enthalpy at different states.

The principles of thermodynamics are also needed for the analyses of air-conditioning systems and processes and the analyses of the processes that involve combustion and other chemical reactions. For such analyses, thermodynamics provides the basic relationships needed to quantify the effects of fluid mixing and chemical reactions on the

properties of the working fluids and on the transfer of energy and effluents to or from the energy-conversion system.

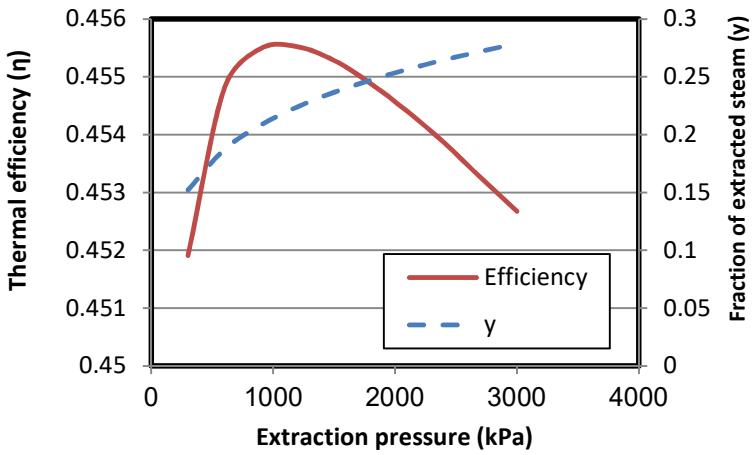

Figure 1.5. The effect of intermediate pressure (P_2) on the fraction of extracted steam (y) and thermal efficiency (η) of a regenerative steam-turbine power plant

1.2. Advantages of computer-aided thermodynamic analyses

Apart from saving time and effort and eliminating possible human errors, computer-aided analyses of energy-conversion systems offer a number of advantages over the traditional methods of analyses that use property tables and charts. An important advantage of computer-aided methods with respect to thermodynamic analyses is their ability to give more realistic results by avoiding unnecessary simplification of the models and by using more accurate estimations of fluid properties. Moreover, they offer reliable techniques for iterative solutions and optimisation analyses. In what follows, these advantages are illustrated by means of relevant examples.

A. Avoiding excessive simplification of the model

In many situations, traditional analytical methods excessively simplify the analytical models; which makes their results grossly deviate from the behaviour of real systems. A good example of this situation is given by the models of internal-combustion (IC) engines. Traditional air-standard models of IC engines, such as the Otto cycle and the Diesel cycle, neglect heat-transfer and friction losses, treat the combustion process as heat-addition from an external source, and use constant specific heats. These assumptions enable the engine processes to be represented by simple closed-form relations for calculating the amount of heat added to the engine and net work from the engine. However, air-standard models usually overestimate the engine's output and thermal efficiency. By comparison, computer-aided models of IC engines, such as those described by Ferguson [2] that take into consideration the geometrical as well as the thermodynamic characteristics of the engines, closely mimic the behaviour of actual IC engines. Therefore, these models can be used to investigate the effect of important design and

operation factors such the ignition or injection timing on the engine performance or the effect of engine speed on the specific fuel consumption. However, the formulation of these models leads to a set of ordinary differential equations that need to be solved simultaneously by using a numerical solver such as the Newton-Raphson method.

B. Accurate representation of fluid properties and processes

The behaviour of real gasses and vapours is frequently modelled by using the following ideal-gas law:

$$P\tilde{v} = R_u T \tag{1.19}$$

Where P is the absolute pressure of the gas, $\tilde{v}$ is the molar specific volume, R_u is the universal gas constant, and T is the absolute temperature of the gas. The ideal gas law can be used with reasonable accuracy for determining the specific volume of a superheated vapour, but when the temperature approaches the saturation line, the value of the specific volume determined by the ideal-gas law departs significantly from the actual volume. Figure 1.6 shows the deviations from the tabulated values by those obtained from the ideal-gas law for refrigerant R134a at 0.2 MPa. The figure shows that the error of the ideal-gas law is more that 2% even at high temperatures and increases as the temperature approaches the saturation value.

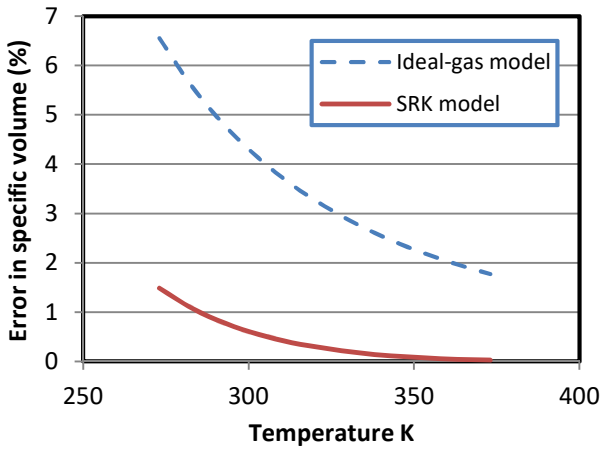

Figure 1.6. Errors in the specific volume of R134a by the ideal-gas law and the SRK equation of state

More accurate estimates can be obtained by using the Soave-Redlich-Kwong (SRK) equation of state [1]:

$$P = \frac{R_u T}{\tilde{v} - b} - \frac{a\alpha}{\tilde{v}(\tilde{v} + b)} \tag{1.20}$$

Where the constants a, b and α are fluid-dependent. For the same case described above, Figure 1.6 shows that the accuracy of the SRK equation remained higher than 99% even close to the saturation line. However, since the SRK equation is implicit in $\widetilde{v}$, it cannot be used directly to determine the specific volume, but has to be solved iteratively. A number of standard iterative procedures (e.g. Newton-Raphson method) can be used to solve the equation, but they are not convenient for hand calculations.

C. Dealing with iterative solutions and optimisation analyses

Thermodynamic analyses involving iterative solutions and optimisation analyses suit computer-aided methods more than manual methods even for simple systems. A good example of thermodynamic analyses that require iterative solutions is the determination of the adiabatic flame temperature by a first-law analysis of the combustion process. Optimisation analyses are needed for determining the best design for a certain energy-utilisation systems such as the optimum intermediate pressure for an air-compression system, the optimum steam-extraction pressure for a regenerative Rankine cycle, and the optimum intermediate pressures for multi-stage and cascade refrigeration systems. While simple optimisation analyses that involve a single design parameter can be performed by means of calculus techniques and graphic tools, optimisation analyses of more complex systems that involve multiple variables require the use of computer-aided techniques.

1.3. Excel as a modelling platform for thermodynamic analyses

Microsoft Excel provides a rich library of built-in functions and powerful graphical tools. Considering its wide availability, the simplicity of its user-interface, and the flexibility of its graphical tools, it is being increasingly used as a teaching aid in various engineering subjects [3-8]. Although Excel is mostly used for dealing with simple computer-aided operations like matrix inversion and multiplication, it is equipped with other tools that make it a capable modelling platform for more challenging types of "What-if" and optimisation analyses. Two of these tools are the Goal Seek command and the Solver add-in. The Visual Basic for Applications (VBA) programming language that comes with Microsoft Office can be used for developing customised user-defined functions (UDFs) and add-ins for thermodynamic analyses. The Developer ribbon of Excel also allows the use of macros that remove the tedium of parametric studies and repetitive calculations.

The main limitation of Excel as modelling platform for thermodynamic analyses is the lack of built-in functions for fluid properties, but this problem could be solved by developing suitable add-ins. The *Thermotable* add-in developed by the Mechanical Engineering Department at the University of Alabama determines the thermodynamic properties of ideal gases, water and superheated steam, and four refrigerants R134a, R22, R410A, and R407C [9-12]. Goodwin [13] also developed an educational Excel add-in, called *TPX* (Thermodynamic Properties for Excel), that determines the properties of five gases (H_2O, H_2, O_2, N_2, CH_4) and refrigerant R-134a. A number of property add-ins have also been developed for research and industrial applications [14, 15]. The American National Institute of Standards and Technology (NIST) developed *REFPROP* that

provides thermophysical properties of various refrigerants and their mixtures [16]. An open-source alternative to *REFPROP*, called *CoolProp*, was developed by Bell [17] at the University of Liege. Optimized Thermal Systems also developed a commercial alternative add-in to *REFPROP* called *XProps* [18].

This book presents an educational add-in, called Thermax, that enables Excel to be used for thermodynamic analyses of various types of energy-conversion systems. Thermax provides property functions for seven groups of working fluids that are used in energy-conversion systems that include:

- Twenty-nine ideal gases,
- Water and superheated steam,
- Twenty-eight refrigerants for vapour-compression refrigeration (VCR) systems,
- Lithium-bromide and ammonia aqua solutions for vapour-absorption refrigeration (VAR) systems,
- Humid air for psychrometric analyses,
- Various types of fuels and chemically-reacting substances,
- Air at standard atmospheric pressure but various temperatures.

In addition to its seven groups of fluid-property functions, Thermax provides a small group of user-defined functions that are useful for general thermofluid analyses. These include two data interpolation functions and a Newton-Raphson solver for non-linear equations such as the SRK equation of state.

1.3. Closure

Chapter 2 describes the fluid property functions provided by Thermax in more details and shows how these functions can be used in Excel's formulae for thermodynamic analyses. Appendix A and Appendix B supplement Chapter 2 by listing the ideal-gases, refrigerants and chemical reactants supported by Thermax and providing the equations used to determine the thermodynamic properties of ideal gases, superheated refrigerants, and humid air. The three chapters that follow Chapter 2 illustrate the use of Thermax functions for the analyses of basic power and refrigeration systems. Chapters 3 and 4 that deal with the analyses of power cycles give examples of analysing the Brayton cycle, the Otto cycle, the Rankine cycles with and without regeneration, the combined Brayton-Rankine cycle, and the organic Rankine cycle. Chapter 5 deals with the analyses and optimisation of single-stage, multi-stage compression, and cascade VCR cycles using refrigerant R134a. Appendix C extends the treatment of Chapter 5 by verifying Thermax functions for refrigerants properties and by presenting an analysis of a cascade VCR system with the two ozone-friendly refrigerants, R507A and R23.

Chapters 6, 7, and 8 show how Thermax property functions can be used to deal with three types of thermodynamic analyses in which the working fluids are mixtures of gaseous or liquid substances. Chapter 6 deals with the analyses of psychrometric processes and illustrates the use of the functions for design analyses of air-conditioning systems.

Chapter 7 focuses on combustion analyses and describes the development of a general Excel sheet for steady-flow combustion analyses. Appendices D and E extend the general Excel sheet to deal with combustion in closed systems and second-law analyses of combustion processes. Chapter 8 illustrates the use of Thermax functions for first-law analyses of single-effect and double-effect VAR cycles using ammonia-water and lithium-bromide-water solutions.

The last four chapters of the book illustrate the use of the Excel-based modelling platform for design analyses and research. Chapters 9, 10, and 11 show how the platform can be used to deal with thermoeconomic optimisation analyses of three power generation cycles which are the air-bottoming cycle, the gas-turbine cycle with inlet-air cooling, and the combined Brayton-Rankine cycle. Chapter 10 highlights the influence of the thermodynamic model of the system to be optimised and shows that the two solution methods offered by Solver can give the designer more than one optimum solution to consider. Chapter 11 shows how the Excel-based model can be used for multi-objective and exergoconomic optimisation of the basic combined cycle. Chapter 12 ventures into a research area by presenting a new power generation cycle for recovering the energy of low-temperature heat sources that combines the Organic Rankine Cycle (ORC) with the Trilateral Flash Cycle (TFC). The new cycle enjoys the merits of the two simple cycles by applying the TFC in the high-temperature circuit and the ORC in the low-temperature circuit and connecting the two cycles via a cascade condenser. The chapter evaluates the thermodynamic performance of the combined cycle with five working fluids of low GWP fluids which are R152a, R1234yf, R600, R600a, and R717.

References

[1] Y.A. Cengel, and M.A. Boles, *Thermodynamics an Engineering Approach*, McGraw-Hill, 7th Edition, 2007.

[2] C.R. Ferguson, *Internal Combustion Engines*, John Wiley & Sons, 1986.

[3] M. Niazkar, S.H. Afzali, Application of Excel Spreadsheet in Engineering Education, First International & National Conference on Engineering Education, Shiraz University, 10-12 November 2015

[4] A. Karimi, Using Excel for the thermodynamic analyses of air-standard cycles and combustion processes, ASME 2009 Lake Buena Vista, Florida, USA.

[5] Z. Ahmadi-Brooghani, Using Spreadsheets as a Computational Tool in Teaching Mechanical Engineering, Proceedings of the 10th WSEAS International Conference on computers, Vouliagmeni, Athens, Greece, July 1315, 2006, 305-310

[6] S.A. Oke, Spreadsheet Applications in Engineering Education: A Review, Int. J. Engng Ed. Vol. 20, 2004, No. 6, 893-901

[7] M.M. El-Awad and A. M. Elseory, Excel as a Modelling Platform for Thermodynamic Optimisation Analyses, University of Khartoum Engineering Journal, Vol. 3 Issue 1, pp. 12-18 (February 2013)

[8] M.M. El-Awad and M.S. Al-Saidi, Excel as an Educational Platform for Design Analyses of Fluid-Thermal Systems, World Journal of Engineering and

Technology Vol.10 No.2, 2022, 434-443, doi: 10.4236/wjet.2022.102025. Scientific Research Publishing.

[9] The University of Alabama, Mechanical Engineering, Excel for Mechanical Engineering project, Internet: http://www.me.ua.edu/excelinme/index.htm (Last accessed July 11, 2019).

[10] J. Huguet, K. Woodbury, R. Taylor, Development of Excel add-in modules for use in thermodynamics curriculum: steam and ideal gas properties, American Society for Engineering Education, 2008, AC 2008-1751.

[11] K. Mahan, J. Huguet, K. Woodbury, R. Taylor, Excel in ME: Extending and refining ubiquitous software tools, American Society for Engineering Education, 2009, AC 2009-2295.

[12] L. Caretto, D. McDaniel, T. Mincer. Spreadsheet calculations of thermodynamic properties, Proceedings of the 2005 American Society for Engineering Education Annual Conference & Exposition, American Society for Engineering Education, 2005.

[13] D. G. Goodwin, ″TPX: thermodynamic properties for Excel", http://termodinamicaparaiq.blogspot.com/p/tpx_12.html (Last accessed July 11, 2019).

[14] T. K. Jack. Computerised calculations of thermo-physical steam and air properties, *Int. J. Pure Appl. Sci. Technol.*, 9(2) (2012), pp. 84-93 (*Available online at* http://ijopaasat.in/yahoo_site_admin/assets/docs/3_IJPAST-276-V9N2.139104407.pdf (Last accessed July 11, 2019).

[15] C.O.C. Oko and E.O.Diemuodeke. MS Excel spreadsheet add-in for thermodynamic properties and process simulation of R152a, *Energy Science and Technology***,** Vol. 5, No. 2, 2013, pp. 63-69.

[16] E.W. Lemmon, M.L. Huber, M.O. McLinden, *NIST Reference Fluid Thermodynamic and Transport Properties— REFPROP* Version 8.0, User's Guide, National Institute of Standards and Technology, Physical and Chemical Properties Division, Boulder, Colorado 80305, 2007.

[17] I. Bell, CoolProp. Available at https://sourceforge.net/projects/coolprop/files/CoolProp/ (Last accessed July 11, 2019).

[18] Optimized Thermal Systems, XProps, A Quick and easy way to call refrigerant properties, http://optimizedthermalsystems.com/index.php/products/xprops, (Last accessed July 11, 2019).

Chapter 2

Thermax property functions

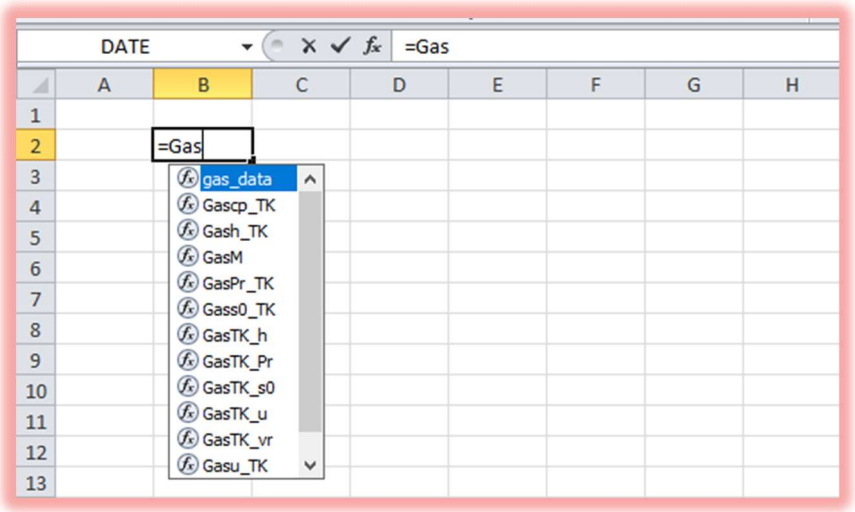

Thermax provides Excel with custom functions that determine the key thermo-physical properties for 29 ideal gases, water and superheated steam, 28 vapour-compression (VC) refrigerants, two binary solutions used in vapour-absorption (VA) refrigeration, humid air for air-conditioning applications, various fuels and chemically reacting substances, and atmospheric air at various temperatures. To help the user select the suitable property function, Thermax functions are divided into seven groups such that each group deals with one substance or similar substances and each group of functions are given a common indicative prefix; e.g. "Gas" for ideal gases, "Wat" for water/steam, and "Ref" for VC refrigerants. The name of each function also indicates its output and input properties. This chapter explains the name style adopted for Thermax functions in more details and shows how it can be utilised by Excel's function wizard to help the user find the required function without having to memorise the names of all the add-in functions. The chapter also describes the procedure for installing the add-in and using its functions in Excel's formulae for thermodynamic analyses.

2.1. The name style for Thermax property functions

Consider the two Thermax functions shown on Figure 2.1. The first function shown on Figure 2.1.a determines the enthalpy of saturated water at a pressure of 500 kPa and quality of 0.8, while that shown on Figure 2.1.b determines the entropy of a superheated refrigerant R134a at a pressure of 200 kPa and temperature of 50°C.

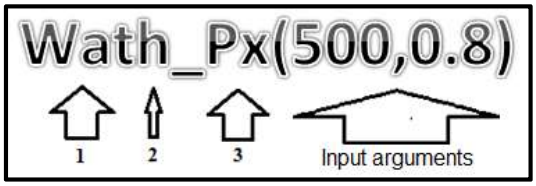

(a)

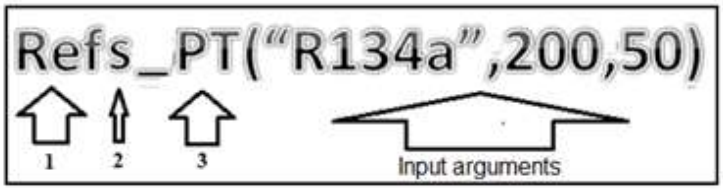

(b)

Figure 2.1. Examples of Thermax functions

Figure 2.1 shows that the name of a function consists of the following three parts:

1. The first three letters (1) refer to the function's group, i.e., "**Wat**" for water/steam and "**Ref**" for vapour-compression refrigerants.
2. The fourth letter (2), which is followed by an underscore, refers to the function's output property, i.e., "**h_**" for enthalpy and "**s_**" for entropy.
3. The letters after the underscore (3) refer to the function's input parameter(s), i.e., "**Px**" for pressure and quality and "**PT**" for pressure and temperature (in °C).

Figure 2.1 also shows the required input parameters for the two functions. While first function (**Wath_Px**) requires two input properties, which are the pressure (500 kPa) and quality (0.8), the second function (**Refs_PT**) requires three input parameters which are the refrigerant name ("R134a"), the pressure (200 kPa), and the temperature (50°C).

For the other groups "**Gas**" stands for ideal gases, "**Psy**" for psychrometric analyses, "**LiB**" and "**Nh3**" for the two binary solutions used in VA refrigeration, "**Chm**" for fuels and chemically reacting substances, and "**Air**" for air at atmospheric pressure. Table 2.1 gives more examples for the add-in functions with their intended usage.

Table 2.1. Examples of Thermax property functions from different groups

#	Thermax function	Output
1	Gash_TK("Air",350)	Determines the enthalpy (h) for air at 350K
2	GasTK_h("Air",500)	Determines the absolute temperature for air given its enthalpy (h=500 kJ/kg)
3	Wats_Tx(150,0.5)	Determines the entropy (s) of saturated water at a temperature of 150°C and quality of 0.5
4	Wath_PT(90,150)	Determines the enthalpy of superheated steam at 90 kPa and 150°C
5	RefPsat_T("R134a",-5)	Determines the saturation pressure (P_{sat}) for refrigerant R134a at -5°C.
6	PsyRh_PTSh(101,30, 0.001)	Determines relative humidity (ϕ) of air at 101 kPa, 30°C, and specific humidity (ω) of 0.001 kg/kg
7	Airdv_T(25)	Determines the dynamic viscosity of air at standard atmospheric pressure and 25°C.
8	Chm_f1("C6H6","M")	Returns the molar mass for benzene (C_6H_6)
9	Chm_f3("N2","M")	Returns the molar mass for nitrogen (N_2)
10	LiBh_TX(20,80)	Determines the enthalpy of water-lithium bromide solution at 20°C and 80% concentration.

The following points should also be noted regarding Thermax and its name style:

1. The add-in adopts only the SI system of units, e.g., pressure unit is kPa.
2. In the Gas-group, the absolute temperature is represented by "**TK**" while in the other groups the temperature in °C is represented by "**T**".
3. Three groups involve more than one substance and, therefore, the functions of these groups require the name of the substance as the first input parameter. These groups are the Gas-group, the Ref-group, and the Chm-group.
4. The input and output properties in most of the functions are represented by one or two letters, e.g. **Gash_TK** and **GasTK_h**, but some properties are represented by three letters like the saturation pressure and saturation temperature, which are

represented by Psat and Tsat in the Wat and Ref groups. Another example is the density of atmospheric air in the Air-group which is represented by **Airrho**.

2.2. Property functions provided by Thermax

The functions provided by each group are described below.

2.2.1. Functions for ideal gases (Gas)

This group of Thermax functions determine the ideal-gas properties for the 29 gasses listed in Appendix A based on the established ideal-gas relationships [1]. The group provides the 12 functions listed in Table 2.2.

Table 2.2. Functions for thermodynamic properties of ideal gases

#	Function	Input [Unit]	Output [Unit]
1	GasM	Gas name	Molar mass, M [kg/kmol]
2	Gascp_TK	Gas name, T[K]	Specific heat, c_p [kJ/kg.K]
3	Gash_TK	Gas name, T[K]	Specific enthalpy, h [kJ/kg]
4	Gasu_TK	Gas name, T[K]	Specific internal energy, u [kJ/kg]
5	Gass0_TK	Gas name, T[K]	Entropy component, s^0 [kJ/kg.K]
6	GasPr_TK	Gas name, T[K]	Relative pressure, P_r [-]
7	Gasvr_TK	Gas name, T[K]	Relative volume, v_r [K]
8	GasTK_h	Gas name, h[kJ/kg]	Absolute temperature, T [K]
9	GasTK_u	Gas name, u[kJ/kg]	Absolute temperature, T [K]
10	GasTK_s0	Gas name, s^0[kJ/kg.K]	Absolute temperature, T [K]
11	GasTK_Pr	Gas name, P_r [-]	Absolute temperature, T [K]
12	GasTK_vr	Gas name, v_r [-]	Absolute temperature, T [K]

The first five functions in Table 2.2 determine the molar mass (M), specific heat (c_p), enthalpy (h), internal energy (u), and the part of entropy change due to temperature change (s^0), respectively. The two functions that follow, **GasPr_TK** and **Gasvr_TK**, determine the relative pressure (P_r) and relative specific volume (v_r) of the ideal gases, respectively. The last five functions in the table are inversion functions that determine the temperature of the ideal gas from its enthalpy (h), internal energy (u), temperature-dependent entropy change (s^0), relative pressure (P_r) or relative specific volume (v_r).

With the exception of the first function, **GasM**, all the functions in this group involve the gas absolute temperature as an input or output parameter. Note that the temperature in the names of all the functions in this group is represented by "TK". An auxiliary function named "**Gas_data**", not shown in the table, stores the values of the four coefficients a_0, a_1, a_2, and a_3 in Equation (A.1) for the 29 gases [1]. The same function is needed by the third function in the combustion and chemical reactions group (**Chm_f3**) to determine the properties of the gases involved in a combustion or chemical reaction process.

2.2.2. Functions for water and superheated steam (Wat)

This group of functions that determine the thermo-physical properties of water and superheated steam can be divided into two subgroups: (a) functions for the properties of saturated water/steam mixture and (b) functions for the properties of superheated steam. Properties of subcooled liquid water can be taken as the corresponding values of saturated liquid water at the given temperature [1].

a) Properties of saturated water/steam mixture

The 20 functions in this subgroup do not use mathematical formulae, but store and interpolate the tabulated data for saturated water provided by ASHRAE [2]. Table 2.3 shows the input and output parameters of the 10 property functions that determine the properties of saturated water/steam mixtures at a given temperature with their relevant units. The corresponding 10 custom functions that provide properties of saturated water-steam mixture at a given pressure are listed in Table 2.4. Properties of water as saturated liquid or saturated vapour can be obtained from the functions number 2 to 9 by assigning the value of the quality x as 0 or 1, respectively.

Table 2.3. Property functions for saturated water/steam at a given temperature

#	Function	Input [Unit]	Output [Unit]
1	WatPsat_T	T [°C]	Saturation pressure, p_s [kPa]
2	Watv_Tx	T [°C], x [-]	Specific volume, v [m^3/kg]
3	Watu_Tx	T [°C], x [-]	Specific internal energy u [kJ/kg]
4	Wath_Tx	T [°C], x [-]	Specific enthalpy, h [kJ/kg]
5	Wats_Tx	T [°C], x [-]	Specific entropy, s [kJ/kg.K]
6	Watcp_Tx	T [°C], x [-]	Specific heat c_p , [kJ/(kg·K)]
7	Watk_Tx	T [°C], x [-]	Thermal cond., k [mW/(m·K)]
8	Watdv_Tx	T [°C], x [-]	Viscosity, μ [Pa·s]
9	Watvs_Tx	T [°C], x [-]	Velocity of sound, [m/s]
10	Watst_T	T [°C]	Surface tension, [mN/m]

Table 2.4. Property functions for saturated water/steam at a given pressure

#	Function	Input [Unit]	Output [Unit]
1	WatTsat_P	P [kPa]	Saturation temperature, T_s [°C]
2	Watv_Px	P [kPa], x [-]	Specific volume, v [m^3/kg]
3	Watu_Px	P [kPa], x [-]	Specific internal energy u [kJ/kg]
4	Wath_Px	P [kPa], x [-]	Specific enthalpy, h [kJ/kg]
5	Wats_Px	P [kPa], x [-]	Specific entropy, s [kJ/kg.K]
6	Watcp_Px	P [kPa], x [-]	Specific heat c_p , [kJ/(kg·K)]
7	Watk_Px	P [kPa], x [-]	Thermal cond., k [mW/(m·K)]
8	Watdv_Px	P [kPa], x [-]	Viscosity, μ [Pa·s]
9	Watvs_Px	P [kPa], x [-]	Velocity of sound, [m/s]
10	Watst_P	P [kPa]	Surface tension, [mN/m]

b) Properties of superheated steam

There are 8 functions in this subgroup that determine the thermodynamic properties of superheated steam as shown in Table 2.5. The first four functions determine the specific volume (v), internal energy (u), enthalpy (h), and entropy (s) of superheated steam given the pressure and temperature according to the formulae provided by Irvine and Liley [3]. The remaining four functions are inverse functions that use iteration to determine the temperature, enthalpy, or entropy from the pressure and another property.

Table 2.5. Properties of superheated steam given the pressure and another property

#	Function	Input [Unit]	Output [Unit]
1	Watv_PT	P, T[°C]	Specific volume, v [m^3/kg]
2	Watu_PT	P, T[°C]	Specific internal energy u [kJ/kg]
3	Wath_PT	P, T[°C]	Specific enthalpy, h [kJ/kg]
4	Wats_PT	P, T[°C]	Specific entropy, s [kJ/kg.K]
5	WatT_Ph	P, h[kJ/kg]	Temperature, T [^{0}C]
6	WatT_Ps	P, s[kJ/kg.K]	Temperature, T [^{0}C]
7	Wath_Ps	P, s[kJ/kg.K]	Specific enthalpy, h [kJ/kg]
8	Wats_Ph	P, h[kJ/kg]	Specific entropy, s [kJ/kg.K]

2.2.3. Functions for vapour-compression refrigerants (Ref)

This group of functions provides the thermo-physical properties for the 28 refrigerants listed in Table A2 of Appendix A. This group can also be divided into two subgroups; (a) for saturated refrigerants and (b) for superheated refrigerants.

a) Properties of saturated refrigerants

As for the water group, the functions for saturated refrigerants do not use mathematical formulae but store and interpolate the tabulated data provided by ASHRAE [2] by using a linear interpolation function. Table 2.6 lists 11 functions in this subgroup that determine the thermo-physical properties of saturated refrigerants at a given pressure and Table 2.7 lists 10 functions that determine the refrigerants properties at a given temperature.

Table 2.6. Properties of saturated refrigerants at a given pressure in kPa and quality

#	Function	Input	Output	Output unit
1	RefTsat_P	*Refrigerant name, P*, x	Saturation temperature, T_{sat}	[^{0}C]
2	Refv_Px	*Refrigerant name, P*, x	Specific volume, v	[m^3/kg]
3	Refu_Px	*Refrigerant name, P*, x	Specific internal energy, u	[kJ/kg]
4	Refh_Px	*Refrigerant name, P*, x	Specific enthalpy, h	[kJ/kg]
5	Refs_Px	*Refrigerant name, P*, x	Specific entropy, s	[kJ/kg.K]
6	Refcp_Px	*Refrigerant name, P*, x	Specific heat, c_p	[kJ/kg.K]
7	Refvs_Px	*Refrigerant name, P*, x	Velocity of sound	[m/s]
8	Refdv_Px	*Refrigerant name, P*, x	Dynamic viscosity, μ	[μPa·s]
9	Refk_Px	*Refrigerant name, P*, x	Thermal conductivity, k	[mW/(m·K)]
10	Refst_P	*Refrigerant name, P*	Surface tension	[mN/m]
11	RefTdew_P	*Refrigerant name, P*	Dew temperature	[^{0}C]

Table 2.7. Properties of saturated refrigerants at a given temperature in °C and quality

#	Function	Input	Output	Output unit
1	RefPsat_T	*Refrigerant name, T, x*	*Saturation temperature,* T_{sat}	[^{0}C]
2	Refv_Tx	*Refrigerant name, T, x*	*Specific volume, v*	[m^3/kg]
3	Refu_Tx	*Refrigerant name, T, x*	*Specific internal energy, u*	[kJ/kg]
4	Refh_Tx	*Refrigerant name, T, x*	*Specific enthalpy, h*	[kJ/kg]
5	Refs_Tx	*Refrigerant name, T, x*	*Specific entropy, s*	[kJ/kg.K]
6	Refcp_Tx	*Refrigerant name, T, x*	*Specific heat,* c_p	[kJ/kg.K]
7	Refvs_Tx	*Refrigerant name, T, x*	*Velocity of sound*	[m/s]
8	Refdv_Tx	*Refrigerant name, T, x*	*Dynamic viscosity,* μ	[μPa·s]
9	Refk_Tx	*Refrigerant name, T, x*	*Thermal conductivity, k*	[mW/(m·K)]
10	Refst_T	*Refrigerant name, T*	*Surface tension*	[mN/m]

Three of the 28 refrigerants are zeotropic blends, which are R404A, R407C, and R410A. For these three refrigerants, the saturation temperature means the bubble temperature, while the dew temperature is given by the last function shown on Table 2.6, **RefTdew_P**.

b) Properties of superheated refrigerants

Table 2.9 lists 8 functions that deal with superheated vapours of refrigerants. The first function in Table 2.9 applies the Redlich-Kwong (SRK) equation of state to determine the specific volume of superheated refrigerants. The following six functions apply Equations (B.18) to (B.23) given in Appendix B to determine the relevant property values. The last function (**Refs_Ph**) is an inversion function that uses an iterative solution to determine the fluid's entropy.

Table 2.9. Properties of superheated refrigerants given the pressure in kPa

#	Function	Input [unit]	Output [unit]
1	Refv_PT	*Refrigerant name, P, T* [°C]	*v* [m^3/kg]
2	Refu_PT	*Refrigerant name, P, T* [°C]	*u* [kJ/kg]
3	Refh_PT	*Refrigerant name, P, T* [°C]	*h* [kJ/kg]
4	Refs_PT	*Refrigerant name, P, T* [°C]	*s* [kJ/kg.K]
5	RefT_Ph	*Refrigerant name, P, h* [kJ/kg]	*T* [°C]
6	RefT_Ps	*Refrigerant name, P, s* [kJ/kg.K]	*T* [°C]
7	Refh_Ps	*Refrigerant name, P, s* [kJ/kg.K]	*h* [kJ/kg]
8	Refs_Ph	*Refrigerant name, P, h* [kJ/kg]	*s* [kJ/kg.K]

It should be noted that the functions in this subgroup apply only for subcritical pressures. Appendix C verifies these functions for R134a by comparing their estimations with the data given by ASHRAE [2].

2.2.4. Functions for psychrometric analyses (Psy)

The functions of this group provide the thermodynamic properties of atmospheric air, which is a mixture of dry air and water-vapour. Appendix B shows the relations used for

the development of these functions which are those commonly used in psychrometric analyses. Table 2.10 lists 14 functions that are included in this group together with their input and output arguments. The letters in the function names have the following meanings: h (specific enthalpy), Db (dry bulb), Dp (dew point), P (pressure), Rh (relative humidity), Sh (specific humidity), v (specific volume), Wb (wet bulb). Case 6 in Table 2.1 shows how the function **PsyRh_PTSh** is used to determine the relative humidity for air given its pressure, temperature, and specific humidity.

Table 2.10. Functions for psychrometric analyses

#	Function	Input [unit]	Output [unit]
1	Psyv_PDbRh	P [kPa], T_{db} [°C], ϕ [%]	v [m^3/kg]
2	PsyRh_PDbSh	P [kPa], T_{db} [°C], ω[kg/kg]	ϕ [%]
3	PsyRh_PDbWb	P [kPa], T_{db} [°C], T_{wb} [°C]	ϕ [%]
4	PsySh_PDbRh	P [kPa], T [°C], ϕ [%]	ω [kg/kg]
5	PsySh_PDbWb	P [kPa], T_{db} [°C], T_{wb} [°C]	ω [kg/kg]
6	Psyh_PDbSh	P [kPa], T [°C], ω[kg/kg]	h [kJ/kg]
7	Psyh_PDbRh	P [kPa], T [°C], ϕ [%]	h [kJ/kg]
8	PsyDp_PDbRh	P [kPa], T_{db} [°C], ϕ [%]	T_{dp} [°C]
9	PsyDp_PDbWb	P [kPa], T_{db} [°C], T_{wb} [°C]	T_{dp} [°C]
10	PsyDb_PRhSh	P [kPa], ϕ [%], ω[kg/kg]	T_{db} [°C]
11	PsyDb_PhSh	P [kPa], h [kJ/kg], ω[kg/kg]	T_{db} [°C]
12	PsyWb_PDbRh	P [kPa], T_{db} [°C], ϕ [%]	T_{wb} [°C]
13	PsyWb_PDbSh	P [kPa], T_{db} [°C], ω[kg/kg]	T_{wb} [°C]
14	PsyWb_PRhSh	P [kPa], ϕ [%], ω[kg/kg]	T_{wb} [°C]

2.2.5. Functions for absorption refrigeration solutions (LiB and NH3)

Thermax provides two groups of property functions for the analyses of vapour-absorption refrigeration systems: (a) water-lithium bromide (H_2O-LiBr) solution and (b) ammonia-water (NH_3-H_2O) solution. Each group has 13 property functions to determine properties of the relevant solution, but they use different formulae.

A. The H_2O-LiBr solution (LiB)

To determine the enthalpy (h), refrigerant temperature (T_r), and refrigerant concentration (X) of the H_2O-LiBr solution, these functions use the formulae given by ASHRAE [2] and to determine the entropy (s) and specific volume (v) the functions use the formulae given by Patek and Klomfar [4] and by Patterson and Perez-Blanco [5], respectively. This group needs two functions that determine the saturation pressure and saturation temperature of the refrigerant, which is water in this case. Although the two properties can be obtained by using the relevant functions in the water group, to make this group self-sufficient it has its own functions that determine these properties from the Antoine equations, which are Equations (B.16) and (B.17) given in Appendix B. Table 2.11 lists the 13 functions in the Lib-group.

Table 2.11. Functions for water-lithium bromide solution

#	Function	Input [unit]	Output [unit]
1	LiBh_TX	T [°C], X [%]	h [kJ/kg]
2	LiBv_TX	T [°C], X [%]	v [m^3/kg]
3	LiBs_TX	T [°C], X [%]	s [kJ/kg.K]
4	LiBT_trX	Tr [°C], X [%]	T [°C]
5	LiBT_prX	Pr [kPa], X [%]	T [°C]
6	LiBT_hX	h [kJ/kg], X [%]	T [°C]
7	LiBTr_TX	T [°C], X [%]	Tr [°C]
8	LiBPr_TX	T [°C], X [%]	Pr [kPa]
9	LiBX_Ttr	T [°C], Tr [°C]	X [%]
10	LiBX_Tpr	T [°C], Pr [kPa]	X [%]
11	LiBT_sX	s [kJ/kg.K], X [%]	T [°C]
12	LiBpr_tr	T [°C]	P_{sat} [kPa]
13	LiBtr_tr	P [kPa]	T_{sat} [°C]

B. The ammonia-water solution (NH3)

To determine the enthalpy of the ammonia-water solution, this group applies the formulae given by Patek and Klomfar [6] and to determine the specific volume it applies that given by Sun [7]. The entropy of NH_3-H_2O solution in the liquid state (s_l) and the vapour state (s_v) are obtained by using the formulae given by El-Shaarawi et al [8]. The relations between refrigerant pressure and temperature of an ammonia-water solution with concentration are taken from Bourseau and Bugarel [9]. Table 2.12 lists the 13 functions in the NH3-group.

Table 2.12. Functions for ammonia-water solution

#	Function	Input [unit]	Output [unit]
1	NH3h_TX	T [°C], X [%]	h [kJ/kg]
2	NH3v_TX	T [°C], X [%]	v [m^3/kg]
3	NH3sl_prX	Pr [kPa], X [%]	s_l [kJ/kg.K]
4	NH3sv_prX	Pr [kPa], X [%]	S_v [kJ/kg.K]
5	NH3T_trX	Tr [°C], X [%]	T [°C]
6	NH3T_prX	Tr [°C], X [%]	T [°C]
7	NH3T_hX	h [kJ/kg], X [%]	T [°C]
8	NH3tr_TX	T [°C], X [%]	Tr [°C]
9	NH3pr_TX	T [°C], X [%]	Pr [kPa]
10	NH3X_Ttr	T [°C], Tr [°C]	X [%]
11	NH3X_Tpr	T [°C], Pr [kPa]	X [%]
12	NH3pr_tr	T [°C]	P_{sat} [kPa]
13	NH3tr_pr	P [kPa]	T_{sat} [°C]

The NH3-group also needs two functions that determine the saturation pressure and saturation temperature of the refrigerant, which is ammonia. In order to make the group

self-sufficient, the group has its own functions that determine these properties instead of using the functions provided by the refrigerants group. Accordingly, the saturation pressure (P_{sat}) of ammonia is obtained from the following equation [7]:

$$P_{sat} = 10^3 \sum_{i=0}^{6} a_i T^i \tag{2.1}$$

Where, T is in °C, P in kPa and values of the six coefficients a_1 to a_6 can be found in Sun [7]. The saturation temperature (T_{sat}) is obtained from Equation (2.1) by iteration.

2.2.6. Functions for combustion and chemical reactions (Chm)

The analyses of combustion and other chemical reactions involve mass and energy balances of the substances involved as reactants or products that can be solids, liquids, or gases. The gases involved are treated as ideal and, therefore, the group of functions for ideal gases "Gas" can be used here. However, combustion analyses require additional data like the heating value, enthalpy of formation, or Gibbs function. The group provided by Thermax for the analyses of combustion processes and chemical reactions consists of the three general functions shown in Table 2.13.

Table 2.13. Functions for thermodynamic properties of reacting systems

#	Function	Input argument	Output property
1	Chm_f1	Substance; property	M, $\bar{h}_f^0$, $\bar{g}_f^0$, $\bar{s}^0$
2	Chm_f2	Substance; property	M, Q_H, Q_L, AF, Hv, α, β, γ, δ
3	Chm_f3	Substance; property, temperature	$\bar{c}_p$, $\bar{h}$, $\bar{u}$, $\bar{s}^0$

All three functions require as input arguments the substance name and the name of the required property. In addition to those, the third function requires the temperature of the substance involved to be provided. The first function, **Chm_f1**, provides the molar mass (M), molar enthalpy of formation ($\bar{h}_f^0$), molar Gibbs function of formation ($\bar{g}_f^0$), and molar absolute entropy ($\bar{s}^0$) for the 29 reacting substances and reaction products that are listed in Table A.3 of Appendix A. Case 8 in Table 2.1 illustrates the use of this function.

The second function, **Chm_f2**, provides additional data needed for combustion analyses involving the 20 fuels and reacting substances listed in Table A.4. These include values of the molar mass (M), gravimetric higher and lower heating values (Q_H and Q_L), stoichiometric air-fuel ratio (AF_s) and heat of vaporisation (H_v). This function also provides the carbon, hydrogen, oxygen, and nitrogen contents of the substance (α, β, γ, δ) based on the general chemical representation $C_\alpha H_\beta O_\gamma N_\delta$. The third function, **Chm_f3**, determines four properties of ideal gases on a unit-mole basis. Case 9 in Table 2.1 shows the required input and the output of this function.

2.2.7. Functions for air at standard atmospheric pressure (Air)

This group provides the thermo-physical properties for air at standard atmospheric pressure as required by fluid-dynamics and heat-transfer analyses. Based on the tabulated data given by Cengel and Ghajar [10], the functions use a linear interpolation function to determine the air density (ρ), specific heat (c_p), thermal conductivity (k), thermal diffusivity (α), dynamic viscosity (μ), kinematic viscosity (ν) and Prandtl number (Pr) at temperatures in the range -150°C to 2000°C. Table 2.14 shows the names of the seven functions in this group with their corresponding output properties. Note that this group also provides a function for determining the specific-heat for air at constant pressure (c_p) which can be used instead of the function provided by the ideal-gas group.

Table 2.14. Properties of air at 1 atm pressure given the temperature in °C

#	Function	Output	Output unit
1	Airrho_T	Density (ρ)	kg/m^3
2	Aircp_T	Specific heat (c_p)	J/Kg.°C
3	Airk_T	Thermal conductivity (k)	W/m.°C
4	Airdf_T	Thermal diffusivity (α)	m^2/s
5	Airdv_T	Dynamic viscosity (μ)	kg/m·s
6	Airkv_T	Kinematic viscosity (ν)	m^2/s
7	AirPr_T	Prandtl number (Pr)	-

2.3. Using Thermax property functions in Excel formulae

Before Thermax functions can be used in Excel's formulae, you have to save it in your computer as an add-in. To do that, open the **Thermax** file and then save it in your computer as an "**Excel Add-in**". Excel comes with a number of add-ins that extend the application's functionality such as the Solver add-in. All add-ins are saved in one folder and active add-ins are automatically loaded when Excel starts up. In order to activate Thermax, open a new Excel sheet and then do the following:

1. Go to **File**, click **Options** and then select **Add-Ins**.
2. From the **Manage** ribbon at the bottom of the menu select **Excel Add-ins** and then press **Go**. The pull-down menu shown on Figure 2.2 will appear to you.
3. To add **Thermax** to the add-ins menu, tick (√) the corresponding box. If for any reason the add-in does not appear in the list, then click on **Browse** and search for it in the destination folder and select it.

The add-in functions can now be used in Excel's formulae just like its built-in functions. The following sections illustrate two methods for using these functions in Excel.

2.3.1. Accessing Thermax functions via the Function Wizard

This method suits the first-time users. To illustrate the method, let us start a formula by entering the equal sign (=) in any cell (say, cell B2). If you now press the *fx* button in the formula ribbon, the **Function Wizard** shown on Figure 2.3 will come up. The Function

Wizard firstly lists the various categories of built-in functions provided by Excel, e.g., financial, mathematical, statistical, etc. Scroll down the list of function categories and select the **User-defined** functions. Then, all the functions provided by Thermax will be listed alphabetically as shown on Figure 2.4.

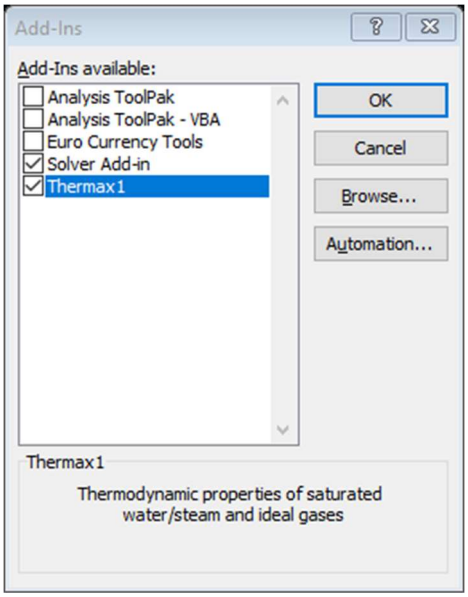

Figure 2.2. Adding Thermax to the menu of Excel add-ins

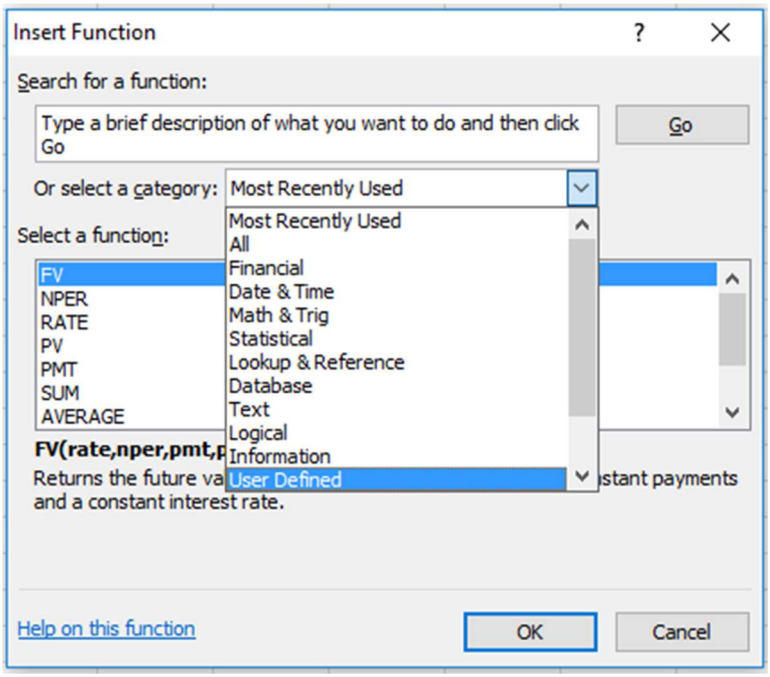

Figure 2.3. Finding the add-in user-defined functions in the Function Wizard

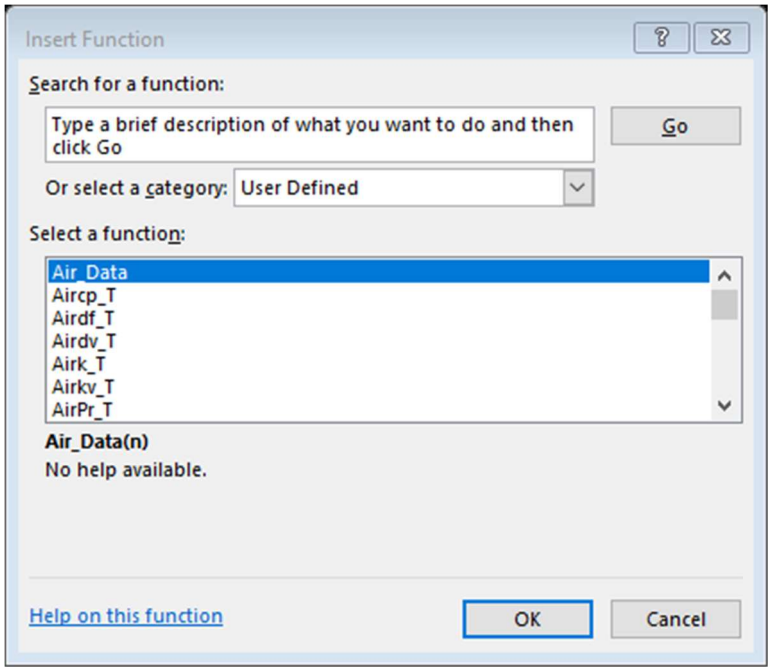

Figure 2.4. Thermax functions listed alphabetically in the User Defined category

The first function in the list of Figure 2.4, **Air_Data**, is an auxiliary function that stores the data for the seven thermophysical properties of air at standard atmospheric pressure. This function is called by other functions in the Air-group in order to determine the values of their respective properties at the required temperature. To start using the add-in functions, let us use it to determine the thermal conductivity (k) of air at 25°C. To do that, go down the list and select the function named **Airk_T**. Upon pressing the OK button, the **Function Arguments** box shown on Figure 2.5 will appear to you.

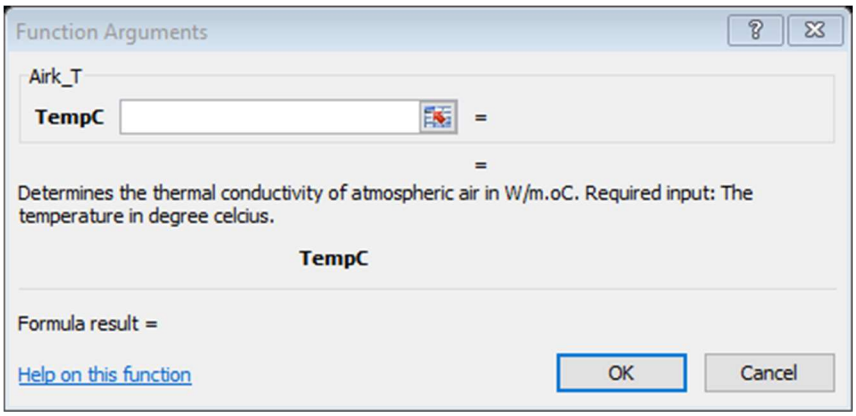

Figure 2.5. The Function Arguments box for the "Airk_T" function

Figure 2.5 shows that this function has one input parameter, which is the temperature in °C "TempC", and gives a brief description of its intended use. Fill the form by entering

the given value of the temperature, 25, as shown on Figure 2.6. Note that the formula ribbon now shows the formula in cell B2, which is "=Airk_T(25)". The form also shows the calculated value of k, which is 0.02551 W/m.°C. When you press the "**OK**" button, this value will appear in the cell B2. Check this value with the tabulated data.

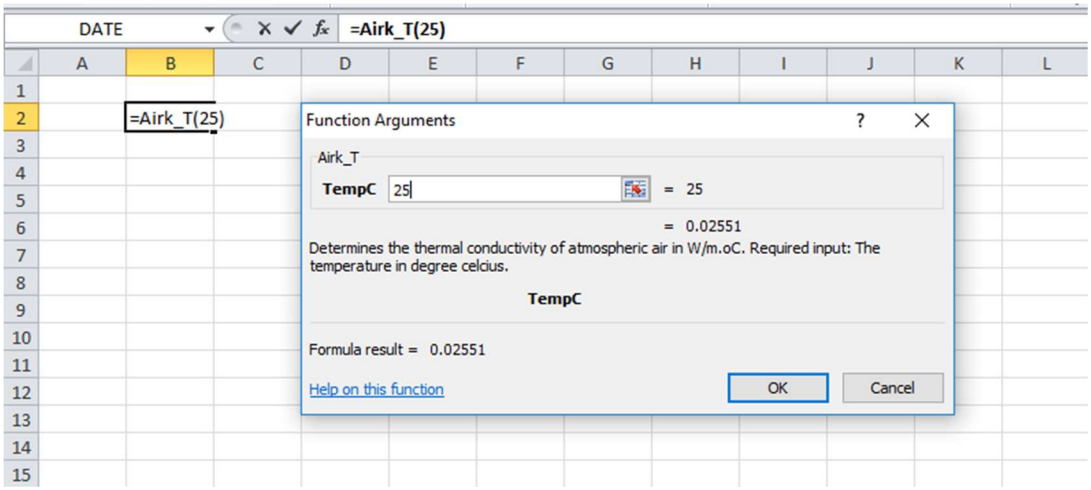

Figure 2.6. Using the function "Airk_T" to determine the thermal conductivity of atmospheric air at 25°C

2.3.2. Direct use of Thermax functions in Excel formulae

It is not necessary to follow the lengthy procedure described above by using the Function Wizard in order to use the add-in property functions. After some practice one can simply type in the formula that contains the property function in the required Excel cell. As mentioned earlier, the style adopted for naming Thermax functions makes it easy to identify the required function and the required input without having to memorise these for all the functions. For illustration, suppose that we want to determine the temperature of carbon-dioxide (CO_2) at which the value of its enthalpy (h) equals 750 kJ/kg. In this case, we need to use the function in the "**Gas**" group that determines the temperature for a given enthalpy value of the gas. Therefore, we start an Excel formula by typing the equal sign "=" in any cell and then type the prefix "Gas". As shown on Figure 2.7, as soon as we type the prefix "Gas" after the equal sign, the user-interface will display all Thermax functions in the ideal-gases group for us to select from.

Since the property we want to find is the temperature, which the Gas-group functions require in absolute degree, we continue the name of the function by adding the letters "TK" immediately after the three-letter prefix "Gas" followed by an underscore. As shown on Figure 2.8, the user-interface then lists only the five functions in Table 2.2 that determine the gas temperature given h, P_r, s^0, u, or v_r. To find the temperature from a known value of enthalpy, we have to select the "**GasTK_h**" function as shown on Figure 2.9. Excel will then ask you to enter the required input parameters. This function requires the name of the gas, which is "CO2", and the value of enthalpy, which is 750 kJ/kg, as

shown on Figure 2.10. Press the "**Enter**" key, and the answer shown on Figure 2.11, which is 817.5544K, will be displayed.

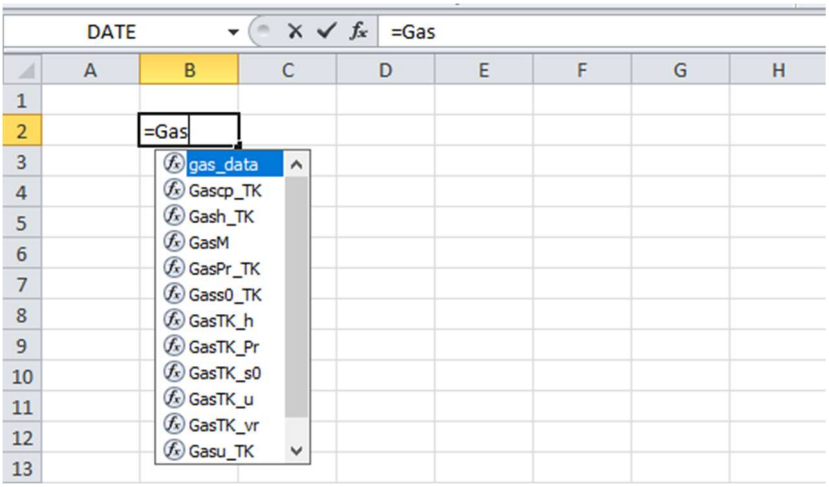

Figure 2.7. Excel UI showing all the functions in the Gas-group

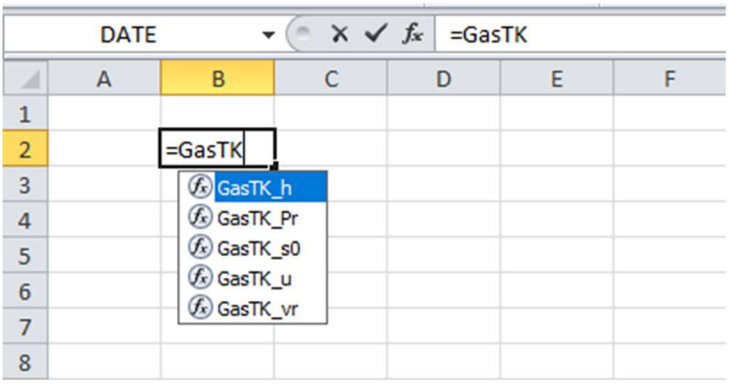

Figure 2.8. UI showing only the five functions that determine the temperature of an ideal gas from known values of h, p_r, s^0, u, or v_r

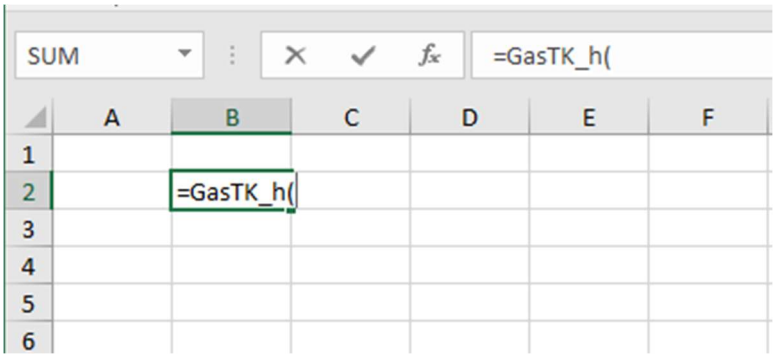

Figure 2.9. The required input for the GasTK_h function

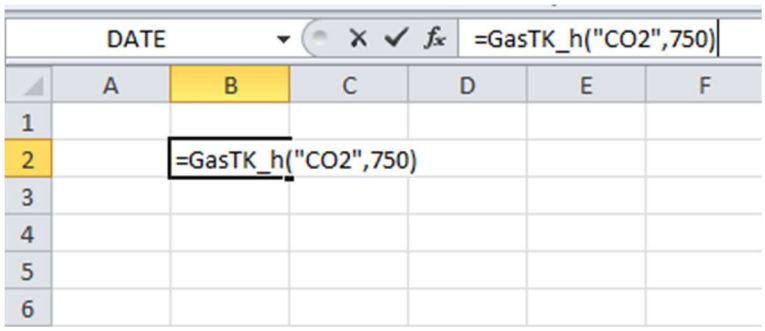

Figure 2.10. The required input for the GasTK_h function

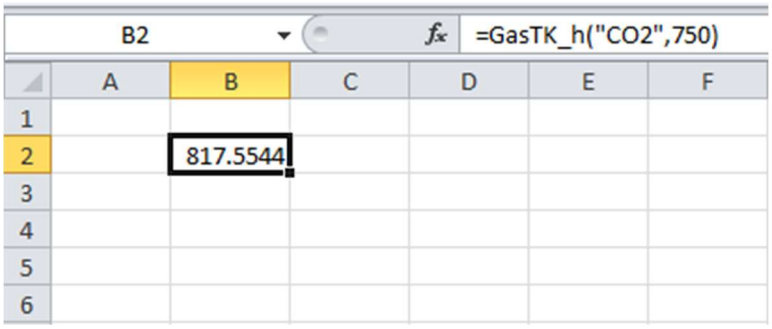

Figure 2.11. The temperature determined by the GasTK_h function

You can always call the **Function Wizard** if you are not certain about the required input parameters by pressing the *fx* button in the formula ribbon and the form shown on Figure 2.12 will appear to you. The form shows the two required input parameters for you to provide. Pressing the "Enter" key or the "OK" button after entering the required data, the function will calculate the corresponding temperature which is 817.5544K as shown on Figure 2.11. This value can be checked by comparison with the tabulated data.

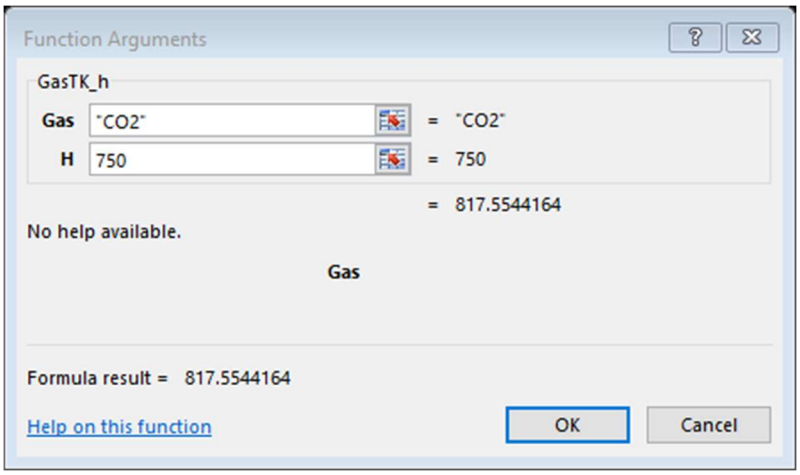

Figure 2.12. The Function Wizard with the required input for the GasTK_h function

2.4. Thermodynamic analysis using Thermax functions

This section shows how Thermax functions can be used in thermodynamic analyses with Excel. The case considered uses the functions in the Gas-group for applying the variable specific-heat method (the exact method) in thermodynamic analyses.

Example 2.1. Thermodynamic analysis with the exact method

Figure 2.13 shows a well-insulated piston–cylinder device that initially contains 0.1 m^3 of air at 100 kPa, 330K. Fifty kJ of heat is transferred to the air causing the air to expand at constant pressure. Treating air as an ideal gas, determine the final temperature inside the cylinder using: (a) the approximate constant-specific heat method, with c_p= 1.005 kJ/kg.K, and (b) the exact variable specific-heat method with Thermax functions.

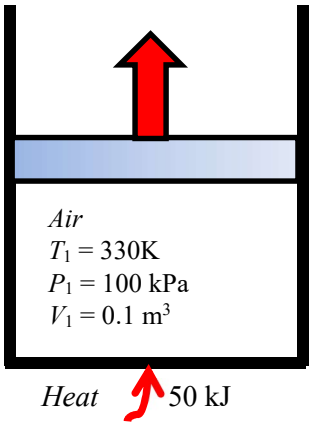

Figure 2.13. Schematic for Example 2.1

(a) Solution with the approximate method

Using the approximate constant specific heat method, the final temperature is determined from:

$$T_2 = T_1 + \frac{Q}{m \times c_p} \tag{2.2}$$

Where m is the mass of air in the piston-cylinder device, c_p is the average value of the specific heat at constant pressure, and Q is the amount of heat added. The mass of air is first calculated from the ideal-gas law:

$$m = \frac{P_1 V_1}{R \times T_1} \tag{2.3}$$

Where R is the gas constant for air, R = 0.287 kJ/kg.K. Substituting for P_1, V_1, R and T_1 in Equation (2.3), leads to m = 0.105585 kg and substituting for m in Equation (2.2) gives T_2 = 801.194K.

(b) Solution with the exact method

To apply the exact method by using Thermax functions, we have to determine the final enthalpy, h_2. From the first law of thermodynamics applied to the closed system that undergoes a constant-pressure process, h_2 is given by:

$$h_2 = h_1 + Q/m \tag{2.4}$$

Once h_2 is found, the final temperature, T_2, can be determined by using the function **GasTK_h** in the Gas-group. Figure 2.14 shows the Excel sheet developed for this example. The given data are inserted at the left-hand side of the sheet together with the gas constant (R_) and specific heat (cp) for air.

H8 fx =(T_2approx-T_2exact)/T_2exact*100

	A	B	C	D	E	F	G	H	I	J	K
1				Approxiamte method			Exact method				
2	T_1	330	K	m	0.106	=P_1*V_1/(R_*T_1)	h_1	330.027	=Gash_TK("Air",T_1)		
3	P_1	100	kPa								
4	V_1	0.1	m3	T_2approx	801.194	=T_1+Q/(m*cp)	h_2	803.577	=h_1+Q/m		
5											
6	Q	50	kJ				T_2exact	781.644	=GasTK_h("Air",h_2)		
7											
8	R_	0.287	kJ/kg.K				Error	2.501	=(T_2approx-T_2exact)/T_2exact*100		
9	cp	1.005	kJ/kg.K								
10											

Figure 2.14. Excel sheet developed for Example 2.1

The calculations part is divided into two parts that determine the final temperature according to the approximate method and the exact method using the corresponding equations given above. Figure 2.14 also reveals the formulae used in these calculations. Note that "cell-labelling" has been used in the Excel formulae. As the figure shows, the answer found by the exact method for T_2 is 781.6K, while the approximate method determines the final temperature as 801.2K. In this case, the approximate constant specific-heat method results in an error of 2.5%.

2.5. Closure

This chapter introduces the Thermax add-in and its seven groups of property functions that determine the thermo-physical properties of various types of working fluids including 29 ideal gases, saturated water and superheated steam, 28 refrigerants, humid air for psychrometric analyses, two aqua solutions for vapour-absorption refrigeration, reacting substances, and air at atmospheric pressure. Thermax property functions are named in a way that helps the user to find the appropriate function via Excel's user-interface and function wizard. The chapter shows how the functions can be used in Excel formulae and illustrates the use of the ideal-gas functions for thermodynamic analyses with the exact variable specific-heat method. There are a number of auxiliary functions that are provided by the add-in its groups but do not appear in the respective tables some of which are mentioned in the following chapters where they are used.

Thermax property functions for ideal-gases, superheated steam, atmospheric humidified air, the two vapour-absorption fluids, and combustion gases use verified equations for these substances [1,3-9]. The functions for saturated water and saturated refrigerants determine the properties by interpolation of the verified data provided by ASHRAE [2]. The functions for atmospheric air at standard pressure also use interpolation of published data [10]. The only group of functions that use equations modified by the author are those developed for superheated refrigerants. The verification of these functions is discussed in Appendix C and a paper published by the author and co-workers [11]. The following six chapters illustrate the use of the various add-in functions for thermodynamic analyses of gas power generation cycles, vapour-power cycles, vapour-compressions refrigeration cycles, air-conditioning processes, combustion processes, and vapour-absorption cycles. The last two chapters of the book illustrate the use of the add-in function for thermo-economic optimisation analyses of energy-conversion systems.

References

[1] Y. A. Cengel and M. A. Boles. *Thermodynamics an Engineering Approach*, McGraw-Hill, 7th Edition, 2007.

[2] American Society of Heating, Refrigeration and Air-Conditioning Engineers, (ASHRAE), Handbook of fundamentals, Atlanta, 2017.

[3] T.F. Irvine Jr. and P.E. Liley. Steam and gas tables with computer equations. Orlando, (FL): Academic Press, 1984.

[4] J. Patek and J. Klomfar. A computationally effective formulation of the thermodynamic properties of LiBr–H2O solutions from 273 to 500 K over full composition range. *International Journal of Refrigeration*, Vol. 29, 2006, pp.566–578.

[5] M.R. Patterson and H. Perez-Blanco, "Numerical fits of the properties of lithium-bromide water solutions", *ASHRAE Trans*. Volume 94, Issue 2, pp. 2059-2077, 1988.

[6] J. Patek and J. Klomfar, "Simple functions for fast calculations of selected thermodynamic properties of the ammonia-water system". *International Journal of Refrigeration,* Vol. 18, No. 4, 1995, pp. 228 -234.

[7] D-W Sun. "Comparison of the performances of NH3-H2O, NH3-LiNO3 and NH3-NaSCN absorption refrigeration systems". *Energy Convers. Mgmt*, Vol. 39, No. 5/6, 1998, pp. 357-368.

[8] M.A.I. El-Shaarawi, S.A.M. Said, M.U. Siddiqui, "New correlation equations for ammonia-water vapor liquid equilibrium (VLE) thermodynamic properties", *ASHRAE Transactions*, 2013, pp. 293-298.

[9] P. Bourseau and R. Bugarel, "Absorption-diffusion machines: comparison of the performances of NH_3-H_2O and NH_3-NaSCN". *International Journal of Refrigeration*, Vol. 9, Issue 4, pp. 206-214.

[10] Y. A. Cengel and A. J. Ghajar. *Heat and Mass Transfer: Fundamentals and Applications*. McGraw Hill, 2011.

[11] M.M. El-Awad, M.S. Al Nabhani, K.S. Al Hinai, A. Younis, Development and Validation of an Excel Add-In for determining the Properties of Various

Refrigerants, Proceedings of the 1st National Conference on Applied Science, Engineering & Technology 2019, CASET – 2K19, 11th June 2019, Ibri, Oman

Exercises

1. Complete the following table by specifying the usage of the given Thermax function according to its name:

#	Function	Output property	Input /properties
1	Gascp_TK("CO2",300)		
2	WatTsat_P(200)		
3	WatT_Ph(200, 3487.7)		
4	RefPsat_T("R134a",0.0)		
5	PsyTs_P(100)		
6	Nh3Pr_TX(200,80)		
7	Airdv_T(500)		
8	Chm_f2("HDL","QL")		

2. Name the appropriate Thermax functions that determine the following properties:

#	Task	Thermax function
1	The enthalpy of saturated liquid water at 25°C	
2	The internal energy of oxygen at 300K	
3	The entropy of superheated steam at 10 kPa, 200°C	
4	The absolute temperature at which the relative pressure of air is equal to 15	
5	The saturation pressure for R-134a at -15°C	
6	The dry-bulb temperature of humid air at P = 101 kPa, ϕ = 50%, ω = 0.01	
7	The enthalpy of ammonia-water solution at 30°C, X= 50%	
8	The higher heating value for gasoline	

3. Using Thermax functions, determine the values of the following fluid properties:

#	Fluid	Given properties	Required property	Value
1	Saturated water	100 kPa, x = 0.5	Enthalpy (h)	
2	Air	700K	Relative volume (v_r)	
3	Steam	100°C, x = 1.0	Entropy (s)	
4	CO_2	450K	Specific heat (c_p)	
5	Hydrogen	h = 2000 *kJ/kg*	Temperature (T)	

Chapter 3

Analyses of gas power cycles

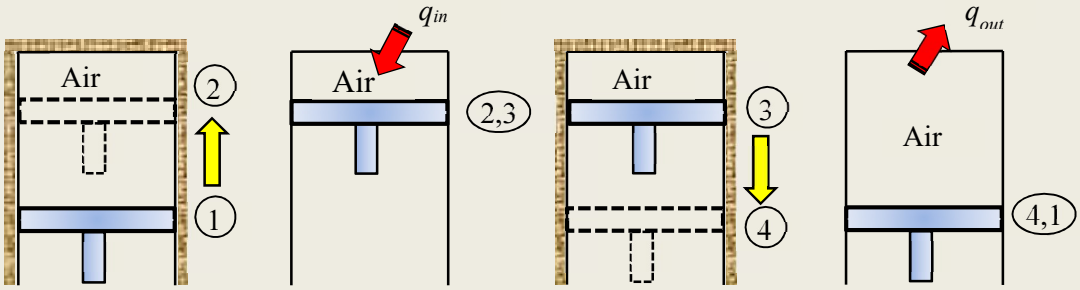

1-2: Isentropic compression

2-3: Heat addition at constant *v*

3-4: Isentropic expansion

4-1: Heat rejection at constant *v*

This chapter illustrates the use of Thermax functions for analysing two important gas power cycles, which are the Brayton cycle for gas turbine and the Otto cycle for spark-ignition internal-combustion engines. For the Brayton cycle both the simple and the regenerative cycles are analysed and for the Otto cycle both energy and exergy analyses are presented. Values of the key parameters of the cycles determined by using Thermax functions are verified against the relevant values given in standard thermodynamics textbooks. The results obtained for the simple Brayton cycle and the Otto cycle are also compared with those obtained by using the "Ideal-Gas" add-in [1].

3.1. The ideal Brayton cycle

The Brayton cycle is the ideal cycle for gas-turbines. Unlike the real gas-turbine cycle, it is a closed cycle with a constant mass of the working fluid going through the system's components as shown on Figure 3.1. The cycle consists of four processes; compression in an ideal gas compressor, heat-addition from a high-temperature source, expansion in an ideal gas turbine, and heat-rejection to a low-temperature sink. Figure 3.2 shows the Brayton cycle on a *T-s* diagram.

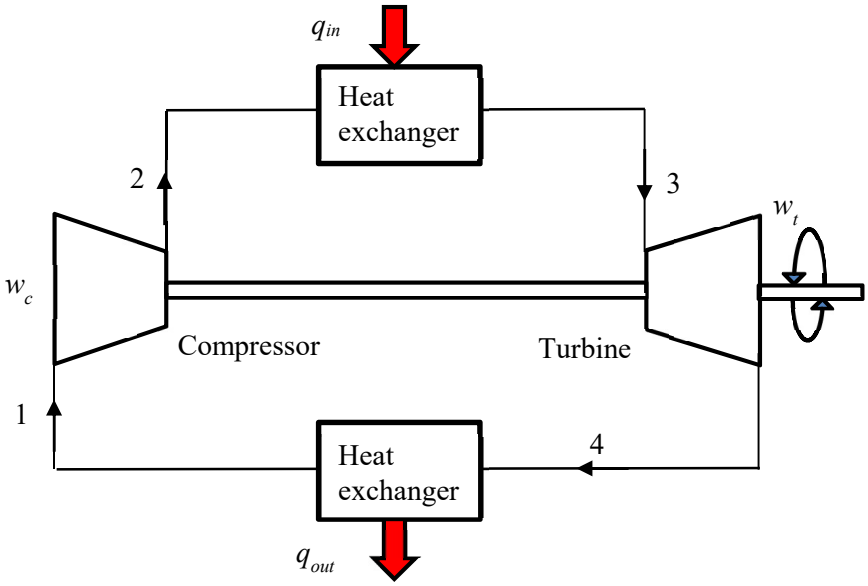

Figure 3.1. Schematic diagram of the closed-cycle gas-turbine

Although the working fluid in the closed cycle can be any suitable gas, in the following analysis it is assumed to be air. Referring to Figure 3.2, the compressor work (w_c) and turbine work (w_t), per unit mass flow rate of the air, are determined from:

$$w_c = (h_2 - h_1) \tag{3.1}$$

$$w_t = (h_3 - h_4) \tag{3.2}$$

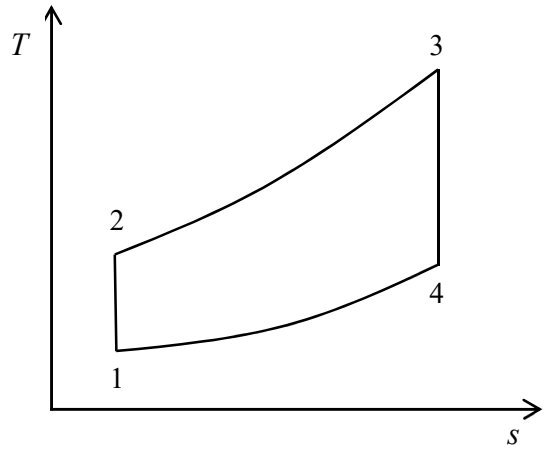

Figure 3.2. *T-s* diagram for the ideal Brayton cycle

Where h_1, h_2, h_3, and h_4 are values of the enthalpy at states, 1, 2, 3, and 4, respectively. The amount of heat addition (q_{in}) per unit mass flow of the air is given by:

$$q_{in} = \left(h_3 - h_2\right) \tag{3.3}$$

Therefore, the net work (w_{net}), back-work ratio (BWR), and thermal efficiency (η) of the cycle are determined from:

$$w_{net} = w_t - w_c \tag{3.4}$$

$$BWR = w_c / w_t \tag{3.5}$$

$$\eta = w_{net} / q_{in} \tag{3.6}$$

Given the compressor's inlet temperature, T_1, and the turbine's inlet temperature, T_3, the discharge temperature from the compressor (T_2) and the discharge temperature from the turbine (T_4) are determined by using the variable specific-heat method of analysis from the corresponding relative pressures P_{r2} and P_{r4} given by:

$$P_{r2} = P_{r1} \times \frac{P_2}{P_1} \tag{3.7}$$

$$P_{r4} = P_{r3} \times \frac{P_4}{P_3} \tag{3.8}$$

Where P_{r1} and P_{r2} are the relative pressures at states 1 and 2, respectively. For the ideal cycle without pressure losses, $P_3 = P_2$ and $P_4 = P_1$. The following example illustrates the procedure for using Thermax property functions for analysing the cycle with Excel. The example is based on Example 9.5 in Cengel and Boles [2].

Example 3.1. Analysis of the simple ideal Brayton cycle

A gas-turbine power plant that operates on an ideal Brayton cycle with air as the working fluid has a pressure ratio of 8. The gas temperature at the compressor inlet is 300 K and at the turbine inlet is 1300 K. Determine (a) the net work per unit mass flow rate of the working fluid, (b) the back work ratio, and (c) the thermal efficiency.

Solution

Figure 3.3 shows the Excel sheet developed for this example using Thermax functions. The figure shows the general layout adopted in this book for sheet arrangement according to which the sheet is divided from left to right into three main parts: (i) Input data, (ii) Intermediate calculations, and (iii) Final results. In the present case, the input data include the given values of the two temperature values at states 1 and 3 (T_1 and T_3) and the pressure ratio (rp). The middle part of the sheet, which is reserved for the calculation of intermediate results, shows the calculated values of the two unknown temperatures T_2 and T_4 and the enthalpy values at the four states in the cycle. The final results are the compressor work (w_c), the turbine work (w_t), the heat input (Q_in), the back work ratio (BWR), and thermal efficiency (η) as shown on the right side of the sheet.

η =(w_t-w_c)/q_in

	A	B	C	D	E	F	G	H	I	J	K	L
1	*Input Data*				*Intermediate calculations*					*Final results*		
2	T_1	300	K	Pr_2	11.06829198		h_1	299.8455		w_c	243.6869	
3												
4	rp	8		T_2	538.1465495		h_2	543.5324		w_t	606.014	
5												
6	T_3	1300	K	Pr_4	41.69167583		h_3	1396.057		q_in	852.5248	
7												
8				T_4	769.2393498		h_4	790.0433		BWR	0.402114	
9												
10										η	0.425005	
11												

Figure 3.3. The Excel sheet developed for Example 3.1

Figure 3.4 shows the formula entered in each cell of the calculations part using Thermax functions. Note that "cell-labelling" has been used in the formulae. Only three Thermax functions from the Gas-group have been used in the Excel model with air as the gas which are: **GasPr_TK**, **GasTK_Pr**, and **Gash_TK**. For the purpose of comparison, a similar Excel sheet was developed by using the IdealGas add-in developed at the University of Alabama [1]. Figure 3.5 shows the Excel sheet and Figure 3.6 reveals the function used in it. Note that the IdealGas functions have the advantage of allowing two systems of

units to be used, but they can only be used for air. By comparison, Thermax functions only use the "SI" system but they can be used for different gases.

=(w_t-w_c)/q_in

	D	E	F	G	H
		Intermediate calculations			
	Pr_2	=GasPr_TK("Air",T_1)*rp		h_1	=Gash_TK("Air",T_1)
	T_2	=GasTK_Pr("Air",Pr_2)		h_2	=Gash_TK("Air",T_2)
	Pr_4	=GasPr_TK("Air",T_3)/rp		h_3	=Gash_TK("Air",T_3)
	T_4	=GasTK_Pr("Air",Pr_4)		h_4	=Gash_TK("Air",T_4)

Figure 3.4. Thermax functions used in the Excel sheet of Example 3.1

η =(w_t-w_c)/q_in

	A	B	C	D	E	F	G	H	I	J	K
1	***Input Data***				***Intermediate calculations***					***Final results***	
2	T_1	300	K	Pr_2	11.01667122		h_1	299.6384		w_c	243.6869
3											
4	rp	8		T_2	538.1465495		h_2	543.3253		w_t	606.014
5											
6	T_3	1300	K	Pr_4	41.49723248		h_3	1395.85		q_in	852.5248
7											
8				T_4	769.2393498		h_4	789.8362		BWR	0.402114
9											
10										η	0.425005
11											

Figure 3.5. Excel sheet for Example 3.1 using the IdealGas add-in

=(w_t-w_c)/q_in

	D	E	F	G	H
		Intermediate calculations			
	Pr_2	= Prel_air(T_1,"si")*rp		h_1	= h_air(T_1,"si")
	T_2	= T_Prel_air(Pr_2,"si")		h_2	= h_air(T_2,"si")
	Pr_4	= Prel_air(T_3,"si")/rp		h_3	= h_air(T_3,"si")
	T_4	= T_Prel_air(Pr_4,"si")		h_4	= h_air(T_4,"si")

Figure 3.6. IdealGas functions used in the Excel sheet of Example 3.1

Table 3.1 shows the values determined by the two property add-ins for the key cycle parameters and their corresponding values given by Cengel and Boles [2]. The figure of

the table shows only minor differences between the values obtained by the property add-ins and those given by Cengel and Boles [2].

Table 3.1. Verification of the two add-ins' results with those of Cengel and Boles [2]

Parameter	Cengel and Boles [2]	Thermax	IdealGas
w_c	244.16	243.69	243.69
w_t	606.60	606.01	606.01
q_{in}	851.62	852.52	852.52
BWR	0.403	0.402	0.402
η	0.426	0.425	0.425

3.2. The regenerative Brayton Cycle

Gas turbines can sustain higher combustion temperatures than those typically met in internal-combustion engines, but the high combustion temperatures lead to high exhaust temperatures as well. By adding a regenerator to the simple gas-turbine system, as shown on Figure 3.7, the energy in the hot exhaust gases that can reach more than 500°C is utilised to preheat the compressed air before it goes to the combustion chamber; a process called *regeneration*. Regeneration reduces the fuel combustion and improves the plant's thermal efficiency, but the cost of the heat-exchanger increases that of the modified system. The economic benefit due to regeneration depends not only on the cost of the heat-exchanger, but also on the system's pressure ratio. While the cost of the heat-exchanger depends on its size and effectiveness, there is a certain value for the pressure ratio that maximises the system's thermal efficiency.

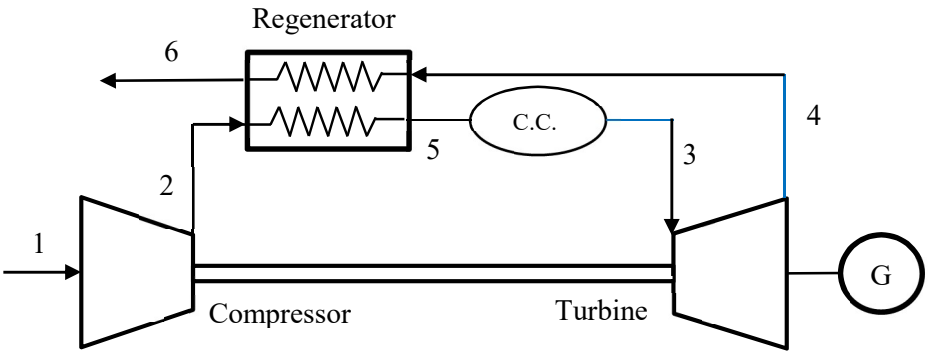

Figure 3.7. Schematic diagram of the regenerative gas-turbine

Figure 3.8 shows the *T-s* diagram for the regenerative Brayton cycle assuming zero pressure losses in the combustion chamber and heat-exchanger. Due to friction losses in both compressor and turbine, the actual exit temperatures from these devices (i.e., T_2 and T_4) are different from the ideal values obtainable by the isentropic compression and expansion processes (T_{2s} and T_{4s}).

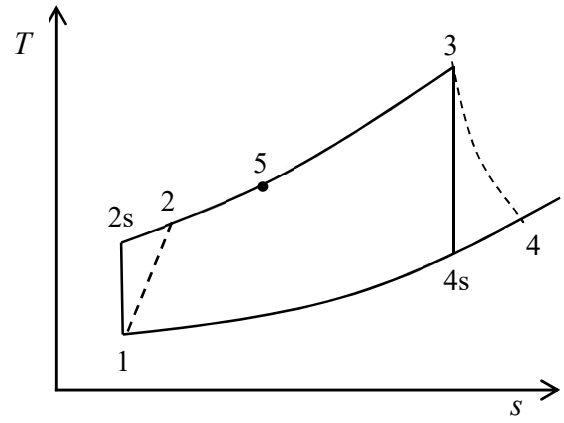

Figure 3.8. *T-s* diagram for the regenerative Brayton cycle

As for the simple Brayton cycle considered earlier, the thermal efficiency (η) is given by:

$$\eta = w_{net} / q_{in} \tag{3.9}$$

Where, w_{net} is the net output work from the plant and q_{in} is its heat input. The net output work for the gas-turbine power plant is the difference between the turbine work output (w_t) and the compressor work input (w_c). Using the numbering scheme of Figures 3.7 and 3.8 to indicate the state of the working fluid entering and leaving the compressor and turbine, the net output work in terms of fluid enthalpies is given by:

$$w_{net} = (h_3 - h_4) - (h_2 - h_1) \tag{3.10}$$

The heat input to the power plant is given by the difference in enthalpies of the combustion gases and the preheated air entering the combustion chamber, i.e.:

$$q_{in} = (h_3 - h_5) \tag{3.11}$$

Given the temperature and pressure of air at the compressor inlet, the ideal relative pressure after the compressor ($P_{r,2s}$) is determined from [2]:

$$P_{r2s} = P_{r1} \frac{P_2}{P_1} = P_{r1}.r_p \tag{3.12}$$

Where, r_p stands for the pressure ratio. P_{r2s} is then used to find T_{2s}, which is the temperature after an ideal isentropic compression process. Once T_{2s} is found, h_{2s} can be determined by using the property function. The actual enthalpy (h_2) is then found from:

$$h_2 = h_1 + (h_{2s} - h_1)/\eta_c \tag{3.13}$$

Where, η_c is the compressor's isentropic efficiency. Similarly, the relative pressure after the expansion process ($P_{r,4s}$) is determined from:

$$P_{r4s} = P_{r3}\frac{P_4}{P_3} = P_{r3} / r_p \tag{3.14}$$

P_{r4s} is then used to find the temperature after an ideal expansion process T_{4s}, from which h_{4s} can be determined. The actual enthalpy (h_4) is then found from:

$$h_4 = h_3 - (h_3 - h_{4s}) \times \eta_t \tag{3.15}$$

Where, η_t is the turbine's isentropic efficiency. The temperature of the compressed air entering the combustion chamber (T_5) and, therefore, the saving in fuel consumption, depends on the effectiveness of the regenerator (ε) which is defined as:

$$\varepsilon = (T_5 - T_2)/(T_4 - T_2) \tag{3.16}$$

Given an estimate for ε, Equation (3.16) can be rearranged to get:

$$T_5 = T_2 + \varepsilon(T_4 - T_2) \tag{3.17}$$

Example 3.2. Analysis of the regenerative Brayton cycle
A gas-turbine power plant operates on a regenerative Brayton cycle with air entering the compressor at 100 kPa, 300 K. Combustion gases leave the combustion chamber at 1400 K. The regenerator effectiveness is 80% and the isentropic efficiency of both the compressor and the turbine is 80%. Determine the pressure ratio that yields the maximum net work output and the maximum thermal efficiency of the plant.

Solution
Figure 3.9 shows the Excel sheet prepared for this example using Thermax functions. The input data shown in the left-side of the sheet includes the air intake temperature (T_1) and pressure (P_1), the pressure ratio (Pratio), and the combustion temperature (T_3). The data part also includes the isentropic efficiency of the compressor (Eff_c), the isentropic efficiency of the turbine (Eff_t), and the regenerator effectiveness (Eff_regen). The middle part of the sheet shows the calculated values of T_2 and T_4. The figure shows the enthalpy values as obtained by using Thermax functions. The formula used in each cell is inserted next to it. The right-side of the sheet shows the main results, which include values of the input compression work, the output expansion work, the net work output, the heat input, and the thermal efficiency.

η =(w_t-w_c)/Q_in

	B	C	D	E	F	G	H	I	J	K	L
1											
2	T_1	300		h_1	299.8455	=Gash_TK("air",T_1)	h_5	890.2033	=h_2+Eff_regen*(h_4-h_2)		
3	P_1	100		Pr_1	1.383536	=GasPr _TK("air",T_1)					
4	Pratio	10		Pr_2s	13.83536	=Pr_1*Pratio	w_c	349.0347	=(h_2-h_1)		
5	T_3	1400		T_2s	572.0764	=GasTK_Pr("air",Pr_2s)	w_t	565.2241	=(h_3-h_4)		
6	Eff_c	0.8		h_2s	579.0732	=Gash _TK("air",T_2s)	w_net	216.1894	=w_t-w_c		
7	Eff_t	0.8		h_2	648.8802	=h_1+(h_2s-h_1)/Eff_c	Q_in	625.5549	=(h_3-h_5)		
8	Eff_regen	0.8		T_2	638.1146	=GasTK_h("air",h_2)	η	0.345596	=(w_t-w_c)/Q_in		
9											
10				h_3	1515.758	=Gash _TK("air",T_3)					
11				Pr_3	454.3223	=GasPr _TK("air",T_3)					
12				Pr_4s	45.43223	=Pr_3/Pratio					
13				T_4s	786.8156	=GasTK_Pr("air",Pr_4s)					
14				h_4s	809.2281	=Gash _TK("air",T_4s)					
15				h_4	950.5341	=h_3-(h_3-h_4s)*Eff_t					
16				T_4	914.5512	=GasTK_h("air",h_4)					
17											

Figure 3.9. The Excel sheet developed for the regenerative Brayton cycle

The sheet shows the results at a pressure ratio of 10 at which the corresponding values of the net output work and thermal efficiency are 216.19 kJ/kg and 0.346, respectively. The value of the pressure-ratio (Pratio) in cell **C4** was changed from 2 to 16 and Figure 3.10 shows the calculated values for the net specific work and thermal efficiency plotted against the pressure ratio. The figure shows that the net output work and thermal efficiency reach their maximum values at different pressure ratios. While the maximum net work output occurs at a pressure ratio of about 8, the maximum thermal efficiency occurs much earlier at a pressure ratio of about 5 or less. Note that exact values of the intermediate pressure that maximise the net wok or thermal efficiency of the cycle can be determined by using the Solver add-in (refer to Exercise 1).

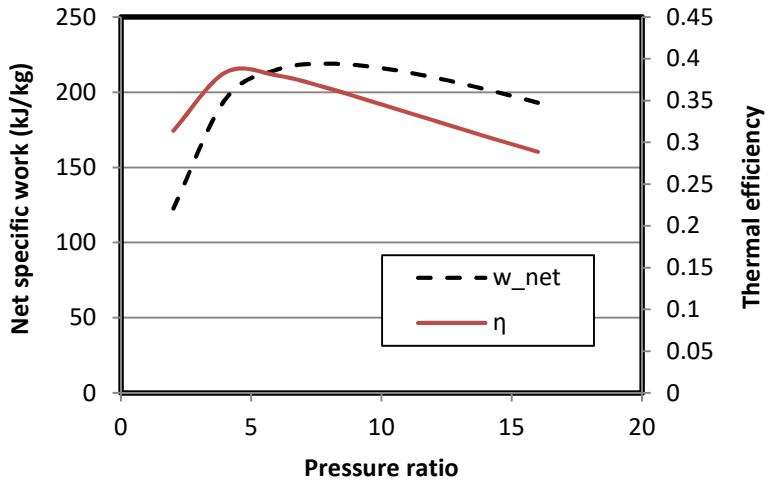

Figure 3.10. Variation of the net specific work and thermal efficiency of the regenerative Brayton cycle with the turbine's pressure ratio

3.3. Energy analysis of the Otto cycle

The Otto cycle and the Diesel cycle are two ideal cycles used for modelling the cycles in internal combustion (I.C.) engines. The Otto cycle is used for modelling spark-ignition I.C. engines, while the Diesel cycle is used for modelling compression-ignition I.C. engines. Both cycles adopt "air-standard" assumptions according to which the working fluid is considered to be air which is treated as an ideal gas. Figure 3.11 shows the four processes that constitute the Otto cycle:

Process 1-2: Adiabatic and reversible compression of air
Process 2-3: Constant-volume heat addition
Process 3-4: Adiabatic and reversible expansion of air
Process 4-1: Constant-volume heat rejection

The *P*-*v* diagram of the Otto cycle is shown on Figure 3.12. Processes 1-2 and 3-4 are isentropic processes because they are both assumed to be adiabatic and reversible.

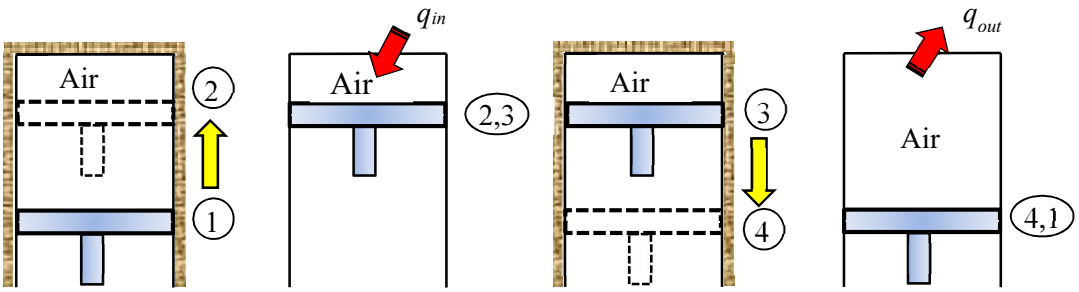

Figure 3.11. The Otto cycle (Adapted from Cengel and Boles [2])

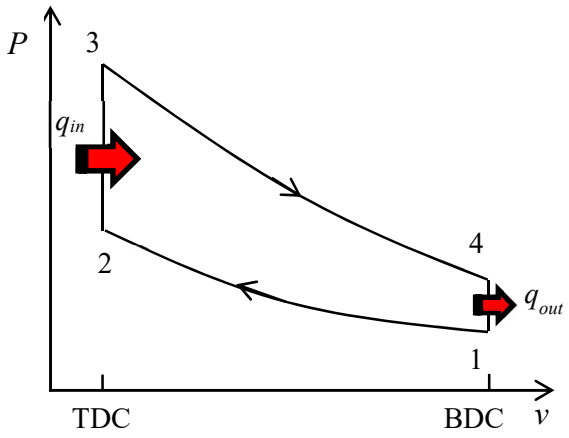

Figure 3.12. *P*-*v* diagram of the Otto cycle (Adapted from Cengel and Boles [2])

The analytical model

The analysis of a cycle that aims to determine its thermal efficiency is called an "energy analysis". For the ideal Otto-cycle shown on Figure 3.12, we have [3]:

$$v_1 = RT_1 / P_1 \tag{3.18}$$

$$v_2 = v_1 / r \tag{3.19}$$

$$v_3 = v_2 \tag{3.20}$$

$$v_4 = v_1 \tag{3.21}$$

Where, R is the gas constant (for air R= 0.287 kJ/kg.K) and r is the compression ratio of the cycle (for modern spark-ignition engines $8 \leq r \leq 11$). Applying the variable specific heat method for or the isentropic compression and expansion processes:

$$\frac{v_{r2}}{v_{r1}} = \frac{v_2}{v_1} = 1/r \tag{3.22}$$

$$\frac{v_{r4}}{v_{r3}} = \frac{v_4}{v_3} = r \tag{3.23}$$

Where, v_r is the relative specific volume. The last two relationships can be used to determine the two temperatures after the compression and expansion processes. The amount of heat added in process 2-3 per kg of the working fluid (q_{in}) is calculated from:

$$q_{in} = \left(u_3 - u_2\right) \tag{3.24}$$

The amount of heat removed per kg of the working fluid (q_{in}) is calculated from:

$$q_{out} = \left(u_4 - u_1\right) \tag{3.25}$$

Applying the first-law of thermodynamics, the net work from the cycle is given by:

$$w_{net} = q_{in} - q_{out} \tag{3.26}$$

Therefore, the thermal efficiency of the Ott cycle (η_{Otto}) is given by:

$$\eta_{Otto} = \frac{w_{net}}{q_{in}} \tag{3.27}$$

The cycle's mean-effective pressure (MEP) is defined as:

$$MEP = \frac{w_{net}}{v_{\max} - v_{\min}} = \frac{w_{net}}{v_1 - v_2} \tag{3.28}$$

Although the above analytical model is based on the usual air-standard assumptions, by adopting the variable specific-heat method it yields more realistic results than those obtainable by adopting the approximate constant specific heat method (refer to Example 2.1). The following example shows how the property functions provided by Thermax and IdealGas [1] can be used to be used for its application.

Example 3.3. Energy analysis of the Otto cycle
An ideal Otto cycle has a compression ratio of 8. At the beginning of the compression process, air is at 100 kPa and 17°C. During the constant-volume heat-addition process, 800 kJ/kg of heat is transferred to air. Accounting for the variation of specific heats of air with temperature, conduct an energy analysis of the cycle to determine:

(i) the net work output and thermal efficiency,
(ii) the mean effective pressure for the cycle.

This example is based on Examples 9-2 in Cengel and Boles [2].

Solution
Figures 3.13 and 3.14 show the Excel sheets developed for analysing the Otto cycle by using property functions for ideal gases provided by Thermax and IdealGAs, respectively. The sheets show the formulae used in the calculation parts and the formula window in each sheet reveals the formula used for calculating the mean effective pressure according to Equation (3.28). Since the IdealGas add-in does not provide a function for determining the gas temperature from its internal energy, the temperature T_3 on Figure 3.14 has been found by using the Goal-Seek command of Excel. Table 3.2 compares the values obtained by the two add-ins to those given by Cengel and Boles [2]. The figures in the table show good agreement between the three solutions.

MEP =w_net/(v_1-v_2)

	B	C	D	E	F	G	H	I	J	K	L
1	**Energy analysis**										
2	rc	8		v_1	0.8323	=R_air*T_1/P_1	u_3	1273.92	=u_2+Q_in	q_out	381.912
3	T_1	290	K	u_1	206.516	=gasu_TK("air",T_1)	T_3	1572.59	=gasTK_u("air",u_3)		
4	P_1	100	kPa	vr_1	676.064	=gasvr_TK("air",T_1)	P_3	4338.19	=(T_3/T_2)*P_2	w_net	**418.088**
5	Q_in	800	kJ/kg	vr_2	84.508	=vr_1/rc_	vr_3	6.06462	=gasvr_TK("air",T_3)		
6				T_2	648.727	=GasTK_vr("air",vr_2)	vr_4	48.5169	=vr_3*rc_	η_I	**0.52261**
7	R_air	0.287		u_2	473.924	=gasu_TK("air",T_2)	T_4	793.117	=GasTK_vr("air",vr_4)		
8				P_2	1789.59	=(T_2/T_1)*rc_*P_1	u_4	588.427	=gasu_TK("air",T_4)	MEP	**574.09**
9				v_2	0.10404	=R_air*T_2/P_2	v_4	0.8323	=v_1		
10											

Figure 3.13. Excel sheet developed for Example 3.3

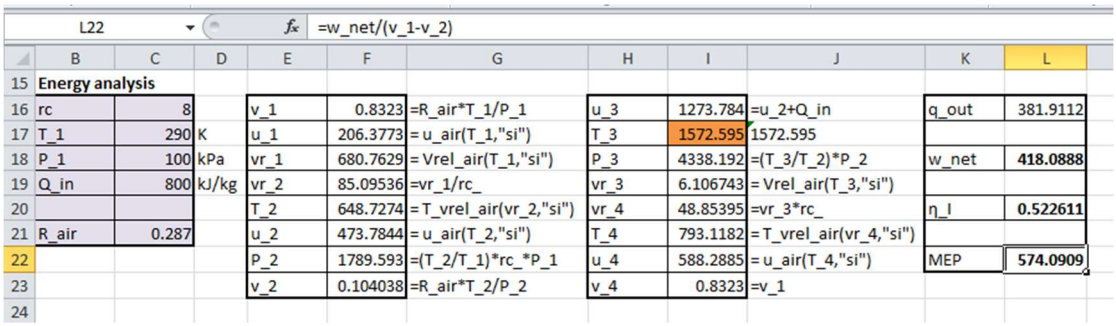

L22 fx =w_net/(v_1-v_2)

	B	C	D	E	F	G	H	I	J	K	L
15	**Energy analysis**										
16	rc	8		v_1	0.8323	=R_air*T_1/P_1	u_3	1273.784	=u_2+Q_in	q_out	381.9112
17	T_1	290	K	u_1	206.3773	= u_air(T_1,"si")	T_3	1572.595	1572.595		
18	P_1	100	kPa	vr_1	680.7629	= Vrel_air(T_1,"si")	P_3	4338.192	=(T_3/T_2)*P_2	w_net	**418.0888**
19	Q_in	800	kJ/kg	vr_2	85.09536	=vr_1/rc_	vr_3	6.106743	= Vrel_air(T_3,"si")		
20				T_2	648.7274	= T_vrel_air(vr_2,"si")	vr_4	48.85395	=vr_3*rc_	η_I	**0.522611**
21	R_air	0.287		u_2	473.7844	= u_air(T_2,"si")	T_4	793.1182	= T_vrel_air(vr_4,"si")		
22				P_2	1789.593	=(T_2/T_1)*rc_*P_1	u_4	588.2885	= u_air(T_4,"si")	MEP	**574.0909**
23				v_2	0.104038	=R_air*T_2/P_2	v_4	0.8323	=v_1		
24											

Figure 3.14. Excel sheet developed for Example 3.3 using the IdealGas add-in

Table 3.2. Key parameters in the energy analysis

Parameter	Cengel and Boles [2]	Thermax	IdealGas
T_2	652.4	648.7	648.7
T_3	1575.1	1572.6	1572.6
T_4	795.6	793.1	793.1
P_2	1799.7	1789.6	1789.6
P_3	4345.0	4338.2	4338.2
q_{out}	381.83	381.91	381.91
w_{net}	418.17	418.09	418.09
η_{Otto}	0.523	0.523	0.523
MEP	574.0	574.1	574.1

Using the approximate method of analysis with fixed values of the specific heat, it can be shown that the thermal efficiency of the Otto cycle is given by [3]:

$$\eta_{otto} = 1 - (1/r_c)^{k-1} \tag{3.29}$$

Where, k is the ratio of specific heats c_p/c_v for air. Substituting $r_c = 8$ and $k = 1.4$ in Equation (3.29), the calculated thermal efficiency is 0.565. It should be noted that values of the thermal efficiency obtained by the exact and the approximate methods are both exaggerated compared to that of actual engines, but that of the variable specific heat method, which is 0.523, is less inaccurate.

3.4. Exergy analysis of the Otto cycle

Energy analyses, such as those presented in the previous sections, evaluate the general performance of energy-conversion systems using overall performance indicators such as the thermal efficiency for power-producing systems and the coefficient of performance (COP) for refrigeration systems. By comparison, *exergy* analyses which are based on the second-law of thermodynamics enable the locations, types, and true magnitudes of waste and loss to be determined. Therefore, exergy analyses can be used in design analyses of thermofluid systems to further the goal of achieving more efficient use of resources [4].

The analytical model

Exergy (ϕ) is a thermodynamic property that measures the ability of the working fluid to do useful work. Per unit mass in a closed system like that of the engine shown on Figure 3.11, exergy is given by [2]:

$$\phi = (u - u_0) - T_0(s - s_0) + P_o(v - v_0) + \frac{V^2}{2} + gz \tag{3.30}$$

Where u is the internal energy and u_0, s_0, and P_0, respectively, refer to the values of the internal energy, entropy and pressure at the dead state which is the surroundings. Neglecting changes in the kinetic and potential energies, and taking into consideration that $v_3 = v_2$ in this case, the exergy input in process 2-3 is determined from:

$$\phi_{input} = (\phi_3 - \phi_2) = (u_3 - u_2) - T_0(s_3 - s_2) \tag{3.31}$$

Exergy of the working fluid can be destroyed in a process because of irreversibilities such as friction losses and heat-transfer over a finite-temperature difference. In general, the exergy destruction (x_{dest}) in a process is determined from:

$$\begin{aligned} x_{dest} &= T_0 s_{gen} = T_0(\Delta s_{sys} - s_{in} + s_{out}) \\ &= T_0\left((s_2 - s_1)_{sys} - \frac{q_{in}}{T_{b,in}} + \frac{q_{out}}{T_{b,out}}\right) \end{aligned} \tag{3.32}$$

Where, s_{gen} refers to the entropy generated in the process. In the Otto cycle, the processes 1-2 and 3-4 are both adiabatic and reversible. Therefore, for these two processes:

$$x_{dest} = 0 \tag{3.33}$$

However, the processes 2-3 and 4-1 both involve heat transfer with the surroundings and that makes them externally irreversible processes. While process 2-3 involves heat addition only, process 4-1 involves heat rejection only. For these two processes, exergy destructions are obtained from:

$$x_{dest} = T_0\left((s_3 - s_2) - \frac{q_{in}}{T_H}\right) \qquad \text{Process 2-3} \tag{3.34}$$

$$x_{dest} = T_0\left((s_1 - s_4) + \frac{q_{out}}{T_L}\right) \qquad \text{Process 4-1} \tag{3.35}$$

The exergy destruction of the whole Otto cycle is the sum of the exergy destructions in the heat-addition and heat-rejection processes. Since $s_2 = s_1$ and $s_4 = s_3$, the exergy destruction in the cycle becomes:

$$x_{dest} = T_0\left(\frac{q_{out}}{T_L} - \frac{q_{in}}{T_H}\right) \tag{3.36}$$

This following example, which is based on Example 9-10 in Cengel and Boles [2], verifies the relevant Thermax functions by comparing their calculations for the exergy analysis with those given by Cengel and Boles [2].

Example 3.4. Exergy analyses of the Otto cycle
Accounting for the variation of specific heats of air with temperature, conduct an exergy analysis for the Otto cycle considered in Example 3.3 to determine:

(i) the exergy destruction associated with the Otto cycle (all four processes as well as the cycle), assuming that heat is transferred to the working fluid from a source at 1700 K and heat is rejected to the surroundings at 290 K, and
(ii) the exergy of the exhaust gases when they are purged.

Solution
The two Excel sheets developed for Example 3.3 were extended for this exergy analysis and Figure 3.15 shows the extension that is needed in the lower part of the sheet using Thermax functions. Table 3.3 shows the functions used in this extension. The sheet using the IdealGas add-in was extended in a similar way. The additional data needed for exergy analysis include the temperature and pressure of the surroundings, temperature of the heat source, and the sink temperature. By obtaining the required entropy values at the different states from the energy part, the two sheets determine the exergy destructions in the four processes of the cycle, the total exergy destruction, and the exergy lost in the heat-rejection process. Table 3.4 compares the calculated values to those given by Cengel and Boles [2]. The figures in the table show a good agreement between the results of the two add-ins and those given by Cengel and Boles [2].

25								
26	**Exergy analysis**							
27	T_0	290	Ed_12	0		Ed_cycle	245.441	kJ/kg
28	P_0	100	Ed_34	0				
29						v_0	0.8323	
30	T_source	1700	Dels23	-0.75607		u_0	206.5157	
31	T_sink	290	Ed_23	82.78839	kJ/kg	Dels40	0.756065	
32								
33			Dels14	-0.75607		E_4	162.6526	kJ/kg
34			Ed_41	162.6526	kJ/kg			
35								

Figure 3.15. Excel sheet developed for Example 3.4 using Thermax functions

Table 3.3. Thermax functions used in exergy analysis of the Otto cycle

Cell	Cell name	Formula
F30	Dels23	=Gass0_TK("air",T_2)-Gass0_TK("air",T_3)-R_air*LN(P_2/P_3)
F31	Ed_23	=T_0*(-Dels23-Q_in/T_source)
F33	Dels14	=Dels23
F34	Ed_14	=T_0*(Dels14+q_out/T_sink)
I27	Ed_cycle	=Ed_23+Ed_41
I29	v_0	=v_1
I30	u_0	=Gasu_TK("air",T_0)
I31	Dels40	=-Dels14
I33	E_4	=(u_4-u_0)-T_0*Dels40-P_0*(v_4-v_0)

Table 3.4. Results of the Otto cycle exergy analysis

	Cengel and Boles [2]	Thermax	IdealGas
$x_{dest,2-3}$	82.2	82.8	82.79
$x_{dest,4-1}$	163.2	162.7	162.65
$x_{dest,Otto}$	245.4	245.4	245.44
ϕ_4	163.2	162.6	162.65

The figures in Table 3.4 show that two thirds of the total exergy supplied to the engine is lost during the heat-rejection process. Therefore, any design efforts that aim to minimise the loss of exergy in the heat-rejection process can effectively improve the performance of the Otto cycle. For example, the lost exergy can be used in a cogeneration system that utilises the heat for producing steam for industrial applications or for air-conditioning purposes. The figures in Table 3.4 also show that the exergy destruction in the heat-addition process are about one third of the total exergy destruction. While increasing the heat-addition temperature will improve the thermal efficiency of the cycle, it will increase the rate of exergy destruction in this process. Therefore, this temperature requires a careful consideration of the two factors among other practical considerations.

3.5. Closure

This chapter illustrates the use of Thermax property functions for the analyses of two basic gas power cycles. With respect to such cycles, property functions in the "Gas" group enable the exact variable specific-heat method to be used instead of the approximate constant-specific heat method. Both the simple and the regenerative Brayton cycles are analysed, while both energy and exergy analyses of the Otto cycle are presented. The various analyses show that the functions provided by Thermax give identical results to those given by the IdealGas add-in [1]. Thermax provides additional functions not provided by IdealGas such as the **GasTK_u** and **GasTK_h** functions that determine the temperature from a given value of internal energy or enthalpy, respectively.

References

[1] The University of Alabama, Mechanical Engineering, Excel for Mechanical Engineering project, Internet: http://www.me.ua.edu/excelinme/index.htm (Last accessed July 19, 2018)

[2] Y. A. Cengel and M. A. Boles. *Thermodynamics an Engineering Approach*, McGraw-Hill, 8th Edition, 2015

[3] W.W. Pulkrabek, Engineering Fundamentals of the Internal Combustion Engine, Second Edition, Pearson Prentice Hall, 2004.

[4] A. Bejan, G. Tsatsaronis, M. Moran, Thermal Design & Optimization, John Wiley $ Sons, 1996.

[5] M.J. Moran and H.N. Shapiro, *Fundamentals of Engineering Thermodynamics*, 5th edition, John Wiley, & Sons. Inc. 2006

Exercises

1. Figure 3.10 shows that the net output work and thermal efficiency of the regenerative Brayton cycle reach their maximum values at different pressure ratios; which is about 8 for the maximum net work output and about 5 or less for the maximum thermal efficiency. Use Solver to determine the exact values of the two optimum pressure ratios.
2. A regenerative gas turbine with intercooling and reheat operates at steady state. Air enters the compressor at 100 kPa, 300 K with a mass flow rate of 5.8 kg/s. The pressure ratio across the two-stage compressor is 10. The pressure ratio across the two-stage turbine is also 10. The intercooler and reheater each operate at 300 kPa. At the inlets to the turbine stages, the temperature is 1400 K. The temperature at the inlet to the second compressor stage is 300 K. The isentropic efficiency of each compressor and turbine stage is 80%. The regenerator effectiveness is 80%. Figure 3.P2 shows the *T-s* diagram of the regenerative gas turbine cycle.

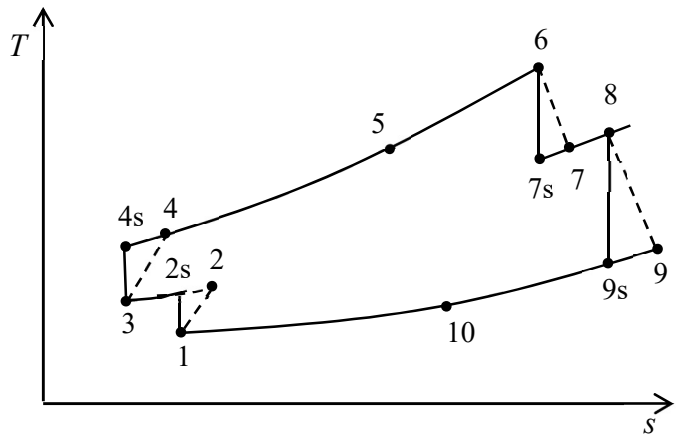

Figure 3.P2. *T-s* diagram for the regenerative gas turbine with intercooling

Develop an Excel sheet to determine: **(a)** the thermal efficiency, **(b)** the back work ratio, **(c)** the net power developed, in kW. Compare your solution with that of Example 9.11 in Moran and Shapiro [5].

3. The air-standard Diesel cycle shown on Figure 3.P3 operates with a compression ratio of 18. At the beginning of the compression process the temperature is 300 K and the pressure is 0.1 MPa. The cutoff ratio for the cycle is 2. Using Thermax or any other property add-in, develop and Excel sheet to determine (a) the temperature and pressure at the end of each process of the cycle, (b) the thermal efficiency, (c) the mean effective pressure, in MPa. Compare your solution with that of Example 9.2 in Moran and Shapiro [5].

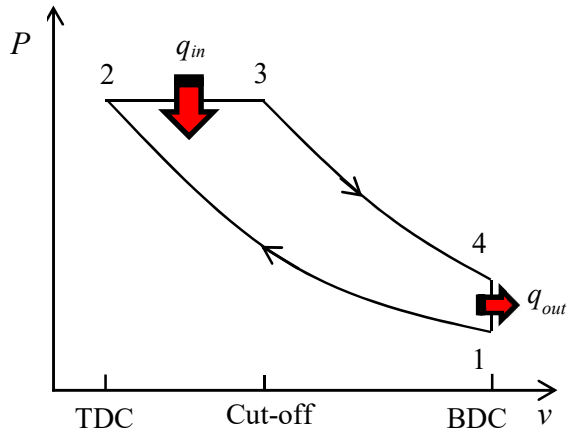

Figure 3.P3. *P-v* diagram of the Diesel cycle

Chapter 4

Analyses of vapour and combined power cycles

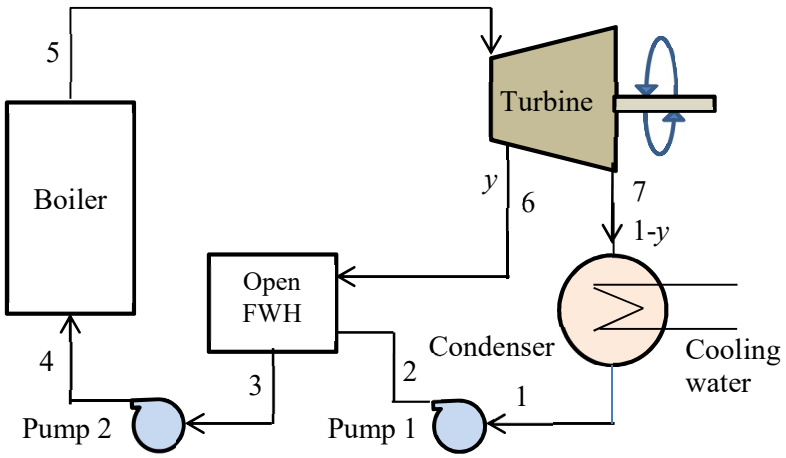

Thermax property functions enable Excel to be used for analysing various vapour and combined power cycles. This chapter illustrates their use for analysing the simple Rankine cycle, Rankine cycle with superheat and reheat, the regenerative Rankine cycle with one and two feed-water heaters, and the combined Brayton-Rankine cycle. The results obtained for the key parameters of these cycles are verified against the relevant values given by standard textbooks. The chapter also illustrates the use of the functions for analysing the simple organic Rankine cycle using different working fluids.

4.1. The ideal simple Rankine cycle

The Rankine cycle is the ideal cycle for steam-turbine power plants. The basic plant shown on Figure 4.1 consists of four components: a boiler, a turbine, a condenser, and a pump. The working fluid, which is water, is pumped at a low temperature to the boiler where it is heated to become saturated steam. The high-pressure steam is then taken to the turbine where it expands to produce work. The steam is completely condensed in the condenser before being pumped back to the boiler. Cooling water removes the heat rejected in the condenser. Figure 4.2 shows the *T-s* diagram for the ideal cycle.

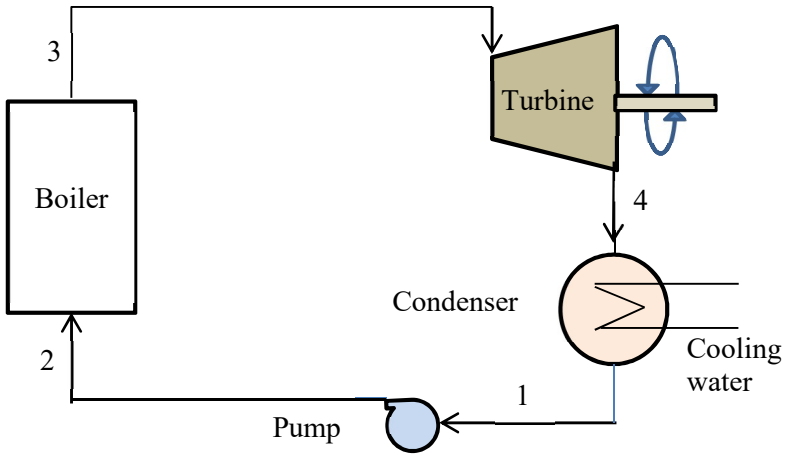

Figure 4.1. Schematic diagram of a simple steam-turbine power plant

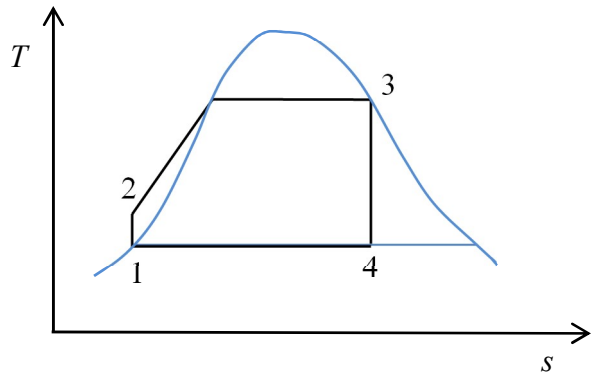

Figure 4.2. *T-s* diagram for the ideal simple Rankine cycle

The pump-work (w_p), turbine-work (w_t), rate of heat addition in the boiler (q_{in}), and rate of heat rejection in the condenser (q_{out}) per unit mass flow of the working fluid are given by:

$$w_p = (h_2 - h_1) \tag{4.1}$$

$$w_t = (h_3 - h_4) \tag{4.2}$$

$$q_{in} = (h_3 - h_2) \tag{4.3}$$

$$q_{out} = (h_4 - h_1) \tag{4.4}$$

Where h_1, h_2, h_3, and h_4 are enthalpy values of the working fluid at the four states indicated on Figures 4.1 and 4.2. The two enthalpy values h_1 and h_3 can be obtained directly from the given pressures by using the relevant Thermax functions, but h_2 and h_4 have to be calculated from:

$$h_2 = h_1 + v_1(P_2 - P_1) \tag{4.5}$$

$$h_4 = h_1 + x_4 h_{fg,P1} \tag{4.6}$$

Where v_1 is the specific volume of saturated liquid water at the condenser pressure, x_4 is the quality at point 4, and $h_{fg,P1}$ is the enthalpy of vaporisation (the difference between the specific enthalpy of saturated steam and saturated liquid water) at the condenser pressure P_1. The quality x_4 is determined from:

$$x_4 = \frac{s_4 - s_1}{s_{fg,P1}} \tag{4.7}$$

Where s_1 and s_4 are the specific entropy values at points 1 and 4, respectively, and $s_{fg,P1}$ is the difference between the specific entropy of saturated steam and saturated liquid water at the condenser pressure P_1. Note that $s_4 = s_3 = s_{g,P2}$.

Once enthalpy values at the states 1 to 4 are determined, and the values of w_p, w_t, q_{in}, and q_{out} are calculated, the different cycle parameters can be calculated as follows:

(a) The thermal efficiency (η):

$$\eta = (w_t - w_p) / q_{in} \tag{4.8}$$

(b) The back work ratio (BWR):

$$BWR = w_p / w_t \tag{4.9}$$

(c) The mass flow rate of the steam (kg/h):

$$\dot{m} = \frac{\dot{W} \times 1000 \times 3600}{(w_t - w_p)} \tag{4.10}$$

Where $\dot{W}$ is the net power of the plant in MW.

(d) The rate of heat transfer in the boiler, ($\dot{Q}_{boiler}$), into the working, in MW:

$$\dot{Q}_{boiler} = \dot{m} q_{in} / 3600 \tag{4.11}$$

(e) The rate of heat transfer from the condenser ($\dot{Q}_{condenser}$), in MW:

$$\dot{Q}_{condenser} = \dot{m} q_{out} / 3600 \tag{4.12}$$

(f) The mass flow rate of the cooling water in kg/h:

$$\dot{m}_{cw} = \frac{\dot{Q}_{out} \times 1000 \times 3600}{(h_{cw,o} - h_{cw,i})} \tag{4.13}$$

Where $h_{cw,i}$ and $h_{cw,o}$ are the enthalpy values of the cooling water entering and exiting the condenser, which are approximated with those of saturated water at the relevant temperatures. The following example, which is based on Example 8.1 in Moran and Shapiro [1], shows how the cycle can be analysed with Thermax property functions.

Example 4.1. Analysis of the simple and ideal Rankine cycle
A steam-turbine power plant that operates on the ideal Rankine cycle has a net power output of 100 MW. Saturated steam enters the turbine at 8.0 MPa and saturated water exits the condenser at 8 kPa. Determine (a) the thermal efficiency of the cycle, (b) the back work ratio, (c) the mass flow rate of the steam, in kg/h, (d) the rate of heat transfer, Q_{in}, into the working fluid as it passes through the boiler, in MW, (e) the rate of heat transfer, Q_{out}, from the condensing steam as it passes through the condenser, in MW, (f) the mass flow rate of the condenser cooling water, in kg/h, if cooling water enters the condenser at 15°C and exits at 35°C. Also, study the effect of increasing the condenser pressure from 8 to 20 kPa on the thermal efficiency, mass-flow rate of the steam, and mass-flow rate of the cooling water.
Solution

The Excel sheet developed for this example is shown on Figure 4.3. The left side of the sheet stores the given data which include the condenser pressure (P_1), the boiler pressure (P_2), the power of the cycle (Power), the temperature of the cooling water entering the condenser (T_cwi), and the temperature of the cooling water leaving the condenser (T_cwo). The central part of the sheet performs the intermediate calculations that determine the values of enthalpy at the four states in the cycle. Table 4.1 shows the formulae used in these calculations with the various property functions provided by Thermax. For example, the enthalpy at point 1 (h_1), which equals the enthalpy of saturated liquid water at the condenser pressure, is obtained by using the add-in function **Wath_Px** with the two input parameters being the condenser pressure and the quality x =0.

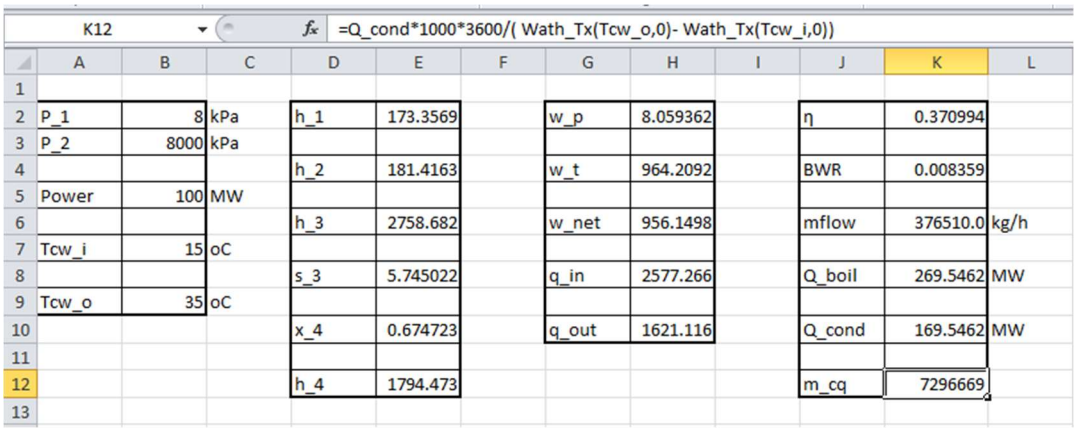

Figure 4.3. The Excel sheet developed for Example 4.1

Table 4.1. Excel formulae with Thermax functions in the sheet of Example 4.1

Cell	Parameter	Excel formula
E2	h_1	=Wath_Px(P_1,0.0)
E4	h_2	=h_1+Watv_Px(P_1,0.0)*(P_2-P_1)
E6	h_3	=Wath_Px(P_2,1.0)
E8	s_3	=Wats_Px(P_2,1.0)
E10	x_4	=(s_3-Wats_Px(P_1,0.0))/(Wats_Px(P_1,1.0) - Wats_Px(P_1,0.0))
E12	h_4	=h_1+x_4*(Wath_Px(P_1,1.0) - Wath_Px(P_1,0.0))

The cells H2 to H10 calculate the values of the pump-work (w_p), the turbine-work (w_t), the net work (w_net = w_t – w_p), the rate of heat addition in the boiler (q_in), and rate of heat rejection in the condenser (q_out). The final results given in the right-side of the sheet include the thermal efficiency (η), the back-work ratio (BWR), the rate of heat addition in the boiler (Q_boil), the rate of heat rejection in the condenser (Q_cond), and the mass flow rate of the cooling water (m_cw). The formula bar in Figure 4.3 reveals the formula in the cell K12 that calculates the mass flow rate of the cooling water from Equation (4.13). Note that the thermal efficiency is 37.1% and x_4 is 0.675.

Table 4.2 compares the values obtained by Thermax functions and those given by Moran and Shapiro [1] for the cycle parameters in the question. The figures show close agreements between the two results.

Table 4.2. Verification of Thermax results for Example 4.1

	Parameter	Moran and Shapiro [1]	Thermax	Deviation (%)
(a)	η	0.371	0.3709	-0.189
(b)	BWR	0.0084	0.0084	0
(c)	$\dot{m}$ (kg/h)	3.77×10^5	3.77×10^5	0.265
(d)	Q_{boiler} (MW)	269.77	269.546	-0.083
(e)	$Q_{condenser}$ (MW)	169.75	169.546	-0.120
(f)	$\dot{m}_{cw}$ (kg/h)	7.3×10^6	7.3×10^6	0

The Excel sheet was used to analyse the effect of increasing condenser pressure on the cycle's efficiency, mass flow rate of the steam and mass flow rate of the cooling water. The resulting percentage changes of the three parameters are shown on Figure 4.4. The figure shows that the thermal efficiency decreases by nearly 6%, while the mass flow rates of both the steam and the cooling water increase by more than 10%.

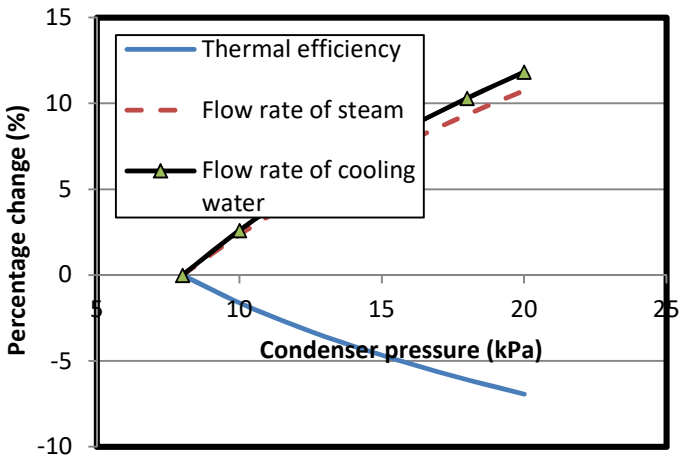

Figure 4.4. Effect of increasing the condenser pressure on the cycle's efficiency, mass flow rate of the steam, and mass flow rate of the cooling water

4.2. The Rankine cycle with superheat and reheat

The thermal efficiency of the simple Rankine cycle can be improved by increasing the boiler pressure and/or reducing the condenser pressure. However, both of these changes increase the wetness fraction of the steam in the last stages of the turbine and may cause erosion of the turbine blades in these stages. This problem can be solved by superheating and/or reheating the steam. Figure 4.5 shows the schematic diagram of a steam-turbine

power plant with super-heating and reheating. Compared to the simple Rankine cycle considered in Example 4.1, this cycle allows lower condenser pressures without exceeding the maximum allowable wetness fraction in the last stages of the low-pressure turbine. Figure 4.6 shows the *T-s* diagram for the cycle.

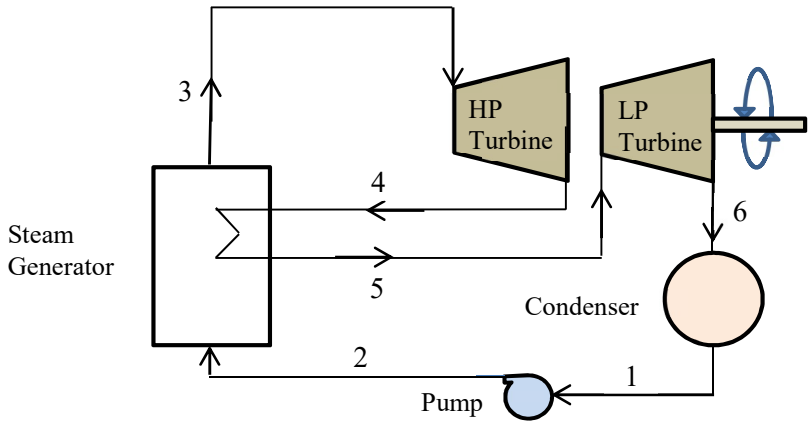

Figure 4.5. Schematic diagram of a steam-turbine power plant with superheating and reheating

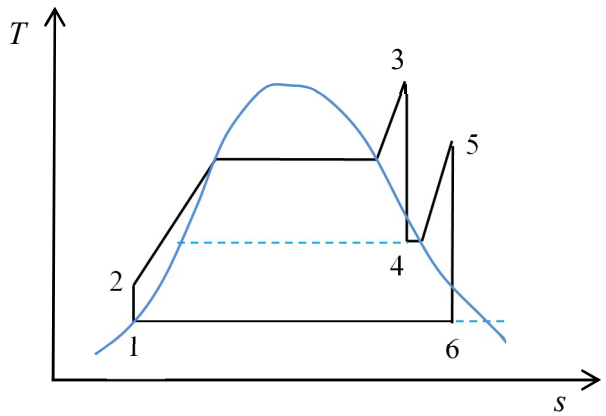

Figure 4.6. *T-s* diagram for the ideal reheat cycle

Since there are two stages of heat addition and two stages of expansion, the relevant equations for the total turbine-work output (w_{out}) and heat-addition (q_{in}) become:

$$w_{out} = \left[\left(h_3 - h_4\right) + \left(h_5 - h_6\right)\right] \tag{4.14}$$

$$q_{in} = \left[\left(h_3 - h_2\right) + \left(h_5 - h_4\right)\right] \tag{4.15}$$

Therefore, the net work-output and thermal efficiency of the cycle are given by:

$$w_{net} = w_{out} - w_{in} \tag{4.16}$$

$$\eta = w_{net} / q_{in} \tag{4.17}$$

Where w_{in} is the pump work input given by:

$$w_{in} = (h_2 - h_1) \tag{4.18}$$

The mass flow rate of steam, $\dot{m}$, in kg per hour, is obtained from the total net power of the plant, $\dot{W}$ in MW, as follows:

$$\dot{m} = \frac{\dot{W} \times 1000 \times 3600}{w_{net}} \tag{4.19}$$

The following example that shows how the superheated and reheated Rankine cycle can be analysed by using Thermax is based on Example 8.3 in Moran and Shapiro [1].

Example 4.2. Analysis of an ideal reheat Rankine cycle
A power plant working on an ideal Rankine cycle with superheat and reheat uses steam as the working fluid to produce a net power output of 100 MW. Superheated steam enters the first-stage turbine at 8.0 MPa, 480°C, where it expands to 0.7 MPa. It is then reheated to 440°C before entering the second-stage turbine and expanding to the condenser pressure of 0.008 MPa. Determine:

(a) the thermal efficiency of the cycle,
(b) the mass flow rate of steam, in kg/h,
(c) the rate of heat transfer from the condensing steam as it passes through the condenser, in MW.

Solution
Figure 4.7 shows the Excel sheet developed for this example. Based on the given data shown on the left side of the sheet, Thermax property functions determine the enthalpy (h), entropy (s), or quality (x) at the six fluid states in the cycle. The enthalpy values at the different states are then used to determine the work and heat interactions according to Equations (4.14) and (4.15). Table 4.3 shows the formulae and Thermax property functions used in the determination of enthalpy and entropy or quality at each state point and the values calculated by Thermax functions for the state and overall cycle parameters. It appears from the table figures that all the values calculated by the present model deviate from those given by Moran and Shapiro [1] by less than 1%.

This example reveals three advantage of the Rankine cycle with superheating and reheating over the simple cycle considered in Example 4.1 that operates between the same

upper and lower pressure levels of 8 MPa and 8 kPa, respectively. The first advantage is that the thermal efficiency of this cycle is 40.5%, while that of the simple cycle is only 37%. The second advantage of the cycle with superheating and reheating is the lower moisture content in the last stages of the low-pressure turbine; which reduces the possibility of turbine's blade erosion. This is indicated by the higher value of the quality at state 6, $x_6 = 0.939$, compared to the corresponding value in the simple cycle, $x_4 = 0.675$. The third important advantage is that the mass flow rate in the cycle with superheating and reheating is lower than that of the simple cycle; which reduces the cost of the boiler and other components in the power plant.

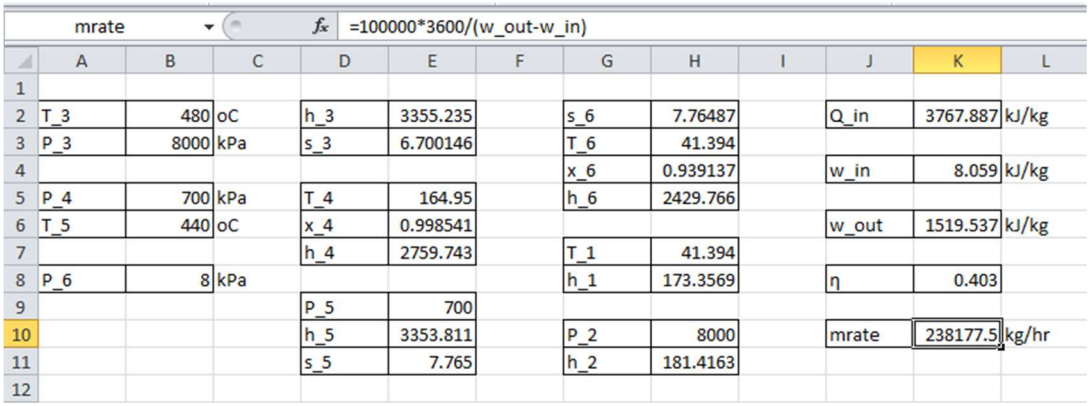

Figure 4.7. Excel sheet developed for the analysis of the reheat Rankine cycle

Table 4.3. Verification of Thermax results for Example 4.2

Name	Excel formula with Thermax functions	Moran & Shapiro [1]	Thermax	Deviation (%)
h_1	=Wath_Tx(T_1,x_1)	173.88	173.3569	-0.301
h_2	=h_1+Watv_Tx(T_1,x1)*(P_2-P_6)	181.94	181.4163	-0.288
h_3	=Wath_pT(P_3,T_3)	3348.4	3355.235	0.2041
s_3	=Wats_pT(P_3,T_3)	6.6586	6.7001	0.6233
x_4	=(s_3-Wats_Tx(T_4,x_4))/Watsfg_T(T_4) *	0.9895	0.9985	0.9096
h_4	=Wath_Tx(T_4,0.0)+x_4*Wathfg_T(T_4) *	2741.8	2759.743	0.6544
h_5	=Wath_pT(P_5,T_5)	3353.3	3353.811	0.0152
s_5	=Wats_pT(P_5,T_5)	7.757	7.765	0.1031
x_6	=(s_6-Wats_Tx(T_6,0.0))/Watsfg_T(T_6) *	0.9382	0.939	0.0853
h_6	=Wath_Tx(T_6,0.0)+x_6*Wathfg_T(T_6) *	2428.5	2429.766	0.0521
η	=w_out/Q_in	0.403	0.403	0

* **Watsfg_T** and **Wathfg_T** return the entropy change and enthalpy of vaporisation for saturated water at the given temperature, respectively. These two functions are not listed in Tables 2.3.

4.3. Regenerative Rankine cycle with a single open feed-water heater

Regeneration in a Rankine cycle refers to the process of preheating the feed-water by the energy of steam that is extracted from the turbine at an intermediate pressure. Regeneration reduces the mass flow rate through the turbine and the work output of the turbine, but improves the thermal efficiency. Figure 4.8 shows a steam-turbine power plant that has a single open feed-water heater (FWH). Heat exchange between the bled steam and the condensate can also take place in a single closed FWH or in multiple open and closed FWHs. Figure 4.9 shows the *T-s* diagram for the system shown on Figure 4.8.

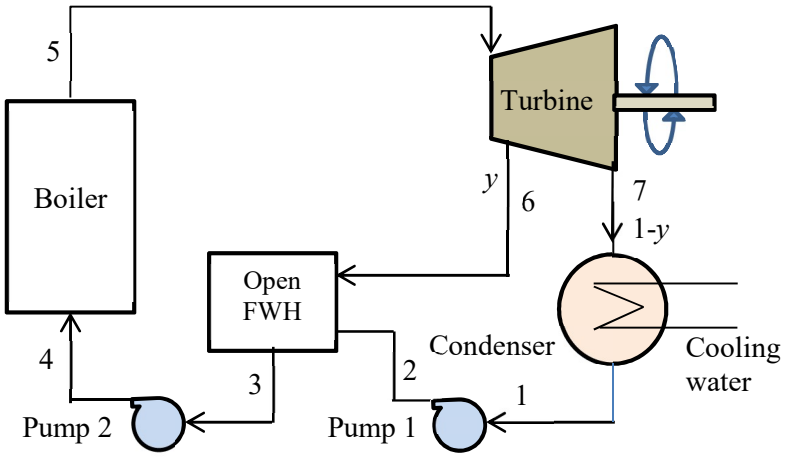

Figure 4.8. Schematic diagram of the steam power plant with regeneration

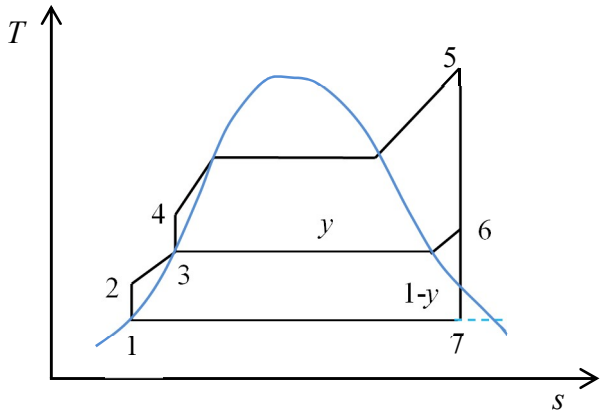

Figure 4.9. *T-s* diagram for the Rankine cycle with regeneration

The main components of the plant shown on Figure 4.8 are a boiler (steam generator), a steam turbine, an open feed-water heater, a condenser, two feed-water pumps, and a connecting pipes system. The working-fluid, which is water, undergoes a complete cycle whereby it leaves the condenser as saturated liquid at P_c and then pumped by the first pump (Pump I) to the pressure in the feed-water heater (P_6). After mixing with the

extracted steam in the open FWH, the feed-water is pumped by the second pump (Pump II) to the boiler pressure (P_b). In the boiler, it is heated to become superheated steam at T_2 before delivered to the steam turbine. The superheated steam expands in the steam turbine to an intermediate pressure (P_6). In the condenser, the steam rejects its heat to a stream of cooling water and, thus, returns to its initial state as saturated liquid water at P_c. The open-feed-water heater does the job of regeneration as well as deaeration.

The analytical model

Per each kilogram of steam exiting the boiler at point 5, a fraction y is extracted and mixed with the condensate in the open feed-water heater. The rest of steam (1-y) completes its expansion in the low-pressure turbine to the condenser pressure ($P_c = P_7 = P_1$). For steady operation, the heat input, turbine's work (w_t), and input work consumed by the two pumps (w_{PI} and w_{PII}) are given by:

$$Q_{in} = h_5 - h_4 \tag{4.20}$$

$$w_t = 1 \times (h_5 - h_6) + (1 - y)(h_6 - h_7) \tag{4.21}$$

$$w_{PI} = v_1 (1 - y)(P_2 - P_1) \tag{4.22}$$

$$w_{PII} = v_3 (P_4 - P_3) \tag{4.23}$$

The enthalpies of the fluid leaving the turbine (h_7) and two pumps (h_2 and h_4) are determined from the corresponding values following isentropic-expansion and isentropic compression (i.e. h_{7s}, h_{2s} and h_{4s}) as follows:

$$h_7 = h_6 - (h_6 - h_{7s}) \times \eta_t \tag{4.24}$$

$$h_2 = h_1 - (h_1 - h_{2s}) / \eta_c \tag{4.25}$$

$$h_4 = h_3 - (h_3 - h_{4s}) / \eta_c \tag{4.26}$$

Where, η_t and η_p are, respectively, the isentropic efficiencies of the two turbines and two pumps. The fraction of steam extracted for regeneration (y) is obtained from mass and energy balance over the feed-water heater:

$$y = \frac{h_3 - h_2}{h_6 - h_2} \tag{4.27}$$

The working fluid at points 2 and 3 is saturated liquid water and, therefore, the enthalpy values at these two points are those of saturated water h_f at the corresponding pressures.

Water leaves the two pumps as compressed liquid and values of its enthalpies at the two discharge points 2 and 3 can be estimated from:

$$h_2 = h_1 + w_{PI} \tag{4.28}$$

$$h_4 = h_3 + w_{PII} \tag{4.29}$$

Since the steam at point 5 is superheated, the value of its enthalpy can be determined from its pressure and temperature. The steam at point 6 is also superheated and its entropy is equal to that at state 5. Therefore, the value of its enthalpy can be obtained from the pressure and entropy using the appropriate Thermax function.

The state of the steam at the last stage of expansion, i.e. point 7, lies in the saturated-mixture region. Therefore, determining its enthalpy needs the dryness fraction at this point to be known. Since the entropy at state 7 also equals that at state 5, the dryness fraction (x_7) is given by:

$$x_7 = \frac{s_5 - s_{f@Pc}}{s_{fg@Pc}} \tag{4.30}$$

Entropy values s_f and s_{fg} at the condenser pressure can be determined by using the appropriate Thermax functions.

An important consideration in the design of a power-generation plant using the regenerative Rankine cycle is the selection of the intermediate pressure at which steam is to be extracted for regeneration. As will be shown later, the maximum values of the thermal efficiency and net work output are obtained at a certain value of this pressure. The following numerical example that illustrates the use of Thermax functions to analyse the cycle is based on an example given by Cengel and Boles [2].

Example 4.3. Regenerative Rankine cycle with a single open feed-water heater
Consider a steam power plant operating on the ideal regenerative Rankine cycle with one open feed-water heaters. Steam enters the turbine at 15 MPa and 600°C and is condensed in the condenser at a pressure of 10 kPa. Some steam leaves the turbine at an intermediate pressure (P_i) and enters the open feed-water heater. Study the effect of the regeneration steam pressure on the net specific output work and thermal efficiency of the plant and determine the most suitable extraction pressure.

Solution
Figure 4.10 shows the Excel sheet prepared for this example. The input data shown in the left-side of the sheet includes the boiler pressure (P_b) and temperature (T_b), the condenser pressure (P_c), the intermediate pressure (P_i), the isentropic efficiency of the two turbines (η_t), and the isentropic efficiency of the two pumps (η_P). Note that both η_t

and η_p have been assigned a value of 1 in this ideal case. The middle part of the sheet shows the calculated enthalpy values obtained by using Thermax functions. Figure 4.11 shows the formulae used in the sheet.

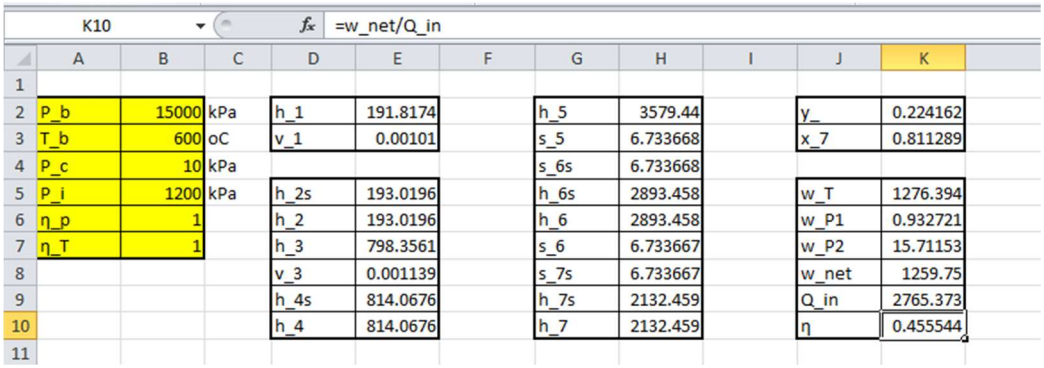

K10 =w_net/Q_in

	A	B	C	D	E	F	G	H	I	J	K
1											
2	P_b	15000	kPa	h_1	191.8174		h_5	3579.44		y_	0.224162
3	T_b	600	oC	v_1	0.00101		s_5	6.733668		x_7	0.811289
4	P_c	10	kPa				s_6s	6.733668			
5	P_i	1200	kPa	h_2s	193.0196		h_6s	2893.458		w_T	1276.394
6	η_p	1		h_2	193.0196		h_6	2893.458		w_P1	0.932721
7	η_T	1		h_3	798.3561		s_6	6.733667		w_P2	15.71153
8				v_3	0.001139		s_7s	6.733667		w_net	1259.75
9				h_4s	814.0676		h_7s	2132.459		Q_in	2765.373
10				h_4	814.0676		h_7	2132.459		η	0.455544
11											

Figure 4.10. The Excel sheet for Example 4.3

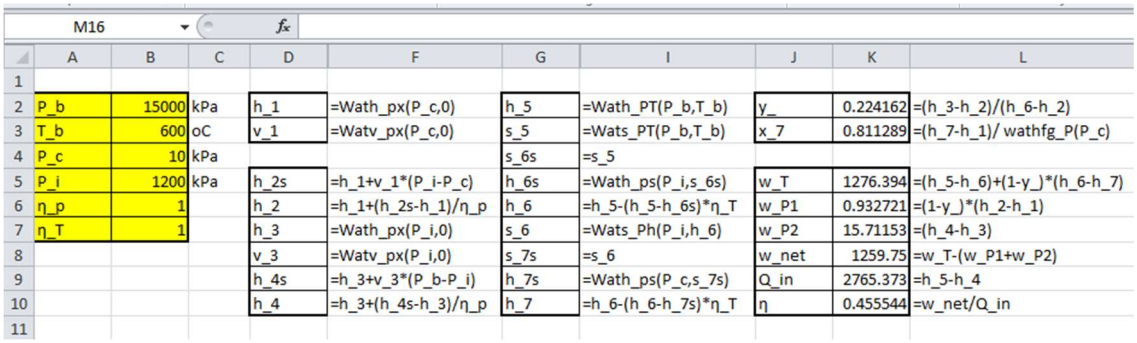

M16

	A	B	C	D	F	G	I	J	K	L
1										
2	P_b	15000	kPa	h_1	=Wath_px(P_c,0)	h_5	=Wath_PT(P_b,T_b)	y_	0.224162	=(h_3-h_2)/(h_6-h_2)
3	T_b	600	oC	v_1	=Watv_px(P_c,0)	s_5	=Wats_PT(P_b,T_b)	x_7	0.811289	=(h_7-h_1)/ wathfg_P(P_c)
4	P_c	10	kPa			s_6s	=s_5			
5	P_i	1200	kPa	h_2s	=h_1+v_1*(P_i-P_c)	h_6s	=Wath_ps(P_i,s_6s)	w_T	1276.394	=(h_5-h_6)+(1-y_)*(h_6-h_7)
6	η_p	1		h_2	=h_1+(h_2s-h_1)/η_p	h_6	=h_5-(h_5-h_6s)*η_T	w_P1	0.932721	=(1-y_)*(h_2-h_1)
7	η_T	1		h_3	=Wath_px(P_i,0)	s_6	=Wats_Ph(P_i,h_6)	w_P2	15.71153	=(h_4-h_3)
8				v_3	=Watv_px(P_i,0)	s_7s	=s_6	w_net	1259.75	=w_T-(w_P1+w_P2)
9				h_4s	=h_3+v_3*(P_b-P_i)	h_7s	=Wath_ps(P_c,s_7s)	Q_in	2765.373	=h_5-h_4
10				h_4	=h_3+(h_4s-h_3)/η_p	h_7	=h_6-(h_6-h_7s)*η_T	η	0.455544	=w_net/Q_in
11										

Figure 4.11. The formulae used in the Excel sheet for Example 4.3

The right-side of the sheet shows the main results, which include the values of y and x_7, the two input work components, the two output work components, the heat input, and the thermal efficiency. Table 4.4 compares the values obtained for the key solution parameters at an intermediate pressure P_i of 1.2 MPa with the corresponding values given by Cengel and Boles [2]. The figures in the table show a good agreement between the present values and those of Cengel and Boles [2] since the maximum deviation between the two results is less than 2%.

To study the effect of the intermediate pressure (P_i) on the system's net output work and thermal efficiency, these were calculated for different values of this pressure. Figure 4.12 shows the variation of the net output work and thermal efficiency with P_i. Clearly, the net work output decreases continuously as the extraction pressure is increased, but the thermal efficiency reaches a maximum value at approximately 1100 kPa. Therefore, the intermediate pressure has to be lower than this value. The optimum value of P_i must be an economic compromise between the revenue generated due to fuel saving and that due to the increased power.

Table 4.4. Verification of Thermax results for Example 4.3

Parameter	Cengel and Boles [2]	Thermax	Deviation (%)
h_1	191.83	191.817	-0.00678
h_2	193.03	193.020	-0.00518
h_3	798.65	798.360	-0.03631
h_4	814.37	814.070	-0.03684
h_5	3582.3	3579.440	-0.07984
h_6	2859.5	2893.458	1.18755
h_7	2114.9	2132.459	0.83025
y	0.2271	0.2242	-1.27697
x_7	0.8037	0.8113	0.94563
η	0.463	0.4555	-1.61987

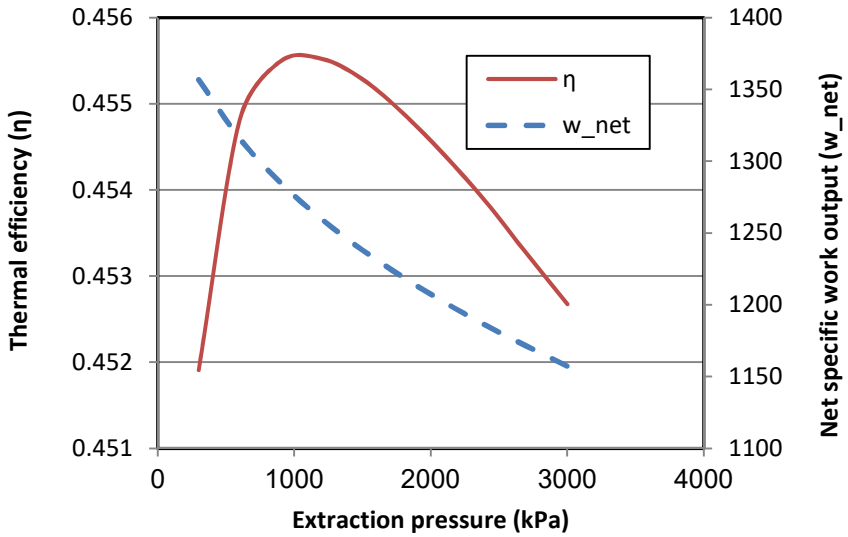

Figure 4.12. Variation of the cycle's net output work and thermal efficiency with the intermediate pressure

4.4. Reheat-regenerative Rankine cycle with two feed-water heaters

Figure 4.13 shows a schematic diagram of a steam power plant that operates on a reheat-regenerative Rankine cycle. Compared to the power plant shown on Figure 4.8, the present power plant adds a low-pressure steam turbine, a reheater, a closed feed-water heater, a third feed-water pump, and a mixing chamber. The additional cost of this equipment should be compensated for by the anticipated increase in both the power and thermal efficiency of the plant. Figure 4.14 shows the *T-s* diagram for the cycle in the ideal situation.

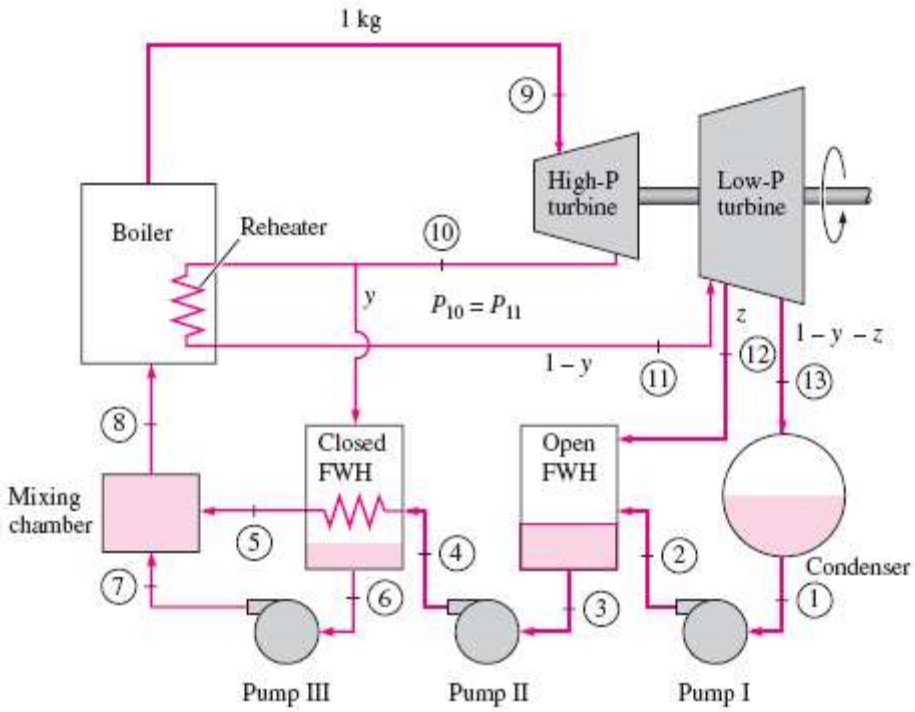

Figure 4.13. A regenerative Rankine cycle with open and closed feed-water heaters (adopted from Cengel and Boles [2])

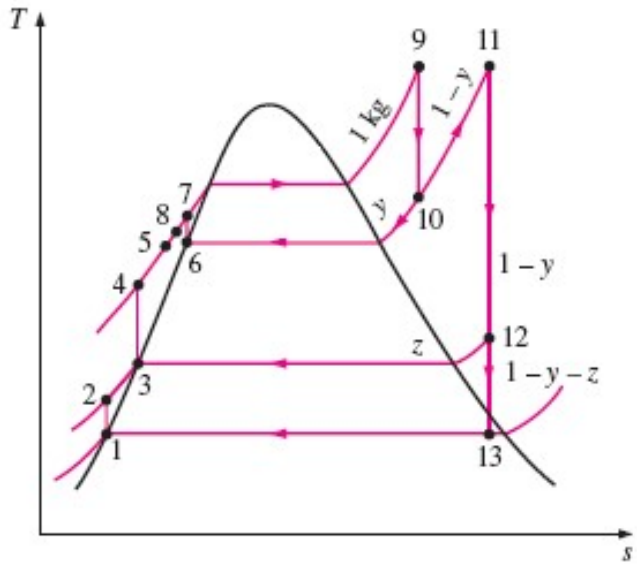

Figure 4.14. *T-s* diagram for the reheat-regenerative Rankine cycle (adopted from Cengel and Boles [2])

The analytical model

In the following model it is assumed that per each kilogram of steam entering and leaving the boiler and high-pressure turbine, a fraction y is passed through the closed feed-water heater. Out of the remaining (1-y) kg that passes through the low-pressure heaters, a fraction z is extracted for regeneration in the open feed-water heater. Therefore, the fraction that passes through the condenser is (1-y-z). The specific work output, work input, and heat input for this power plant are given by:

$$w_{out} = 1 \times (h_9 - h_{10}) + (1 - y)(h_{11} - h_{12}) + (1 - y - z)(h_{12} - h_{13}) \tag{4.31}$$

$$w_{in} = (1 - y - z)(h_2 - h_1) + (1 - y)(h_4 - h_3) + y(h_7 - h_6) \tag{4.32}$$

$$Q_{in} = 1 \times (h_9 - h_8) + (1 - y)(h_{11} - h_{10}) \tag{4.33}$$

Steam at points 9 and 11 is superheated and, therefore, enthalpy values at these two points (h_9 and h_{11}) can be determined from the known values of pressure and temperature. Steam at points 10 and 12 are also superheated at the reheat pressure and extraction pressure, respectively. The other known property at these two points is entropy, which leads to $s_{10}=s_9$ and $s_{12}=s_{11}$ in the case of ideal isentropic expansion. At point 13 the working fluid is saturated liquid-vapour mixture at the condenser pressure. The entropy of the fluid leaving the low-pressure turbine at point 13 is determined from the known condenser pressure and entropy at point 13 which, for isentropic expansion, equals that at point 12, i.e. $s_{13}=s_{12}$. Since the water at points 1, 3 and 6 is saturated liquid at the condenser pressure, its enthalpy at these points equal the enthalpies of saturated liquid water at the corresponding pressures, i.e. $h_1=h_{f@P1}$, $h_3=h_{f@P3}$, and $h_6=h_{f@P6}$. Water leaves the three pumps as compressed-liquid and its enthalpies at points 2, 4, and 7 are obtained from:

$$h_2 = h_1 + v_1(P_2 - P_1)/\eta_P \tag{4.34}$$

$$h_4 = h_3 + v_3(P_4 - P_3)/\eta_P \tag{4.35}$$

$$h_7 = h_6 + v_6(P_7 - P_6)/\eta_P \tag{4.36}$$

Where, η_P is the pump's isentropic efficiency.

The fraction z is determined from mass and energy balance over the open FWH assuming that the feed-water leaves the heater as saturated liquid. This leads to:

$$z = \frac{(1 - y)(h_3 - h_2)}{(h_{12} - h_2)} \tag{4.37}$$

Since the two streams entering the closed feed-water heater are at different pressures and leave it unmixed, the temperature of the feed-water at point 5 can take any value between T_4 and T_{10}. In the present analysis it is assumed that the feed-water leaves the closed FWH at the saturation temperature corresponding to the reheater pressure (P_{rh}), i.e. $T_5=T_6 =T_{sat@Prh}$. Once the value of h_5 is known, the mass fraction y can be determined according to the following relationship:

$$y = \frac{(h_5 - h_4)}{(h_{10} - h_6) + (h_5 - h_4)} \tag{4.38}$$

The enthalpy at state 8 is also obtained by energy balance as:

$$h_8 = (1 - y)h_5 + yh_7 \tag{4.39}$$

The following numerical example, which is adapted from Example 10.6 given by Cengel and Boles [2], analyses the cycle's performance and proves its advantages compared to the cycle with a single feed-water heater considered in Example 4.3.

Example 4.4. Analysis of the regenerative Rankine cycle with two heaters
Consider a steam power plant that operates on an ideal reheat–regenerative Rankine cycle with one open feed-water heater, one closed feed-water heater, and one reheater. Steam enters the turbine at 15 MPa and 600°C and is condensed in the condenser at a pressure of 10 kPa. Some steam is extracted from the turbine at 4 MPa for the closed feed-water heater, and the remaining steam is reheated at the same pressure to 600°C. The extracted steam is completely condensed in the heater and is pumped to 15 MPa before it mixes with the feed-water at the same pressure. Steam for the open feed-water heater is extracted from the low-pressure turbine at a pressure of 0.5 MPa. The feed-water is heated in the closed-feed-water heater to the saturation temperature at the feed-water heater pressure (i.e., 4 MPa).

Solution
Figure 4.15 shows the Excel sheet developed for this example and Figure 4.16 reveals the formulae used in the sheet. The sheet can account for anisotropic compression and expansion, but for this ideal case the isotropic efficiencies of the pumps and turbines are assigned values of 100%. The formula window reveals the formula used for the calculation of h_5. Note that the function **Wath_Px(P_rh,0)** is used to determine the value of h_f at the reheat pressure (P_rh). Figure 4.15 shows that the net specific work is 1397.186 kJ while the thermal efficiency is 48.255%. Compared to the regenerative cycle with a single feedwater heater, the net specific work increased by 10.91 % while the thermal efficiency increased by 5.93%. Table 4.5 compares the values of the important cycle parameters obtained in the present analyses with their corresponding values given by Cengel and Boles [2].

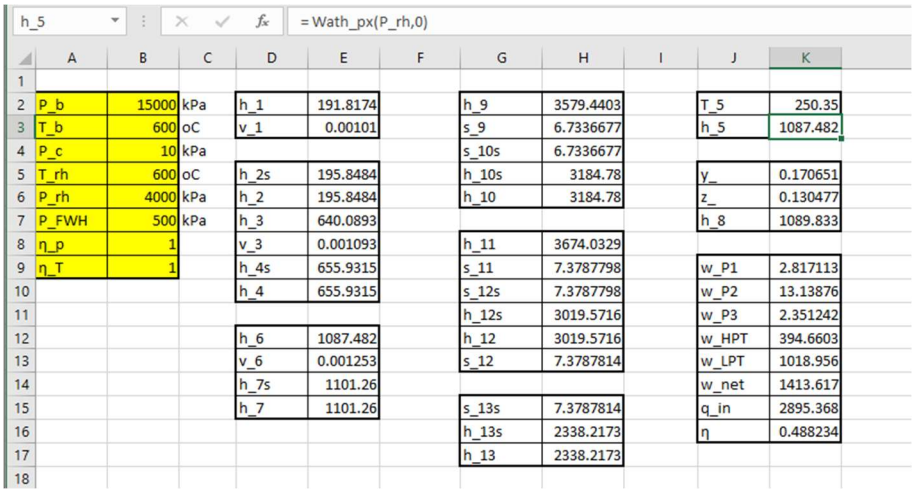

h_5 = Wath_px(P_rh,0)

	A	B	C	D	E	F	G	H	I	J	K
1											
2	P_b	15000	kPa	h_1	191.8174		h_9	3579.4403		T_5	250.35
3	T_b	600	oC	v_1	0.00101		s_9	6.7336677		h_5	1087.482
4	P_c	10	kPa				s_10s	6.7336677			
5	T_rh	600	oC	h_2s	195.8484		h_10s	3184.78		y_	0.170651
6	P_rh	4000	kPa	h_2	195.8484		h_10	3184.78		z_	0.130477
7	P_FWH	500	kPa	h_3	640.0893					h_8	1089.833
8	η_p	1		v_3	0.001093		h_11	3674.0329			
9	η_T	1		h_4s	655.9315		s_11	7.3787798		w_P1	2.817113
10				h_4	655.9315		s_12s	7.3787798		w_P2	13.13876
11							h_12s	3019.5716		w_P3	2.351242
12				h_6	1087.482		h_12	3019.5716		w_HPT	394.6603
13				v_6	0.001253		s_12	7.3787814		w_LPT	1018.956
14				h_7s	1101.26					w_net	1413.617
15				h_7	1101.26		s_13s	7.3787814		q_in	2895.368
16							h_13s	2338.2173		η	0.488234
17							h_13	2338.2173			
18											

Figure 4.15. Excel sheet for Example 4.4

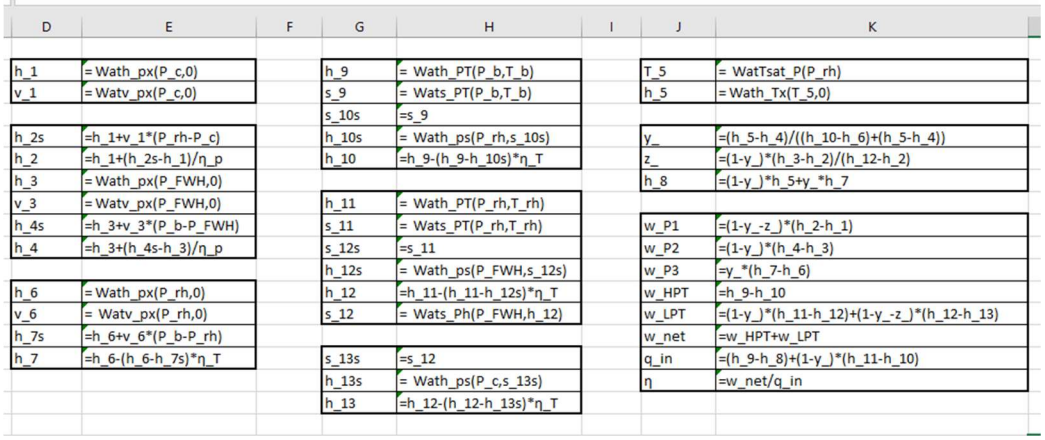

D	E	F	G	H	I	J	K
h_1	= Wath_px(P_c,0)		h_9	= Wath_PT(P_b,T_b)		T_5	= WatTsat_P(P_rh)
v_1	= Watv_px(P_c,0)		s_9	= Wats_PT(P_b,T_b)		h_5	= Wath_Tx(T_5,0)
			s_10s	=s_9			
h_2s	=h_1+v_1*(P_rh-P_c)		h_10s	= Wath_ps(P_rh,s_10s)		y_	=(h_5-h_4)/((h_10-h_6)+(h_5-h_4))
h_2	=h_1+(h_2s-h_1)/η_p		h_10	=h_9-(h_9-h_10s)*η_T		z_	=(1-y_)*(h_3-h_2)/(h_12-h_2)
h_3	= Wath_px(P_FWH,0)					h_8	=(1-y_)*h_5+y_*h_7
v_3	= Watv_px(P_FWH,0)		h_11	= Wath_PT(P_rh,T_rh)			
h_4s	=h_3+v_3*(P_b-P_FWH)		s_11	= Wats_PT(P_rh,T_rh)		w_P1	=(1-y_-z_)*(h_2-h_1)
h_4	=h_3+(h_4s-h_3)/η_p		s_12s	=s_11		w_P2	=(1-y_)*(h_4-h_3)
			h_12s	= Wath_ps(P_FWH,s_12s)		w_P3	=y_*(h_7-h_6)
h_6	= Wath_px(P_rh,0)		h_12	=h_11-(h_11-h_12s)*η_T		w_HPT	=h_9-h_10
v_6	= Watv_px(P_rh,0)		s_12	= Wats_Ph(P_FWH,h_12)		w_LPT	=(1-y_)*(h_11-h_12)+(1-y_-z_)*(h_12-h_13)
h_7s	=h_6+v_6*(P_b-P_rh)					w_net	=w_HPT+w_LPT
h_7	=h_6-(h_6-h_7s)*η_T		s_13s	=s_12		q_in	=(h_9-h_8)+(1-y_)*(h_11-h_10)
			h_13s	= Wath_ps(P_c,s_13s)		η	=w_net/q_in
			h_13	=h_12-(h_12-h_13s)*η_T			

Figure 4.16. Excel formulae used for Example 4.4

Table 4.5. Verification of Thermax results for Example 4.4

Parameter	Cengel and Boles [2]	Thermax	Deviation (%)
h_8	1089.8	1089.833	0.00303
h_9	3583.1	3579.440	-0.10214
h_{10}	3155.0	3184.78	0.94390
h_{11}	3674.9	3674.033	-0.02360
h_{12}	3014.8	3019.572	0.15827
h_{13}	2335.7	2338.217	0.10778
y	0.1766	0.171	-3.36863
z	0.1306	0.131	0.57504
η	0.492	0.488	-0.81301

The figures in Table 4.5 show good agreements between the present enthalpy values and those of Cengel and Boles [2] for all the fluid states, but the calculated value of the steam fraction, y, deviates from the corresponding values given by Cengel and Boles [2] by about 3%. As a result, the calculated value for the cycle's efficiency deviates by 1.92% from that that given by Cengel and Boles [2].

4.5. First and second-law analyses of the combined Brayton-Rankine cycle

The combined Brayton-Rankine cycle, or simply the combined-cycle (CC), captures the exhaust gas energy and utilises it for steam generation in a heat-recovery steam generator (HRSG). When expanded in a steam turbine, the generated steam produces additional power so that the overall efficiency of the plant can be increased by 50 – 60 present. Figure 4.17 shows a schematic diagram of the CC power plant.

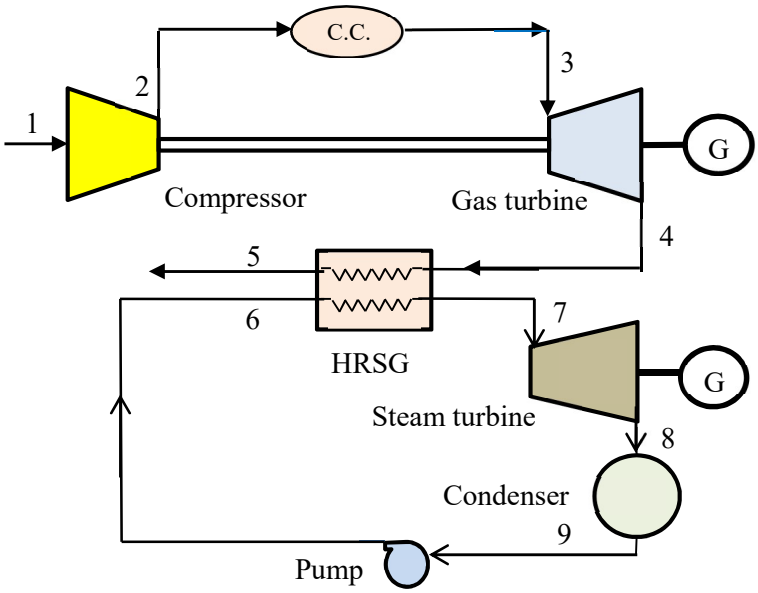

Figure 4.17. A schematic diagram for a combined-cycle power plant

Air enters the compressor of the gas-turbine at state 1 where it is compressed to state 2 and heated in the combustion chamber to state 3. After expanding in the gas turbine, the exhaust gas leaves at state 4 and then passes through the HRSG where part of its energy is used to produce steam for the steam power-plant and eventually leaves the heat exchanger at state 5. The feed-water of the steam-turbine system enter the HRSG as compressed liquid at state (6) before being heated to become superheated steam at state (7). It is then delivered to the steam turbine where it expands to the condenser pressure at state (8). After leaving the condenser as saturated liquid water at state (9), the feed-water is pumped by the first feed-water pump to state (6). Usually the temperature of the gas at point 5 is not allowed to drop below 150°C in order to avoid condensation of the water vapour in the gas that will lead to corrosion of the duct and chimney. Figure 4.18 shows the *T-s* diagram of the cycle.

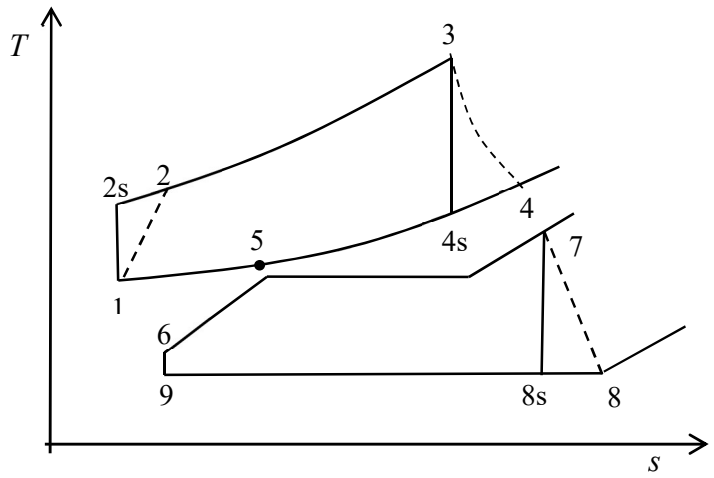

Figure 4.18. *T-s* diagram for the combined-cycle power plant

Note that states 2s and 4s are the states after idealised isentropic compression and expansion in the Brayton cycle, while the states 2 and 4 are the actual corresponding states. Similarly, state 8s in the Rankine cycle is that after an idealised isentropic expansion in the steam turbine, while state 8 is the actual corresponding state.

4.5.1. First-law analysis of the combined cycle

For steady-state operation and negligible heat transfer with the surroundings, the energy rejected by the Brayton cycle equals that gained by the Rankine cycle. Neglecting friction losses and changes in kinetic and potential energy, energy balance in the HRSG gives:

$$\dot{m}_s\left(h_7 - h_6\right) = \dot{m}_g\left(h_4 - h_5\right) \tag{4.40}$$

Where $\dot{m}_g$ and $\dot{m}_s$ are the mass flow rates of the gas-turbine exhaust and the steam, respectively. Knowing both the inlet and exit temperatures of the exhaust gas and the steam, Equation (4.40) can be used to relate the mass flow rates in the Brayton and Rankine cycles as follows:

$$\frac{\dot{m}_s}{\dot{m}_g} = \frac{\left(h_4 - h_5\right)}{\left(h_7 - h_6\right)} \tag{4.41}$$

Given the total net power of the combined plant, $\dot{W}$, in MW, the mass flow rate of the gas in the gas-turbine cycle can be obtained from:

$$\dot{m}_g = \frac{\dot{W} \times 1000}{\left[\left(h_3 - h_4\right) - \left(h_2 - h_1\right)\right] + \dfrac{\dot{m}_s}{\dot{m}_g}\left[\left(h_7 - h_8\right) - \left(h_6 - h_9\right)\right]} \tag{4.42}$$

Having determined the mass flow rate in the gas-turbine ($\dot{m}_g$), the corresponding mass flow rate of steam in the steam-turbine ($\dot{m}_s$) can be calculated from Equation (4.40).

Enthalpy values h_2, h_4 and h_8 are determined as follows:

$$h_2 = h_1 + (h_{2s} - h_1)/\eta_c \tag{4.43}$$

$$h_4 = h_3 - (h_3 - h_{4s}) \times \eta_{gt} \tag{4.44}$$

$$h_8 = h_7 - (h_7 - h_{8s}) \times \eta_{st} \tag{4.45}$$

Where η_c, η_{gt}, and η_{st}, refer to the isentropic (adiabatic) efficiencies of the air-compressor, the gas-turbine, and the steam-turbine, respectively. The thermal efficiency for the Brayton cycle alone ($\eta_{Brayton}$) is given by:

$$\eta_{Brayton} = (W_{GT} - W_C)/Q_{in} \tag{4.46}$$

Where Q_{in} is the heat input and W_{GT} the work produced by the gas-turbine and W_{C} is the work input to the compressor. The thermal efficiency of the combined plant is given by:

$$\eta_{combined} = \frac{(W_{GT} - W_C) + (W_{ST} - W_p)}{Q_{in}} \tag{4.47}$$

Where W_{ST} is the work produced by the steam-turbine plant and W_{p} is the work consumed by the pump. In terms of fluid flow rates and enthalpies, the five quantities on the right-hand sides of Equations (4.46) and (4.47) can be expressed as:

$$Q_{in} = \dot{m}_g (h_3 - h_2) \tag{4.48}$$

$$W_{GT} = \dot{m}_g (h_3 - h_4) \tag{4.49}$$

$$W_C = \dot{m}_g (h_2 - h_1) \tag{4.50}$$

$$W_{ST} = \dot{m}_s (h_7 - h_8) \tag{4.51}$$

$$W_p = \dot{m}_s v_9 (P_6 - P_9) \tag{4.52}$$

The following example is based on Example 9.13 in Moran and Shapiro [1].

Example 4.5. Energy analysis of the combined Brayton-Rankine cycle

In a 45-MW combined-cycle system such as the one shown on Figure 4.17, air enters the compressor at 300K and 100 kPa. The compressor pressure ratio is 12 and air leaves the combustion chamber at 1400 K. The isentropic efficiencies of the compressor and gas-turbine are 84% and 88%, respectively. The exhaust gases are used to produce steam in the HRSG at 8 MPa and 500°C. The exhaust gases leave the HRSG at 400K. The condenser pressure is 8 kPa. The isentropic efficiencies of the steam-turbine and pump are 90% and 80%, respectively. Determine the mass flow rates in the gas-turbine and the steam-turbine cycles and the overall thermal efficiency of the plant.

Solution

Figure 4.19 shows the Excel sheet developed for this example by using Thermax functions. The top part of the sheet deals with the analysis of the Brayton cycle, while the bottom part deals with that of the Rankine cycle. The Brayton cycle is analysed by using property functions from the Gas-group of Thermax as shown in Example 4.1, while the Rankine cycle is analysed by functions from the Wat-group as shown in Example 4.4. The development of this sheet is left as an exercise to the reader (Exercise 4.6).

H20 =w_total/Q_in

	A	B	C	D	E	F	G	H	I	J	K	L
1	P_power	45	MW									
2	T_1	300		h_1	299.845		P_3	1200		P_4	100	
3	P_1	100		Pr_1	1.38E+00		h_3	1515.758		P_5	100	
4	T_3	1400		Pr_2s	1.66E+01		Pr_3	4.54E+02		w_c	368.951	
5	Pratio	12		T_2s	601.209		Pr_4s	3.79E+01		w_t	657.122	
6				h_2s	609.764		T_4s	749.921		w_net	288.171	
7	Eff_c	0.84		h_2	668.797		h_4s	769.029				
8	Eff_t	0.88		T_2	656.809		h_4	858.636		Eff_therm	0.340	
9				P_2	1200		T_4	831.820				
10	T_5	400	K				h_5	401.001				
11												
12	P_6	8000		T_9	41.394		mratio	0.154				
13	P_7	8000		h_9	173.357		m_gas	100.676	kg/s			
14	T_7	400	oC	v_9	0.001		m_vap	15.504	kg/s			
15	P_8	8		h_6	183.431							
16	P_9	8		h_7	3155.111		w_gas	29.012	MW			
17				s_7	6.392		w_vap	15.988	MW			
18	Eff_p	0.8		T_8	41.394		w_total	45.000	MW			
19	Eff_Ts	0.9		s_8s	6.392		Q_in	85.268	MW			
20				x_8s	0.759		Eff_total	0.528				
21				h_8s	1998.098							
22				h_8	2113.800							
23												

Figure 4.19. Excel sheet developed for Example 4.5 using Thermax

Table 4.6 compares the calculated values of enthalpies at various points in the cycle with their corresponding values obtained by Moran and Shapiro [1]. As the figures indicate, the difference between the values calculated by Thermax and those given by Moran and Shapiro [1] are minor.

Table 4.6. Verification of Thermax results for energy analysis of the combined cycle

Quantity	Moran and Shapiro [1]	Thermax	Deviation (%)
h_1	300.19	299.845	-0.115
h_2	669.79	668.797	-0.148
h_3	1515.42	1515.758	0.022
h_4	858.02	858.636	0.072
h_5	400.98	401.000	0.005
h_9	173.88	173.357	-0.301
h_6	183.96	183.431	-0.287
h_7	3138.30	3155.111	0.536
h_8	2104.74	2113.800	0.431
$\dot{m}_g$	100.87	100.676	-0.192
$\dot{m}_v$	15.60	15.504	-0.615
$\eta_{Brayton}$	-	0.340	-
η_{CC}	-	0.528	-

The figure in Table 4.6 show that the thermal efficiency of the simple Brayton cycle is only 34%, while that of the combined cycle reached 52.8%. It should also be mentioned that the gas-turbine and steam-turbine systems in the combined cycle need not be simple systems as shown on Figure 4.17 since both of them can adopt various measures that improve their efficiencies. For example, the gas-turbine can have intercooling and reheating and the Rankine cycle can have single or multiple feed-water heaters.

4.5.2. Second-law analysis of the combined cycle

First-law analyses, also called "energy analyses" or "energetic analyses", are useful for evaluating the overall performance of energy-conversion systems. The performance indicator used in such analyses is the thermal efficiency in the case of power-producing systems or the coefficient of performance (COP) in the case of refrigeration and heat-pump systems. By comparison, second-law or exergy analyses aim to identify the locations and magnitudes of energy losses in the system. Therefore, exergy analyses are more useful than energy analyses for designing more efficient energy systems. This section illustrates the application of the method to the combined cycle in Example 4.5.

For open systems (control volumes), the specific flow exergy (ε_f) is defined as [1]:

$$\varepsilon_f = (h - h_0) - T_0(s - s_0) + \frac{V^2}{2} + gz \tag{4.53}$$

Where T_0 is the dead-state temperature and h_0 and s_0 are values of enthalpy and entropy of the working fluid at the dead-state (T_0, P_0). The last two terms that represent contributions from kinetic and potential energy are usually small compared to the other terms and can be neglected as follows:

$$\varepsilon_f = (h - h_0) - T_0(s - s_0) \tag{4.54}$$

In general, the rate of exergy increase or decrease across any open system that involves work transfer ($\dot{W}$) and heat transfer ($\dot{Q}$) with its surroundings is governed by [1]:

$$\frac{dE_{cv}}{dt} = \sum_j \left(1 - \frac{T_0}{T_j}\right)\dot{Q}_j - \left(\dot{W}_{cv} - P_0 \frac{dV_{cv}}{dt}\right) + \sum_i \dot{m}_i \varepsilon_{fi} - \sum_e \dot{m}_e \varepsilon_{fe} - \dot{E}_d \tag{4.55}$$

Where $\dot{E}_d$ refers to the rate of exergy destruction and suffices *i* and *e* refer to the inlet and exit conditions of the fluid. The sign convention of heat-in (+) and work-out (+) applies in Equation (4.55), which for steady, single-pass flow devices, reduces to:

$$\dot{E}_d = \left(1 - \frac{T_0}{T}\right)\dot{Q} - \dot{W}_{cv} + \dot{m}(\varepsilon_{fi} - \varepsilon_{fe}) \tag{4.56}$$

Furthermore, for devices that involve only adiabatic process (e.g. the air-compressor, gas-turbine, pump and steam turbine), the equation becomes:

$$\dot{E}_d = -\dot{W}_{cv} + \dot{m}(\varepsilon_{fi} - \varepsilon_{fe}) \tag{4.57}$$

Alternatively, the rate of exergy destruction for these devices can obtained from the following relationship:

$$\dot{E}_d = \dot{m} T_0 (s_e - s_i) \tag{4.58}$$

Applying Equation (4.58) to the gas-turbine cycle:

$$\dot{E}_{d,compressor} = \dot{m}_g T_0 (s_2 - s_1) \tag{4.59}$$

$$\dot{E}_{d,airturbine} = \dot{m}_g T_0 (s_4 - s_3) \tag{4.60}$$

Similarly, for the steam-turbine cycle:

$$\dot{E}_{d,pump} = \dot{m}_s T_0 \left(s_6 - s_9\right) \tag{4.61}$$

$$\dot{E}_{d,steamturbine} = \dot{m}_s T_0 \left(s_8 - s_7\right) \tag{4.62}$$

For the steam generator that does involves neither work nor heat-transfer, Equation (4.55) becomes:

$$\dot{\mathrm{E}}_d = \sum_i \dot{m}_i \varepsilon_{fi} - \sum_e \dot{m}_o \varepsilon_{fe} = \dot{m}_g \left(\varepsilon_5 - \varepsilon_4\right) + \dot{m}_s \left(\varepsilon_7 - \varepsilon_6\right) \tag{4.63}$$

The net exergy increase of the gas passing through the combustion chamber is:

$$\dot{E}_{gain,c.c.} = \dot{m}_g \left(\varepsilon_{f3} - \varepsilon_{f2}\right) \tag{4.64}$$

The rate of exergy loss with the exhaust gas is given by:

$$\dot{E}_{loss,exhaust} = \dot{m}_g \left(\varepsilon_{f5} - \varepsilon_{f1}\right) \tag{4.65}$$

Finally, the rate of exergy loss in the condenser is given by:

$$\dot{E}_{loss,condenser} = \dot{m}_s \left(\varepsilon_{f8} - \varepsilon_{f9}\right) \tag{4.66}$$

Figure 4.20 shows the extensions needed for the Excel sheet used for energy analysis of the combined cycle shown on Figure 4.19.

27	**Exsrgy analysis**					**Exergy gain**		
28	T_0	300	s0_1	1.7008641		Combustor	59.4193041	MW
29	P_0	100	s0_2	2.5079358		Exhaust	1.39802075	MW
30			s0_3	3.36378917		Cooling water	1.38936042	MW
31	Ra	0.287	s0_4	2.76400997				
32			s0_5	1.99176039		**Exergy destruction**		
33						Air turbine	3.42465226	MW
34			s_9	0.59085656		Compressor	2.83613766	MW
35			s_6	0.59085656				
36						Steam turbine	1.71098343	MW
37			x_8	0.80762937		Pump	0	MW
38			s_8	6.76028731		Heat exchange	3.66014956	MW
39								

Figure 4.20. Extension to the Excel sheet of the combined cycle in Example 4.5 required for the exergy analysis

The additional data required by exergy analysis include: the reference temperature (T_0), the reference pressure (P_0), and the gas constant for air (R_air). Based on these data, the sheet calculates entropy values of the air and water at various locations and then determines the rates of exergy gains and exergy destructions in the different system components from the relevant equations. Figure 4.21 reveals Thermax property functions used in these calculations and Table 4.7 compares values of the key parameters in the exergy analysis to those given by Moran and Shapiro [1].

		Exergy gain	
s0_1	=gass0_TK("air",T_1)	Combustor	=m_gas*(h_3-h_2-T_0*(s0_3-s0_2-Ra*LN(P_3/P_2)))/1000
s0_2	=gass0_TK("air",T_2)	Exhaust	=m_gas*(h_5-h_1-T_0*(s0_5-s0_1-Ra*LN(P_5/P_1)))/1000
s0_3	=gass0_TK("air",T_3)	Cooling water	=m_vap*((h_8-h_9)-T_0*(s_8-s_9))/1000
s0_4	=gass0_TK("air",T_4)		
s0_5	=gass0_TK("air",T_5)	**Exergy destruction**	
		Air turbine	=m_gas*T_0*(s0_4-s0_3-Ra*LN(P_4/P_3))/1000
s_9	=Wats_Px(P_9,0)	Compressor	=m_gas*T_0*(s0_2-s0_1-Ra*LN(P_2/P_1))/1000
s_6	=s_9		
		Steam turbine	=m_vap*T_0*(s_8-s_7)/1000
x_8	=(h_8-h_9)/(wath_px(P_8,1)-h_9)	Pump	=m_vap*T_0*(s_6-s_9)/1000
s_8	=s_6+x_8*(Wats_Px(P_8,1)-s_6)	Heat exchanger	=T_0*(m_gas*(s0_5-s0_4)+m_vap*(s_7-s_6))/1000

Figure 4.21. Thermax functions used in exergy analysis of the combined cycle

Table 4.7. Accuracy of Thermax results for exergy analysis of the combined cycle

	Moran and Shapiro [1]	Thermax	Deviation (%)
Net exergy loss in the exhaust gas at state 5	1.39	1.400	0.7194
Exergy loss in the condenser cooling water	1.41	1.389	-1.4894
Exergy destruction in air-turbine	3.42	3.425	0.1462
Exergy destruction in the compressor	2.83	2.836	0.2120
Exergy destruction in the steam turbine	1.71	1.711	0.0585
Exergy destruction in the pump	0.02	0.00	-100
Exergy destruction in the heat exchanger	3.68	3.660	-0.5435

In general, Table 4.7 shows very small differences (less than 1%) between the present values and those obtained by Moran and Shapiro [1] except for the rate of exergy destruction in the pump which has been neglected in the present analysis by specifying $s_6 = s_9$. Moran and Shapiro [1] obtained the value shown on the table by accounting for the small difference between s_6 and s_9,

Exergy analysis of the combined cycle indicates that the maximum rate of exergy destruction occurs in the HRSG (3.660 MW) followed closely by the air-turbine (3.425 MW) and the air-compressor (2.836 MW). Exergy losses in the exhaust gas and the cooling water of the condenser have similar magnitudes and each one amounts to around 1.4 MW.

4.6. First-law analysis of the organic Rankine cycle with different fluids

The organic Rankine cycle (ORC) is a power cycle that allows heat recovery from low temperature sources such as industrial waste heat, geothermal heat, solar ponds, etc. [3]. The recovered thermal energy can be converted into useful work and then into electricity. The working principle of the ORC is the same as that of the conventional Rankine cycle but, unlike the conventional cycle, the ORC uses a high molecular mass organic fluid instead of water. Figure 4.22 shows a schematic of the simple ORC system. The working fluid is pumped to a boiler (evaporator) where it is evaporated, passes through a turbine (expander) and finally condensed. Figure 2.23 shows the *T-s* diagram of the simple ORC cycle that takes into consideration the losses in the pump and expander due to irreversibilities but neglects pressure losses.

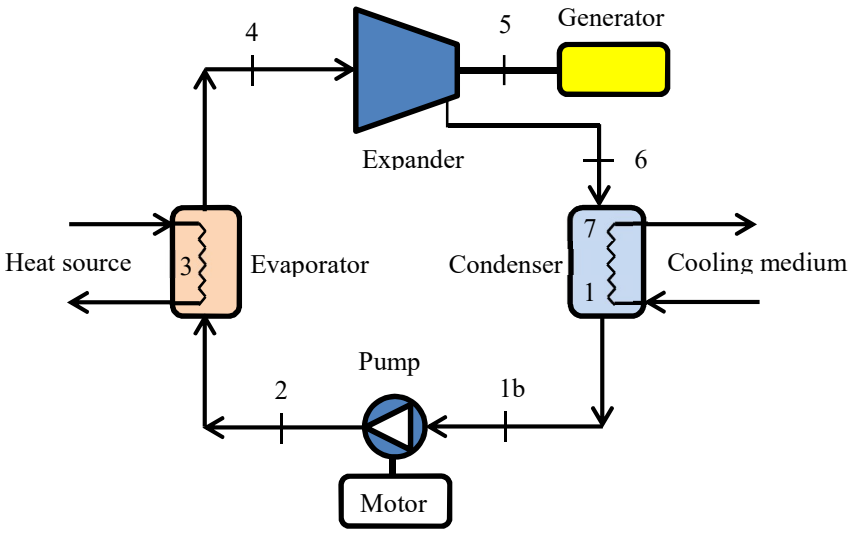

Figure 4.22. Schematic diagram for a simple organic Rankine cycle (adapted from [3])

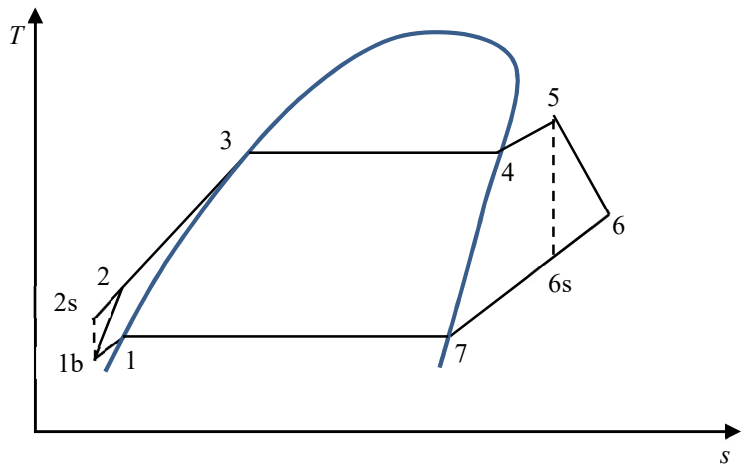

Figure 4.23. *T-s* diagram of the simple ORC

Certain chlorofluorocarbon refrigerants and hydrocarbons are usually used as working fluids for ORCs due to safety and environmental considerations. Table 4.8 shows the characteristics of three suitable fluids, which are R123, R134a, and R290 (propane) [4].

Table 4.8. Characteristics of three candidate fluids for ORC applications [4]

	$T_{critical}$ (°C)	$P_{critical}$ (bar)	Mw (g/mol)	$T_{normalboiling}$ (°C)	ODP	GWP	Safety group
R123	183.68	36.618	152.93	27.82	0.02	77	B1
R134a	101.06	40.593	102.0	-26.07	0.005	1430	A1
R290	96.67	42.359	44.1	−42.09	0	3.3	A2

The design parameters of the ORC system include the temperature of the available energy source and that of the cooling medium, the degree of subcooling and degree of superheating, and the isentropic efficiencies of the pump and expander. The performance of the system is measured in terms of the fluid's mass-flow rates, net work-output, rate of waste-heat recovered, and thermal efficiency. The following example compares the performance of the simple ORC cycle by using R123, R134a, and R290.

Example 4.6. First-law analysis of the simple ORC with three fluids
A simple ORC system is to be used for recovering waste heat that is available at 110°C while the temperature of the cooling medium is 30°C. The ORC system is to be evaluated with three working fluids: R123, R134a, and R290, under the following conditions:

Evaporator temperature (T_e) = 90°C
Condenser temperature (T_c) = 45°C
Degree of superheating (ΔT_{sheat}) = 5°C
Degree of subcooling (ΔT_{scool}) = 5°C

The performance of the three fluids is to be compared for the same evaporator capacity of 10 kW for preheating and vaporising the working fluid. Assuming the energy loss from the evaporator to be negligible for excellent thermal insulation and taking the isentropic efficiencies of the expander and the isentropic pump's efficiency as 85%, determine:

a. The required mass flow rate of the fluid
b. The net work from the cycle
c. The total rate of heat recovered from the high-temperature source
d. The thermal efficiency of the cycle

Solution
For specified values of the evaporator and condenser temperatures, the temperatures of the subcooled liquid (T_{1b}) and superheated vapour (T_5) are determined from:

$$T_{1b} = T_e - \Delta T_{scool} \tag{4.67}$$

$$T_5 = T_c + \Delta T_{sheat} \tag{4.68}$$

Enthalpy values at the different states are determined as follows:

$$h_{1b} \approx h_{f@T_{1b}} \text{ (subcooled liquid)} \tag{4.69}$$

$$h_{2s} \approx h_{1b} + v_{1b}\left(p_c - p_e\right) \tag{4.70}$$

$$h_2 \approx h_1 + \left(h_{2s} - h_{1b}\right)/\eta_p \tag{4.71}$$

$$h_3 = h_{f@T_c} \tag{4.72}$$

$$h_4 = h_{g@T_c} \tag{4.73}$$

$$h_5 = h\left(p_c, T_5\right) \text{ (superheated vapour)} \tag{4.74}$$

$$h_{6s} = h\left(p_e, s_5\right) \text{ (superheated vapour)} \tag{4.75}$$

$$h_6 = h_5 - \left(h_5 - h_{6s}\right) \times \eta_t \tag{4.76}$$

The mass flow rate of the working fluid can be determined from the knowledge of the nominal waste heat capacity of the evaporator, $\dot{Q}_{evap} = 10\,\text{kW}$, i.e.:

$$\dot{m} = \dot{Q}_{evap}/\left(h_4 - h_2\right) = 10/\left(h_4 - h_2\right) \tag{4.77}$$

Therefore, the recovered waste heat, $\dot{Q}_{waste}$, can be determined from:

$$\dot{Q}_{waste} = \dot{m}\left(h_5 - h_2\right) = \dot{Q}_{evap} + \dot{m}\left(h_5 - h_4\right) \tag{4.79}$$

The net work, $\dot{W}$, and thermal efficiency, η, are determined from:

$$\dot{W} = \dot{m}\left(h_5 - h_6\right) \tag{4.78}$$

$$\eta = \dot{W}/\dot{Q}_{waste} \tag{4.80}$$

Figures 4.24, 4.25, and 4.26 show the Excel-aided model developed for analysing the cycle with R123, R134a, and R290, respectively, as the working fluid.

m_f =10/(h_4-h_2)

	A	B	C	D	E	F	G	H	I	J	K	L
1	ORC2											
2	Fluid	R123										
3	T_high	110	oC	P_cond	624.23		h_3	294.45		w_t	17.99312	
4	T_low	25	oC	P_evap	181.76		h_4	434.43		w_p	0.368822	
5				P_ratio	3.434					w_net	0.910952	kW
6	T_cond	90	oC				h_5	438.2985				
7	T_evap	45	oC	T_1	40	oC	s_5	1.692784		q_in	10.19995	kW
8				T_5	95	oC				q_out	9.289002	kW
9	ηt	0.85		m_f	0.051687	kg/s	s_6s	1.692784				
10	ηp	0.85					h_6s	417.1302		η_th	8.930943	%
11				h_1	240.59		h_6	420.3054				
12	Δ_scool	5	oC	h_2s	240.9035							
13	Δ_sheat	5	oC	h_2	240.9588							
14												

Figure 4.24. The Excel-aided model with R123 as the working fluid

m_f =10/(h_4-h_2)

	A	B	C	D	E	F	G	H	I	J	K	L
1	ORC2											
2	Fluid	R134a										
3	T_high	110	oC	P_cond	3244.2		h_3	342.93		w_t	15.70966	
4	T_low	25	oC	P_evap	1160.2		h_4	425.42		w_p	2.179283	
5				P_ratio	2.796					w_net	0.811024	kW
6	T_cond	90	oC				h_5	432.229				
7	T_evap	45	oC	T_1	40	oC	s_5	1.684829		q_in	10.40814	kW
8				T_5	95	oC				q_out	9.597116	kW
9	ηt	0.85		m_f	0.059941	kg/s	s_6s	1.684829				
10	ηp	0.85					h_6s	413.7471		η_th	7.79221	%
11				h_1	256.41		h_6	416.5194				
12	Δ_scool	5	oC	h_2s	258.2624							
13	Δ_sheat	5	oC	h_2	258.5893							
14												

Figure 4.25. The Excel-aided model with R134a as the working fluid

m_f =10/(h_4-h_2)

	A	B	C	D	E	F	G	H	I	J	K	L
1	ORC2											
2	Fluid	R290										
3	T_high	110	oC	P_cond	3764.1		h_3	483.71		w_t	29.47707	
4	T_low	25	oC	P_evap	1534.6		h_4	616.47		w_p	5.722047	
5				P_ratio	2.453					w_net	0.78245	kW
6	T_cond	90	oC				h_5	629.6308				
7	T_evap	45	oC	T_1	40	oC	s_5	2.263208		q_in	10.43349	kW
8				T_5	95	oC				q_out	9.651044	kW
9	ηt	0.85		m_f	0.032938	kg/s	s_6s	2.263208				
10	ηp	0.85					h_6s	594.9519		η_th	7.499406	%
11				h_1	307.15		h_6	600.1537				
12	Δ_scool	5	oC	h_2s	312.0137							
13	Δ_sheat	5	oC	h_2	312.872							
14												

Figure 4.26. The Excel-aided model with R290 as the working fluid

Figure 4.27 compares the performance of the three fluids in terms of their mass-flow rates, net work-output, rate of waste-heat recovered, and thermal efficiency. The figure shows that the lowest mass flow rate is that of R290, but this fluid also gives the lowest net work and thermal efficiency even though it recovers the maximum rate of waste heat. Comparing R123 and R134a, the figure shows that R123 gives the highest net work and thermal efficiency with less energy input and mass flow rate. Accordingly, among the three candidate fluids, R123 offers the best performance followed by R134a and then R290. Note that the thermal efficiencies are very low compared to values of the conventional Rankine cycle discussed earlier.

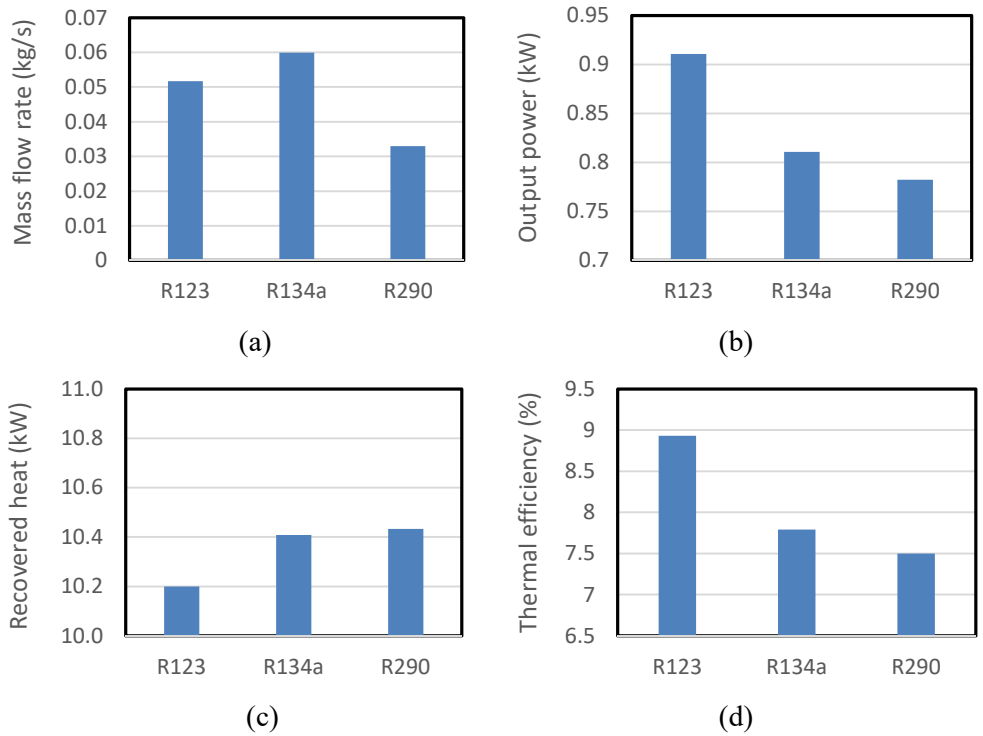

Figure 4.27. Comparison of (a) the mass flow rate, (b) net-work, (c) recovered heat, and (d) thermal efficiency of the ORC using three working fluids

4.7. Closure

Thermax property functions enable Excel to be used for thermodynamic analyses of various vapour power cycles. The chapter illustrates this capability by analysing the simple Rankine cycle, the Rankine cycle with superheat and reheat, the regenerative Rankine cycle with one feedwater heater and with two heaters, and the combined Brayton-Rankine cycle. The analyses of these cycles illustrate the advantages of the various improvements made to the simple Rankine cycle gained by increasing the net-work output and the thermal efficiency. Comparisons of the results obtained by using Thermax functions with those given by Moran and Shapiro [1] and by Cengel and Boles [2] prove the accuracy of the relevant Thermax property functions in the “Wat” group

and the "Gas" group. The chapter also illustrates the use of the functions in the "Ref" group for energy analysis of the organic Rankine cycle with R123, R134a, and R290 as working fluids.

References

[6] M.J. Moran and H.N. Shapiro, *Fundamentals of Engineering Thermodynamics*, 5th edition, John Wiley, & Sons. Inc. 2006

[7] Y. A. Cengel and M. A. Boles. *Thermodynamics an Engineering Approach*, McGraw-Hill, 8th Edition, 2015

[8] A. H. Tarrad, A Steady-State Evaluation of Simple Organic Rankine Cycle (SORC) with Low-Temperature Grade Waste Heat Source, Journal of Power and Energy Engineering, 2020, 8, 15-31

[9] American Society of Heating, Refrigeration and Air-Conditioning Engineers, (ASHRAE), Handbook of fundamentals, Atlanta, 2017.

Exercises

1. Using the Excel sheet developed for Example 4.1, study the effect of increasing the boiler pressure (P_b) on the thermal efficiency and wetness fraction at the last stages of the low-pressure turbine. Plot these two parameters for the following values of P_b: 7, 10, 15, 20 MPa.
2. By making suitable extensions to the Excel sheet developed for first-law analyses of the simple ideal Rankine cycle in Example 4.1, develop an Excel sheet for second-law analysis of the cycle. Verify your results by comparison with those obtained by Cengel and Boles [2] in their EXAMPLE 10–7.
3. Using the Excel sheet developed for Example 4.2, study the effect of varying the reheat pressure on the dryness fraction of steam at the last stages of the turbine (x_6), the net specific work, and thermal efficiency.
4. A steam power plant operates on an ideal reheat-regenerative Rankine cycle and has a net power output of 80 MW. Steam enters the high-pressure turbine at 10 MPa and 550°C and leaves at 0.8 MPa. Some steam is extracted at this pressure to heat the feed-water in an open feed-water heater. The rest of the steam is reheated to 500°C and is expanded in the low-pressure turbine to the condenser pressure of 10 kPa. Make the necessary modifications to the Excel sheet developed for Example 4.2 and use the modified sheet to study the effect of the intermediate pressure on the net work output and thermal efficiency. Use Solver to determine the exact value of the intermediate pressure that maximises the thermal efficiency.
5. Consider the steam power plant shown on Figure 4.P5 that operates with reheat and one closed feed-water heater. Steam enters the high-pressure turbine at 15 MPa and 600°C where it expands to a pressure of 700 kPa after which it is returned to the steam generator house for reheating to a temperature of 550°C. The steam then expands in the low-pressure turbine and then condensed in the condenser at a pressure of 10 kPa. Some steam leaves the low-pressure turbine at an intermediate pressure P_i = 0.3 MPa and enters the closed feed-water heater. The extracted steam exits the feed-water heat as saturated liquid at the same pressure.

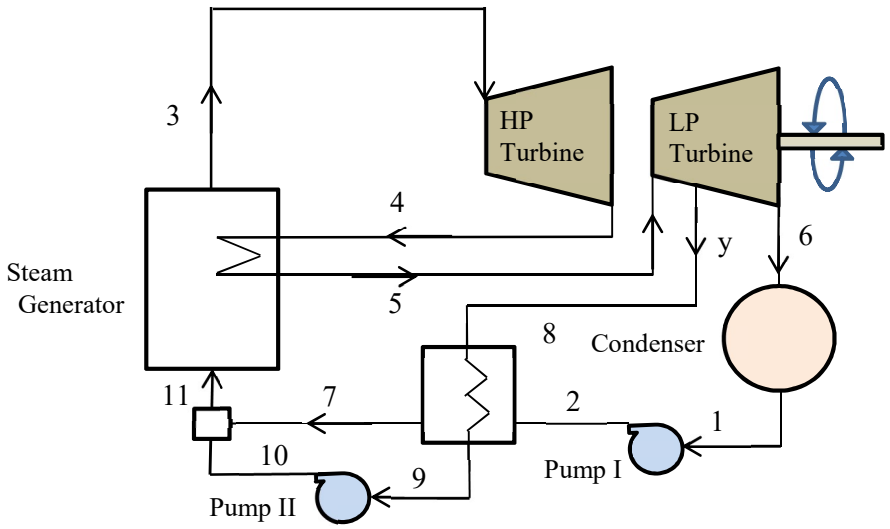

Figure 4.P5 (adapted from Cengel and Boles [2])

Using the ideal regenerative Rankine cycle model, develop an Excel sheet to determine: (i) the fraction of steam extracted from the turbine (y) and (ii) the thermal efficiency of the cycle (η). Use the Excel sheet to study the effect of varying the steam extraction pressure (P_8) on y and η. Use Solver to determine the exact value of the extraction pressure that maximises the thermal efficiency.

6. Develop the Excel sheet used to analyse the combined Brayton-Rankine cycle in Example 4.5. Use the Excel sheet to study the effects of the temperature T_5 on the overall thermal efficiency of the plant $\eta_{combined}$ and mass flow rates of the fluids in the two cycles, $\dot{m}_g$ and $\dot{m}_s$, by varying the value of T_5 from 200 to 600K.
7. Following the procedure applied in Example 4.6, select three other suitable working fluids for the ORC system, one of which is a hydrocarbon, and evaluate their thermodynamic performance at the same conditions of the example.
8. Study the effect of superheating on the performance of the three working fluids of the ORC system in Example 4.6 by repeating the analysis with ΔT_{sheat} = 0ºC, 10ºC and 15ºC. Use the same heating capacity of 10 kW for preheating and vaporizing the working fluid in the evaporator at 90˚C and keep the value of the fluid mass flow rate constant at that of ΔT_{sheat} = 0ºC for each candidate fluid regardless of the superheat degree.
9. The thermal efficiency of the organic Rankine cycle of Example 4.6 is much lower than that of the simple Rankine cycle of Example 4.1. What is *the* reason?
10. The thermal efficiency of the organic Rankine cycle of Example 4.6 using R123 is higher than those of the other two fluids. What is *the* reason?

12

Thermodynamic evaluation of a combined ORC-TFC cycle for power generation from low-grade energy sources

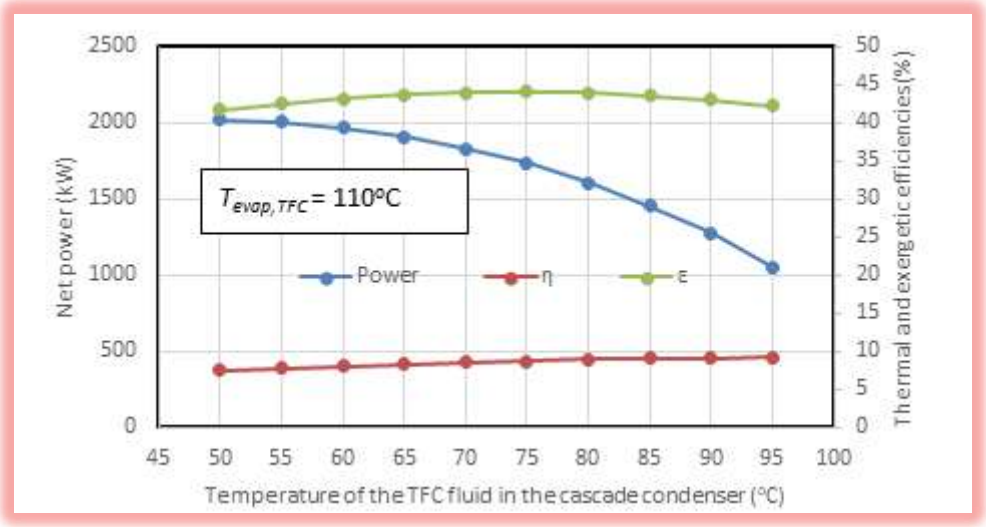

This chapter presents a combined power generation cycle for recovering the energy of low-grade heat sources that connects the Organic Rankine Cycle (ORC) with the Trilateral Flash Cycle (TFC) via a cascade condenser. By applying the TFC in the high-temperature circuit and the ORC in the low-temperature circuit, the combined cycle enjoys the merits of the two subsidiary cycles. The Excel-based model developed for evaluating the thermodynamic performance of the cycle determines the fluid properties by using Thermax functions for the refrigerants' group. The accuracy of the functions is checked by comparing their estimations with relevant published data for the basic ORC and TFC cycles with a number of relevant fluids. The performance of the combined cycle is first evaluated by comparing it with those of the simple TFC and simple ORC with R152a as the working fluid in all three cycles. It is then evaluated with five fluids of low GWP which are R1234yf in the ORC circuit and R152a, R600, R600a, or R717 in the TFC circuit. Finally, performance of the combined cycle using the pair R152a/R1234yf is compared with that using R152a as the single fluid at the cascade-condenser temperature that simultaneously maximises the cycle's power, thermal efficiency, and exergetic efficiency as determined by using the MIDACO multi-objective solver.

12.1. Literature review

The mounting concerns about the damage to the environment and the climate changes due to the use of fossil-fuels for electricity generation have inspired intensive research for the development of new technologies that utilise alternative energy sources such as solar and geothermal energy and waste heat from industries. One of the promising technologies for the utilisation of such energy sources is the organic Rankine cycle (ORC) [1-3]. Unlike the conventional Rankine cycle that requires steam at very high temperatures before expanding in the turbine, the ORC can be adapted to heat sources at low and moderate temperatures by using an organic fluid as the working fluid instead of steam. Efficiency is the main concern about the cycle and, like the conventional cycle, various modifications to the simple ORC have been considered for improving it such as reheating, regeneration, and recuperation [1]. Although such modifications are effective, they do not address an inherent drawback of the ORC which is the mismatch between the temperature of a finite heating source and that of the working fluid during the heat-addition process in the evaporator since the temperature of the working fluid remains constant while that of the heating source drops [4]. To solve this problem, the trilateral flash cycle has been proposed. In this cycle the saturated liquid fluid is not allowed to vaporise during the heat recovery process but taken directly to expand in a two-phase expander [4-7]. However, the technology of TFC expanders is relatively immature and, therefore, they are less efficient compared to the conventional turbines [1,5].

Most previous researchers developed theoretical models for comparing the performance of the ORC and TFC from thermodynamics and thermoeconomic viewpoints or compared them with other cycles such as the Kalina cycle. For example, Bidgoli and Yanagihara [2] analysed an ORC system to recover the waste heat from the intercoolers of the compression units of a large processing plant. By using Aspen HYSYS [8], they compared the performance of various working fluids including R123, n-butane, n-

pentane, hexane, and n-heptane. Their results showed that a net power of up to 40 MW could be generated with R123. Wolf et al. [3] investigated a solar powered ORC using pure iso-pentane and two iso-pentane/CO_2 zeotropic mixtures. Modelling of the system was done by using EES (engineering equation solver) software [9] while determining the thermodynamic properties by using REFPROP [10]. They conducted both exergy and exergo-economic analyses and their study showed that the investigated unit was capable of co-producing approximately 30 kW electricity and 160 kW district heating with a exergetic efficiency exceeding 60%. Therefore, the unit was able to compete with existing renewable power generating systems in terms of specific cost of electricity.

Skiadopoulos et al. [4] assessed the potential of the TFC as a promising higher efficiency alternative to the ORC for solar energy exploitation. The system they studied consisted of a field of evacuated tube collectors and a TFC engine. To develop their analytical model, the thermodynamic properties of the fluids involved were calculated by using the CoolProp library [11] wrapper for Matlab [12]. Their results showed that the efficiency of the TFC was highly dependent on the quality of the working fluid at the onset of expansion and the operating pressure ratio, but the cycle could achieve a thermal efficiency of up to 11%. For the scale of the system they considered, the levelized cost of electricity (LCOE) of the power system was estimated to be in the region of 0.26 - 0.32 €/kWh, indicating that it may be a competitive solution for solar energy exploitation. Yari et al. [5] considered a low-grade heat source with a temperature of 120^{o}C and conducted parametric studies for several working fluids in ORC and TFC cycles by using the EES software. Their results showed that increasing the inlet temperature of the TFC expander increases the net output power and decreases the product cost, but this was not the case for the ORC system. The cycles were then optimised for either maximising the net output power or minimising the product cost. Although the TFC could achieve a higher net output power compared with the ORC system, they found that its product cost was greatly affected by the expander's isentropic efficiency.

Lykas et al. [6] compared two innovative designs feeding with the same low-temperature (80-100^{o}C) heat source. The first design was an ORC system in which a small fraction of the supplied waste heat was continuously provided to the expander with the aim of approaching a quasi-isothermal process instead of the adiabatic one. The second design was the TFC. They performed parametric thermodynamic analyses of the two cycles, with R1234ze(E), R1234yf, R1233zd(E), and R134a as working fluids through Aspen Plus software [13]. By avoiding the temperature decrease due to the expansion process, their results for the modified ORC design showed that the cycle's thermal efficiency and power production increased compared to the adiabatic expansion process. Accordingly, the ORC with nearly isothermal expansion achieved higher values of both electrical and exergy efficiencies, reaching maximum values of 10.51% and 52.27%, respectively. They also showed that the electrical and exergy efficiencies determined for this cycle are higher than those of the TFC. Their techno-economic study of this cycle conducted by using Aspen Process Economic Analyzer (APEA) with the four working fluids showed that R1233zd(E) was the most proper working fluid for the cycle.

Some researchers studied the utilisation of the ORC for cogeneration. For example, Sun et al. [14] investigated the ORC cycle combined with the Absorption Refrigeration Cycle (ARC) and the Ejector Refrigeration Cycle (ERC) to recover the waste heat from the flue gas for generating both power and cooling for external uses. Their results, with R113 as the working fluid, showed that the net power output, refrigerating capacity, and exergy efficiency of the ORC-ARC combination are all higher than those of the ORC-ERC combination for evaporation temperatures of the basic ORC exceeding 153°C. Toujani et al. [15] combined the ORC with the vapour compression refrigeration (VCR) cycle for cogeneration with a negative cold (-10–0◦C) and a positive cold (0–10◦C) applications. They examined three configurations in terms of the net power, refrigeration capacity and overall efficiency and they used n-hexane as working fluids for the ORC and R600 for the VCC. Their results obtained by using the EES software showed that, for a hot spring of 1000 kW, the cycle could provide simultaneously, a maximum net work of 17 kW and a maximum net cooling capacity of 160 kW and an overall coefficient of the order of 0.3. For the production of positive cold, their results showed that the basic ORC cycle (without recovery) was the most suitable option.

Few researchers reported the results of theoretical studies of cascade ORC systems or hybrid systems involving ORC with steam turbines. For example, Oko et al. [16] presented exergoeconomic analysis of a 100 kW solar driven ORC power plant. They considered a cascade cycle of R134a and R290 as working fluids and developed their model in Microsoft Excel and MATLAB environments. They determined the energy and exergy efficiencies of the proposed plant at the optimal collector operation as 18.92 and 21.61%, respectively. The total capital investment, LCOE, payback period and the earning power of the investment were estimated to be 352 US$/kW, 0.0072 US$/kWh, 2 years 7 months, and 14.3%, respectively. Najjar and Qatramez [17] modelled a hybrid system consisting of a single flash geothermal cycle operating on a steam turbine and ORC using n-butane, isobutane, R11, and R123. The highest energy efficiency of 18.76% and net power output of 24,887MW were obtained with R11. Mokarram and Mosaffa [18] studied a cycle that integrated a steam turbine and a trans-critical ORC using R245fa. They showed that the system could produce 7.2% more power compared to a similar cycle operating in subcritical conditions. With a maximum energy and exergy efficiencies of 14.66% and 55.15%, respectively, the system's LCOE was 0.2018 USD/kWh.

Liu et al. [19] studied a two stage subcritical saturated ORC system with a heat source temperature of 100~150 C with four different organic working fluids. The EES software was used to study the ORC power generation system. They analysed the variations of the exergy efficiencies for the single-stage/two-stage systems, heaters, and condensers with the heat source temperature and also studied the effects of the mass split ratio of the geothermal fluid flowing into the preheaters and the exergy efficiency of the heater based on the condition when the exergy efficiency was maximised for the two-stage system. They found that the exergy efficiency of the two-stage system was affected by the evaporation temperatures of the organic working fluid in both the high temperature and low temperature cycles and had a maximum value and that, under the same heat sink and

heat source parameters, the exergy efficiency of the two-stage system was larger than that of the single-stage system.

The brief literature review given above and the more comprehensive review given in [20] indicate that a cycle that combines the TFC in the high-temperature circuit (HTC) and the ORC in the low-temperature circuit (LTC) has not been considered before. While minimising the mismatch between the working fluid and the heat source for the ORC, the new cycle enables a turbine to be used in the LTC instead of the two-phase expander that, according to [4, 5, and 6], is the main factor for degrading the efficiency of the TFC. Moreover, different organic fluids can be used in the HTC and LTC that suit the high and low temperature ranges better than a single fluid. Needless to say that such a cycle also gives cogeneration systems more flexibility than a single ORC or LTC. In this regard, the present chapter contributes to knowledge by presenting a thermodynamic evaluation and multi-objective optimisation of this new cycle using a single working fluid as well as various environment-friendly fluids. From another perspective, the literature review shows that most researchers used commercial software [8-13] for their analyses. However, the use of general-purpose software can encourage independent researchers and engineering students to contribute to the development of innovative ORC and TFC systems using suitable fluids [21, 22]. In this respect, the model used in the present study uses Microsoft Excel as the modelling platform with special VBA functions to determine the thermodynamic properties of the working fluids. While the versatile solver that comes with Excel can be used for single-objective optimisation analyses, the free version of the MIDACO solver [23] or the Solver-TOPSIS technique described in [24] can be used for multi-objective optimisation analyses.

12.2. The ORC, TFC, and the proposed combined ORC-TFC cycle

Figure 12.1 shows schematic diagrams of the simple ORC and TFC systems and Figure 12.2 shows their respective *T-s* diagrams. As Figure 12.1.a shows, the ORC system has the same components as those of the conventional steam-turbine power plant which are the evaporator (boiler), the turbine, the condenser, and the pump. Organic fluids are used in the ORC instead of water because they have higher boiling pressures at low temperatures and, therefore, suit the low-temperature applications better. To avoid the problem of blade erosion at the last turbine stages, dry or isentropic fluids are usually selected for which the saturated liquid-vapour curves have negative or infinite slopes, respectively [1,19]. The TFC system also uses organic fluids, but the TFC system is different from the ORC system in that it heats the working fluid without going into the vaporisation process so that the hot pressurised fluid expands in the two-phase region. As Figure 12.2.b shows, this cycle leads to a uniform temperature glide between the heat source and the working fluid; which reduces the losses during the heat-transfer process and improves the performance of the TFC systems. Typically, TFC systems can provide 50% more work than ORC systems for the same energy input, but they need sophisticated expanders that can adequately handle the liquid-phase presence during the expansion process [1]. Apart from increasing the investment cost, two-phase expanders are generally less efficient than conventional vapour turbines.

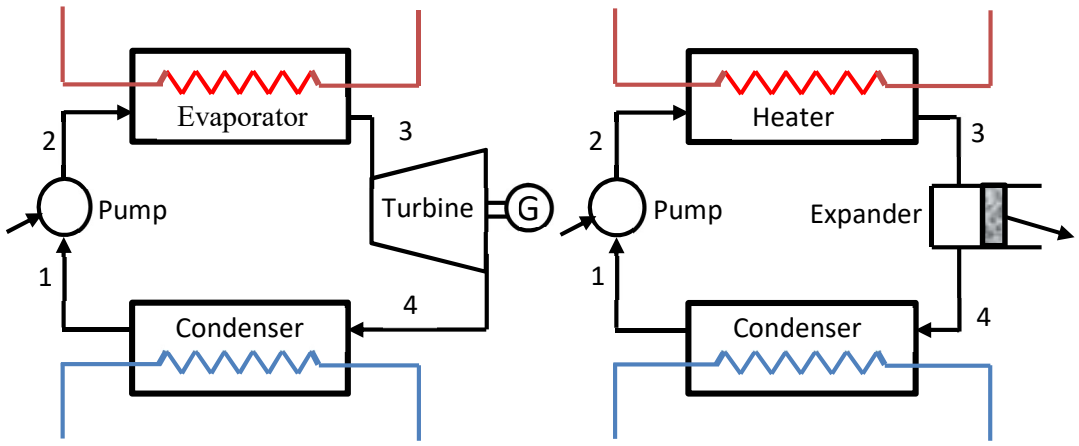

(a) (b)

Figure 12.1. Schematic diagrams of: (a) the ORC system and (b) the TFC system

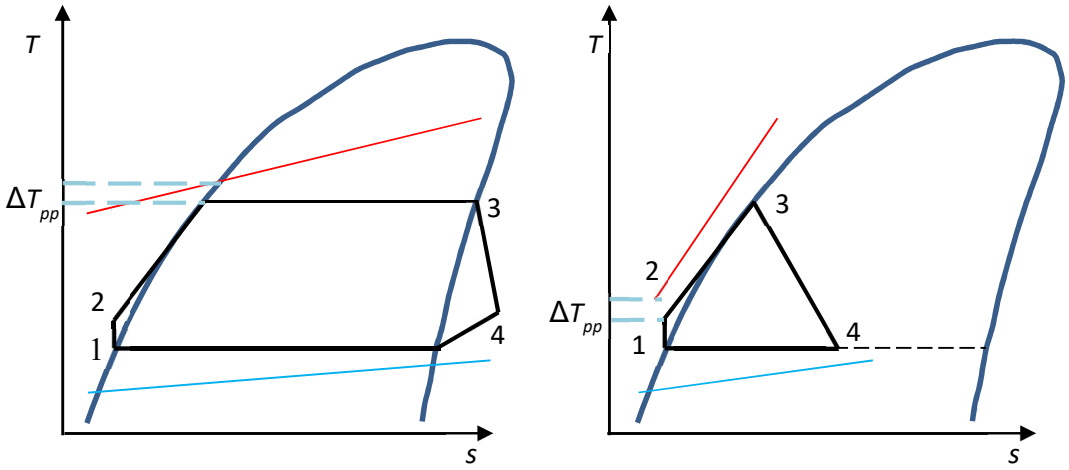

(a) (b)

Figure 12.2. *T-s* diagrams of: (a) the ORC cycle and (b) the TFC cycle

Figure 12.3.a shows a schematic diagram of the combined-cycle system in which the heat source is first used to heat the working fluid of the TFC circuit and then heat the working fluid of the ORC circuit. After expanding in the two-phase expander to produce power, the working fluid of the TFC circuit is condensed by the cooler working fluid of the ORC circuit in a cascade condenser (cc) before being pumped into the TFC heater. The ORC system shown on Figure 12.3.a is a recuperative system in which the superheated fluid exiting the turbine is used to heat the cold fluid exiting the pump in an internal heat-exchanger (IHEX). Accordingly, the initially superheated fluid exiting the turbine enters the condenser of the ORC as saturated vapour. In the condenser, the working fluid is cooled by the cold-sink fluid to the saturated-liquid state and then pumped into the cold

side of the IHEX. After the IHEX, the fluid is heated by the heat source to the state of saturated liquid before entering the cascade condenser where it is heated further by the condensing fluid of the TFC circuit until it becomes saturated vapour.

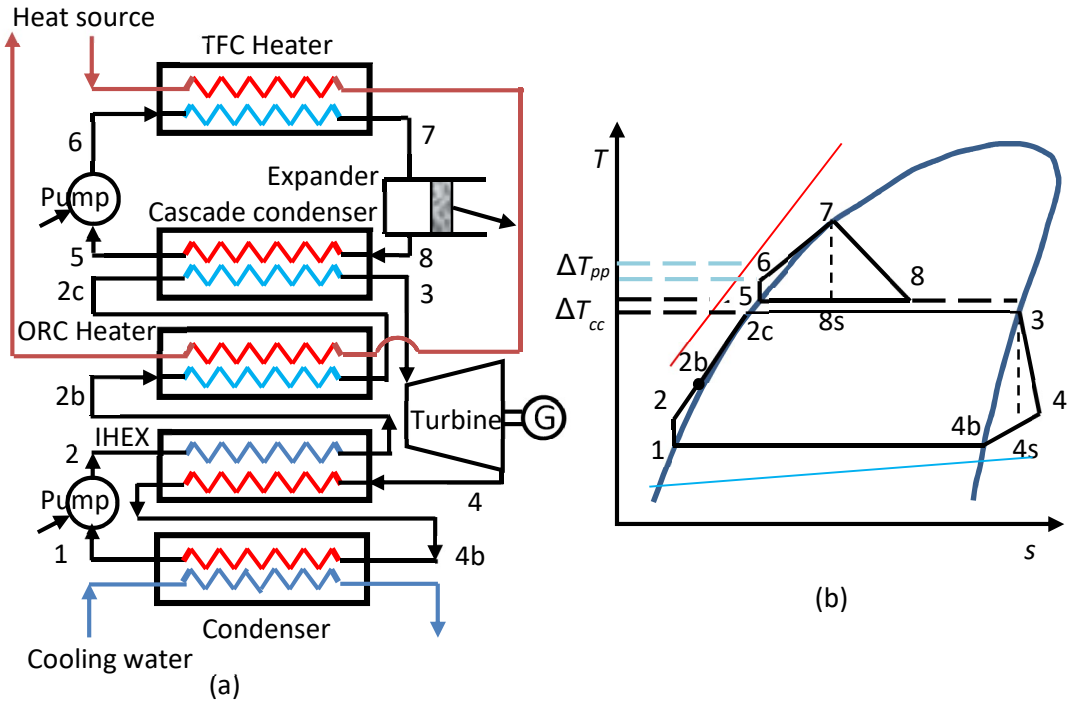

Figure 12.3. Schematic and *T-s* diagrams for the combined ORC-TFC cycle

Figure 12.3.b shows the *T-s* diagram of the combined cycle. Unlike the TFC cycle in which the pinch point occurs where the heating fluid exits the system, that of the combined cycle occurs in the middle of the heating process which forces the heating source to exit the system at a higher temperature than that of the TFC. Although this limits the amount of heat recovered and the work produced by the ORC circuit, the combined cycle can still produce more work than the simple ORC alone because of the additional work produced by the TFC circuit. Compared to a simple TFC, the combined cycle may not be able to produce the same power but it can have a higher thermal efficiency by replacing the two-phase expander with the single-phase turbine and by allowing two different working fluids to be used in the TFC and ORC circuits that lead to a better overall performance than a single fluid.

12.3. The analytical model for the combined cycle

The analytical model for the present thermodynamic analyses assumes steady-state operation and neglect pressure losses and heat-transfer losses in the various components. However, the losses due to irreversibility in the pumps, the turbine, and the two-phase expander are taken into consideration via the relevant the isentropic efficiencies [25].

12.3.1. The analytical model for the TFC circuit

Given the pinch-point temperature difference, ΔT_{pp}, the temperature of the heat source exiting the heater of the TFC, $T_{hso,TFC}$, is determined from:

$$T_{hso,TFC} = T_6 + \Delta T_{pp} \tag{12.1}$$

Given the inlet temperature of the heat source, $T_{hs,in}$, and its mass flow rate, $\dot{m}_{hs}$, the rate of heat transfer from the heat source (a stream of hot-water) to the working fluid of the TFC, $\dot{Q}_{hs,TFC}$, and the mass flow rate of the working fluid, $\dot{m}_{TFC}$, are calculated from:

$$\dot{Q}_{hs,TFC} = \dot{m}_{hs} c_p \left(T_{hs,in} - T_{hso,TFC}\right) \tag{12.2}$$

$$\dot{m}_{TFC} = \dot{Q}_{hs,TFC} / \left(h_7 - h_6\right) \tag{12.3}$$

The specific work, in kJ per kg, of the working fluid in the TFC during the two-phase expansion process is evaluated from the enthalpy change as follows:

$$w_{exp} = \left(h_7 - h_{8s}\right) \times \eta_{exp} \tag{12.4}$$

Where η_{exp} is the isentropic efficiency of the expander and h_{8s} is the enthalpy of the fluid after an isentropic expansion (refer to Figure 12.3.b). The TFC pump specific work is given by:

$$w_{p,TFC} = v_5 \left(p_{eva,TFC} - p_{cc,TFC}\right) / \eta_{p,TFC} \tag{12.5}$$

Where $p_{eva,TFC}$ and $p_{cc,TFC}$ are the pressures of the TFC fluid in the evaporator and cascade-condenser, respectively. Equation (12.6) is then used to determine the enthalpy of the fluid at state 6 after the pump:

$$h_6 = h_5 + w_{p,TFC} \tag{12.6}$$

The thermal efficiency of the TFC circuit alone is given by:

$$\eta_{TFC} = \dot{m}_{TFC} \left(w_{exp} - w_{p,TFC}\right) / \dot{Q}_{hs,TFC} \tag{12.7}$$

12.3.2. The analytical model for the ORC circuit

Referring to Figure 12.3b, the mass flow rate of the working fluid in the ORC circuit is given by:

$$\dot{m}_{ORC} = \dot{m}_{TFC} \left(h_8 - h_5\right) / \left(h_3 - h_{2c}\right) \tag{12.8}$$

The pump specific work is given by:

$$w_{p,ORC} = v_1\left(p_{cc,ORC} - p_{con,ORC}\right)/\eta_{p,ORC} \tag{12.9}$$

Where $\eta_{p,ORC}$ is the isentropic efficiency of the ORC pump. Energy balance over the IHEX gives:

$$h_{2b} = h_2 + \left(h_4 - h_{4b}\right) \tag{12.10}$$

Where h_{4b} is the enthalpy of the saturated vapour at the condenser pressure. The enthalpy h_4 is determined by taking into consideration the irreversibility of the turbine as follows:

$$h_4 = h_3 + \left(h_3 - h_{4s}\right)\times\eta_t \tag{12.11}$$

Where h_{4s} is the enthalpy after an isentropic expansion and η_t is the isentropic efficiency of the turbine. The turbine's specific work is then calculated from:

$$w_t = h_3 - h_4 \tag{12.12}$$

The thermal efficiency of the ORC circuit alone is given by:

$$\eta_{ORC} = \dot{m}_{ORC}\left(w_t - w_{p,ORC}\right)/\dot{Q}_{hs,TFC} \tag{12.13}$$

Where $\dot{Q}_{hs,ORC}$ is the heat recovered in the ORC circuit, which is given by:

$$\dot{Q}_{hs,ORC} = \dot{m}_{ORC}\left(h_{2c} - h_{2b}\right) \tag{12.14}$$

12.3.3. The analytical model for the combined cycle

The total heat recovered from the heat source and total net power produced by the combined cycle, respectively, are given by:

$$\dot{Q}_{hs,tot} = \dot{Q}_{hs,TFC} + \dot{Q}_{hs,ORC} \tag{12.15}$$

$$\dot{W}_{tot} = \dot{m}_{ORC}\left(w_t - w_{p,ORC}\right) + \dot{m}_{TFC}\left(w_{exp} - w_{p,TFC}\right) \tag{12.16}$$

The overall thermal efficiency and the second-law (exergetic) efficiency of the cycle are given by:

$$\eta_{tot} = \dot{W}_{tot}/\dot{Q}_{hs,tot} \tag{12.17}$$

$$\varepsilon_{tot} = \dot{W}_{tot} / \dot{E}_{hs,in} \tag{12.18}$$

Where $\dot{E}_{hs,in}$ in Equation (12.18) is the rate of exergy flow of the heat source entering the system following the definition adopted by Yari et al. [5]:

$$\dot{E}_{hs,in} = \dot{m}_{hs}\left[\left(h_{hs,in} - h_0\right) - T_0\left(s_{hs,in} - s_0\right)\right] \tag{12.19}$$

The temperature of the heat source exiting the system is given by:

$$T_{hs,out} = T_{hs,in} - \dot{Q}_{hs,tot} / \dot{m}_{hs} c_p \tag{12.20}$$

Where c_p is the specific heat of the heating medium.

12.4. Excel models for the ORC and TFC and their validation

The Excel-based models developed for the present analyses determine the thermal fluid properties by using the Thermax add-in [26] that provides property functions for ideal gases, saturated water and superheated steam, 28 synthetic and natural refrigerants, humid-air for psychrometric analyses, two aqua solutions for vapour-absorption refrigeration, combustion and chemically-reacting substances, and atmospheric air at various temperatures. Regarding the functions associated with the present analyses, which are those of the refrigerants group, the functions for saturated liquids and saturated vapours interpolate the data given by ASHRAE [27]. The functions that determine the enthalpy and entropy of superheated refrigerants use ideal-gas equations in which the specific heat is determined at an adjusted pressure by multiplying the actual pressure by a "compressibility factor" for which an average value of 0.5 is adopted [28]. Although this approximation enables the functions to be used for supercritical conditions, the accuracy of the functions needs to be verified. El-Awad et al. [28] assessed their accuracy for the analyses a simple VCR system by comparing their estimations with the values provided by Atalay and Conan [29], who used REFPROP, for two ozone-friendly refrigerants, R410A and R1234yf, and two natural refrigerants, R290 and, R744. El-Awad et al. [28] also analysed a cascade VCR system with R507A in the high-temperature circuit and R23 in the low-temperature circuit and compared the results of the functions with those obtained by Parekh and Tailor [30] who used EES. In what follows, the functions are verified for the present analyses by comparing the results of the models developed for the simple ORC and TFC cycles with relevant published data.

12.4.1. The ORC model and its validation

Yari et al. [5] analysed the simple ORC with a heat source at 120°C with the data shown on Table 12.1. Their results for seven working fluids, which are: R134a, R1234yf and R152a, propane (R290), n-butane (R600), iso-butane (R600a), and ammonia (R717), were used to verify Thermax property functions for this cycle and Figure 12.4 shows the Excel-aided model developed for the system. The sheet consists of four blocks of cells.

The first block on the left side of the sheet stores the specified data, while the second and third blocks in the middle perform the calculations for the ORC cycle. The fourth block on the right side of the sheet determines the overall cycle parameters that include the total amount of recovered heat (Qhs_tot), the net power produced by the system (Work_net), the exit temperature of the heating source (Ths_out), and the overall energetic (therm_eff) and exergetic (exg_eff) efficiencies. The sheet uses R152a as the working fluid, but the name of the fluid is stored as a variable so that it can be used for other fluids. The "Run" button shown in the figure is linked to a macro that records the model's calculations for the first fluid so that the same calculations can easily be repeated for the other fluids.

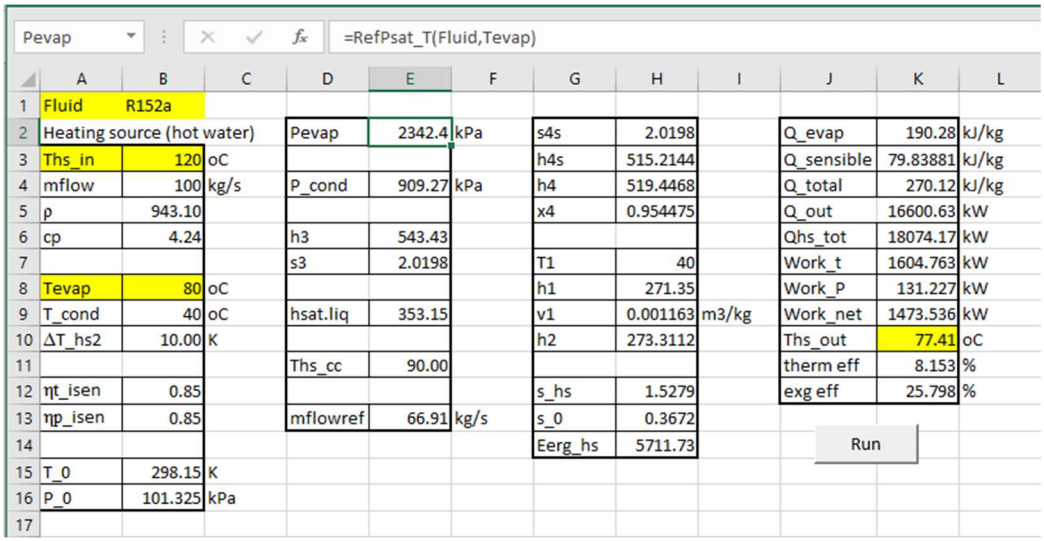

Figure 12.4. The Excel-aided model for the simple ORC with the data given by [5]

Table 12.1. Values of the parameters used for validating the simple ORC model [5]

Parameter	Value
T_{hs} (°C)	120
$\dot{m}_{hs}$ (kg/s)	100
T_{cond} (°C)	40
ΔT_{pp} (K)	10
η_p (%)	85
η_t (%)	85

The system's power output, thermal efficiency, and exergetic efficiency were calculated at various values of the turbine's inlet temperature, T_3, which is the temperature of the working fluid in the evaporator. The results obtained by the present model for the seven fluids are compared on Figures 12.5 and 12.6 with those obtained by Yari et al [5] who developed their model by using the EES software. The two figures show close agreement between the results of the present model and their model.

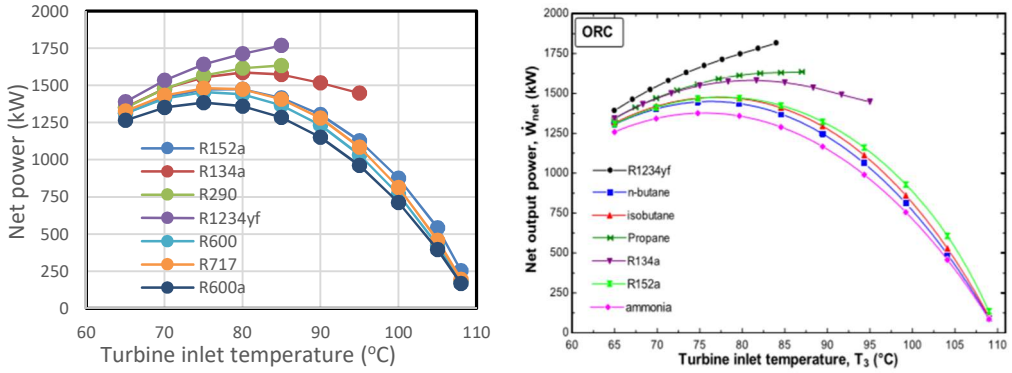

(a) (b)

Figure 12.5. Comparison of (a) the model's estimations for the net power of the ORC at various values of T_3 with (b) the reference [5]

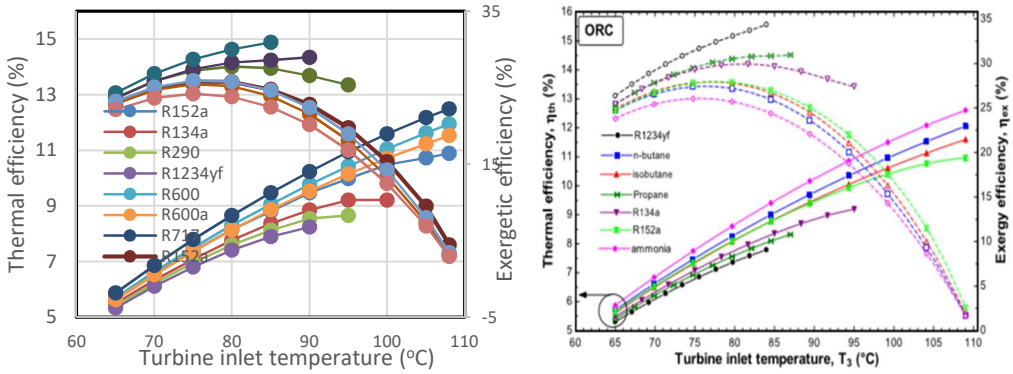

(a) (b)

Figure 12.6. Comparison of (a) the model's estimations for thermal efficiency and exergetic efficiency of the ORC at various values of T_3 with (b) the reference [5]

12.4.2. The TFC model and its validation

Figure 12.7 shows the model developed for the TFC using the data provided by Lai et al. [6] who analysed the cycle with a heat source at 80°C. In their analyses, the mass flow rate of the heat source was 4.16 kg/s, the heat sink temperature was maintained at 30°C, the fluid's inlet temperature to the condenser was 37°C, and the isentropic efficiency of the pump was 0.7. Lai et al. [6] fixed the operating temperature at the inlet of the pump (T_2) at 35°C. The model shown on Figure 12.7 uses the same data, but T_2 is evaluated by the model and not fixed. For their analyses, Lai et al. [6] selected four working fluids that are commonly used in low-grade power generation systems, which are R134a, R236fa, R245fa, and R1233zd. They evaluated the fluid properties by using the REFPROP software. Since R236fa is not supported by Thermax, comparison will be made with the other three fluids, which are R134a, R245fa, and R1233zd. Figure 12.8. that shows the results obtained by the present model also shows a close agreement with the results of the reference model shown on Figure 12.9. While R236fa and R1233zd have comparable power and thermal efficiency, R134a has considerably lower values.

ηnozzle =0.865+0.00175*(1/Refv_Tx(Fluid_TFC,Tcond_TFC,1))

	A	B	C	D	E	F	G	H	I	J	K	L	M	N	
1	Fluid_ORC			TFC cycle											
2	Fluid_TFC	R134a		Ths_out	42.00		s2	1.18013		x4	0.248143		Workt_TFC	26.34512	kW
3	Heating source (hot water)						h3	295.765		ηrotor	0.655647		Workp_TFC	18.270	kW
4	Ths_in	80	oC	Pevap_TFC	1890.2		s3	1.30885					Worknet_TFC	8.075621	kW
5	mflow	4.160	kg/s	Pcond_TFC	937.5		ss4	1.30885		ED_exp	2.2291	kW			
6	ρ	971.80		h1	251.955		xss4	0.247247		ED_cc_TFC	0.258	kW	Q_TFC	663.4618	kW
7	cp	4.20		s1	1.1764		hss4	293.0338		ED_pump_1	17.30465	kW	η_TFC	1.217	%
8	TFC			mf_TFC	15.56109		ηnozzle	0.945441					ε_TFC	9.891473	%
9	Tevap_TFC	65		v1	0.000863	m3/kg	wnozzle	2.582203		shs_in	1.0756				
10	Tcond_TFC	37		h2	253.1291		h4	293.1828		s_0	0.3672		Button 1		
11				T2	37.79358		s4	1.30933		Exerg_hs	81.64				
12	ΔT_hs2	5.00	K												
13	ηp	0.7													
14															
15	T_0	298.15	K												
16	P_0	101.325	kPa												
17															

Figure 12.7. The Excel-aided model for the TFC using R134a with the data of [6]

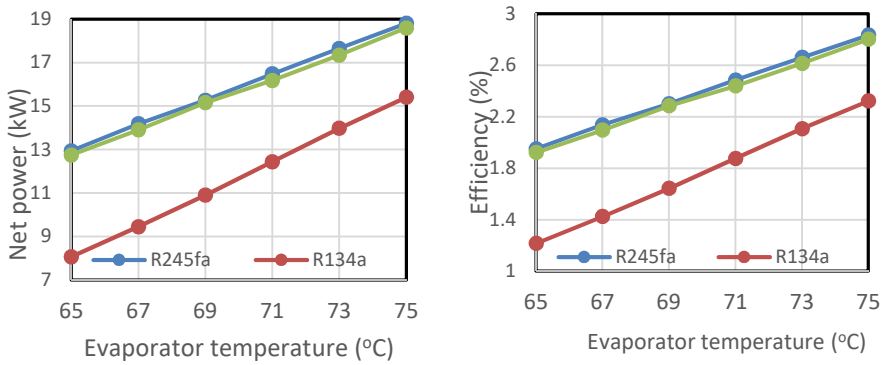

(a) (b)

Figure 12.8. Variations of the net power and thermal efficiency of the TFC with the evaporation temperature as obtained by the present model

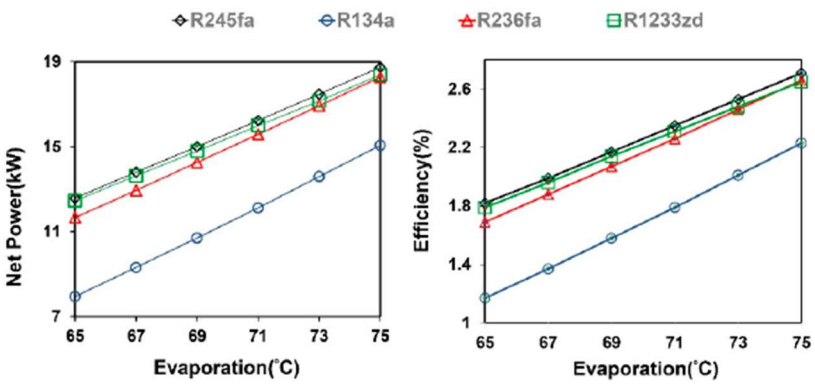

(a) (b)

Figure 12.9. Variations of the net power and thermal efficiency of the TFC with the evaporation temperature as given by Lai et al. [6]

12.5. The Excel model for the combined cycle and comparison with the ORC and TFC using R152a only

Figure 12.10 shows the model developed for the combined cycle in which the first block of cells on the left side of the sheet stores the specified data, while the second and third blocks in the middle perform the calculations for the TFC and ORC circuits, respectively. The fourth block on the right side of the sheet determines the overall cycle parameters. The names of the working fluids in the TFC and ORC circuits are stored as variables so that the model can be used for different fluid pairs, but for the present comparison R152a is used in both circuits. The cascade-condenser temperature difference is taken as 3°C. Figure 10.12 shows that the temperature of the TFC fluid in the cascade condenser, Tcc_TFC, and that of the ORC fluid, Tcc_ORC, are specified as 83°C and 80°C, respectively.

Pevap_TFC =RefPsat_T(Fluid_TFC,Tevap_TFC)

	A	B	C	D	E	F	G	H	I	J	K	L	M	N	O
1	**Working fluids**			**TFC cycle**									**TFC**		
2	Fluid_TFC	R152a		T_hsi	93.00		s6	1.508015		h8	434.86189		Workt_TFC	656.4599	kW
3	Fluid_ORC	R152a					h7	439.22		s8	1.7098828		Workp_TFC	433.9989	kW
4	**Heating source (hot water)**			Pevap_TFC	4243.2		s7	1.7058					Worknet_TFC	222.4611	kW
5	T_hs	120	oC	Pcc_TFC	2503.08								Q_TFC	11458.8	kW
6	mflow	100	kg/s	h5	360.266		ss8	1.7058					η_TFC	1.941	%
7	ρ	943.10	kg/m3	s5	1.50023		xss8	0.40023							
8	cp	4.24	kJ/kg.K	mf_TFC	150.62947		hss8	433.4092		s_hs	1.5279		**ORC**		
9	**TFC**			v5	0.0014074	m3/kg				s_0	0.3672		Q_sensible	91.67203	kJ/kg
10	Tevap_TFC	110	oC	h6	363.1472					Exerg_hs	3472.92		Q_ORC	5413.38	kW
11	Tcc_TFC	83	oC	T6	84.214554								Workt_ORC	1416.248	kW
12	ΔTcc	3	K	**ORC cycle**									Workp_ORC	115.811	kW
13	ΔT_hs2	10	K	Tcc_ORC	80	oC	s4s	2.0198		h2	273.31119		Worknet_ORC	1300.436	kW
14	**ORC**			Pcc_ORC	2342.4	kPa	h4s	515.2144		T2	41.037827		η_ORC	7.811	%
15	Tcond_ORC	40	oC	Pcond_ORC	909.27	kPa	h4	519.4468		s2	1.2472232				
16	ΔT_sc	0.00	K				T4	40					**Overall parameters**		
17	ηt_isen	0.85		h3	543.43		s4	2.033315		h2b	261.47797		Q_total	16872.18	kW
18	ηp_isen	0.85		s3	2.0198					T2b	34.724121	kJ/kg	T_hsout	80.24	oC
19	ηx_isen	0.75		h2c	353.15		T1	40	oC	s2b	1.2098085	kg/s	Q_out	15349.28	kW
20	T_0	298.15	K	s2c	1.481		h1	271.35	kJ/kg						
21	P_0	101.325	kPa				v1	0.001163	m3/kg	Qevap_ORC	190.28	kW	W_total	1522.897	kW
22				h4b	531.28		s1	1.2411		mf_ORC	59.05	kW	η_overall	9.026	%
23				s4b	2.0711								ε_overall	43.85063	%
24															

Figure 12.10. Excel-aided model for the combined cycle using R152a with the data shown on Table 12.1

By fixing value of the temperature of the TFC fluid entering the expander at 110°C, the power, thermal efficiency, and exergetic efficiency of the combined cycle were calculated at various values of the cascade-condenser temperature in the cycle with R152a as the single working fluid. The results are plotted on Figure 12.11 which shows that the thermal efficiency of the combined cycle increases steadily with the temperature of the ORC fluid in the cascade condenser, but its power drops while the exergetic efficiency has a maximum value at the cascade temperature of 75°C. Clearly, the combined cycle has a certain cascade temperature that gives the best trade-off between its produced power, thermal efficiency, and exergetic efficiency. Initially, the performance of the combined cycle will be compared to that of the ORC and TFC cycles using the same working fluid in all three cycles, which is R152a. The comparison will be for a heat-source at 120°C and using the data shown on Table 12.1.

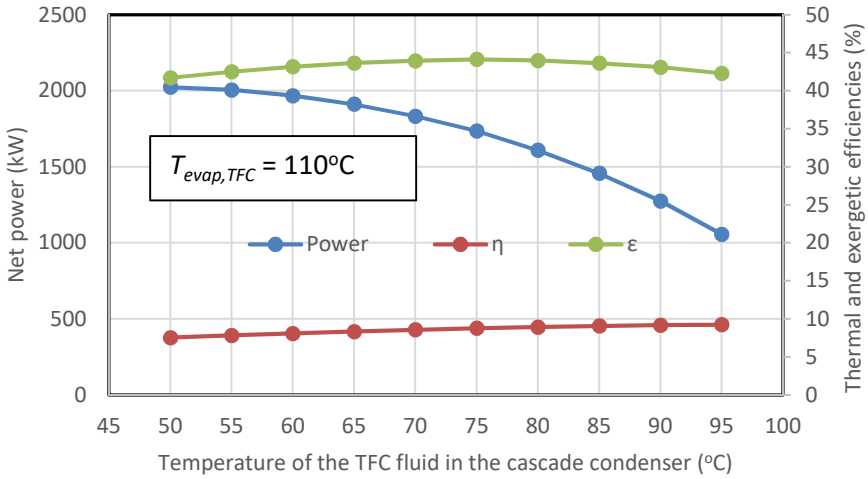

Figure 12.11. Variation of the combined-cycle's power and thermal and exergetic efficiencies with the temperature of the TFC fluid in the cascade condenser

In order to make comparison with the TFC at a heat-source of 120°C and using the input data of Table 12.1, the TFC model shown on Figure 12.7 has to be modified. Figure 12.12 shows the modified TFC model with R152a as the working fluid. The temperature of the TFC fluid entering the TFC expander is taken as 110°C for both the TFC and the combined cycle and the isentropic efficiency of the TFC expander is specified as 75% for both cycles. Also note that the condenser temperature for the TFC is now 40°C and pinch-point temperature difference is 10°C. Figures 12.5 shows that the ORC has a certain temperature in its evaporator that maximises its output power, which is 80°C. Therefore, the comparison with the ORC will be based on the cycle's performance at this temperature as shown on Figure 12.4.

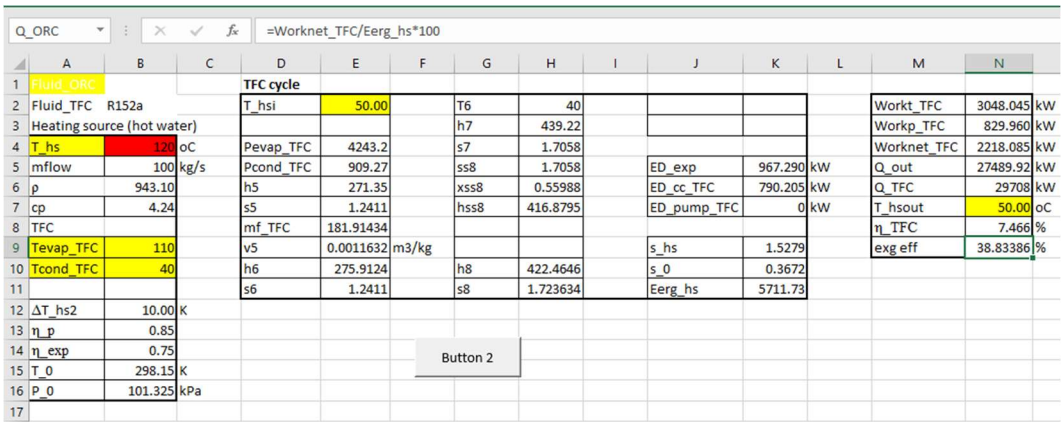

Figure 12.12. The modified model for the TFC cycle using R152a with the data of Table 12.1

Table 12.2 compares the values obtained by the three cycles for a number of performance indicators. For the TFC and ORC cycles, the relevant values are obtained from Figure 12.12 and Figure 12.4, respectively. For the combined cycle, three sets of values are shown which correspond to three values of the temperature of the ORC fluid in the cascade condenser, Tcc_ORC, which are 70°C (CC-70), 80°C (CC-80), and 90°C (CC-90). The table figures show that the lowest exit temperature for the heat source is that of the TFC, which is 50°C, and the highest exit temperature is that of the combined cycle CC_90, which is 90.72°C.

Table 12.2. Performance parameters of the ORC, TFC, and the combined cycle

	TFC	ORC	CC-70	CC-80	CC-90
Ths,out (°C)	50	77.41	71.75	80.24	90.72
Qin (kW)	29708	18074.17	20479.42	16872.18	12427.7
Qout (kW)	27489.92	16600.63	18700.75	15349.28	11278.86
Power (kW)	2218.085	1473.536	1778.665	1522.897	1148.837
Thermal efficiency (%)	7.466	8.153	8.685	9.026	9.244
Exergetic efficiency (%)	38.834	25.798	31.141	43.851	20.114

Figures 12.13 and 12.14 compare amount of heat recovered, power produced, thermal efficiency, and exergetic efficiency of the three cycles. Figures 12.13 shows that the simple TFC recovers the most energy and produces the most power compared to the other two cycles. The figure also shows that both the heat recovered and power produced by the combined cycle decrease as the cascade temperature is increased. The recovered energy and power produced by the combined cycle are lower than those of the TFC for all three cascade temperatures, but higher than that of the ORC for cascade temperatures of 80°C and below. Figure 12.13.a shows that at the cascade temperature of 80°C the combined cycle recovers less amount of energy from the heat source compared to the other two cycles and, therefore, rejects less energy to the cooling water in the condenser; which means that the cooling system can be smaller and less expensive.

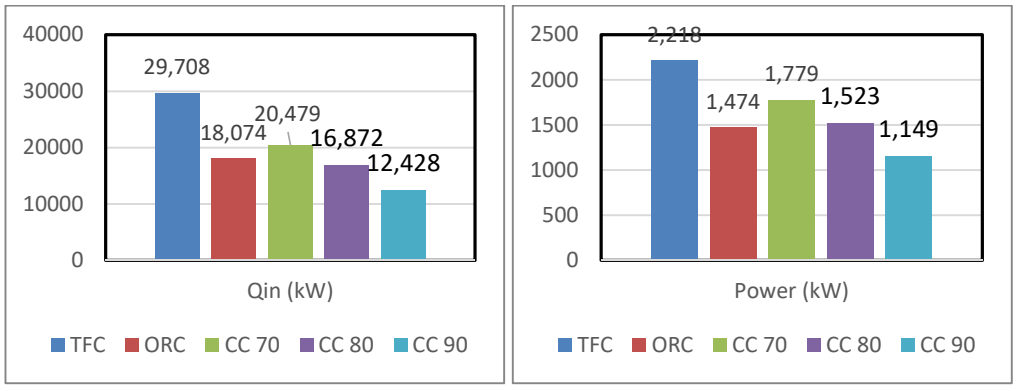

Figure 12.13. Comparison of the recovered heating source energy and power produced by the combined cycle with those of the simple TFC and ORC

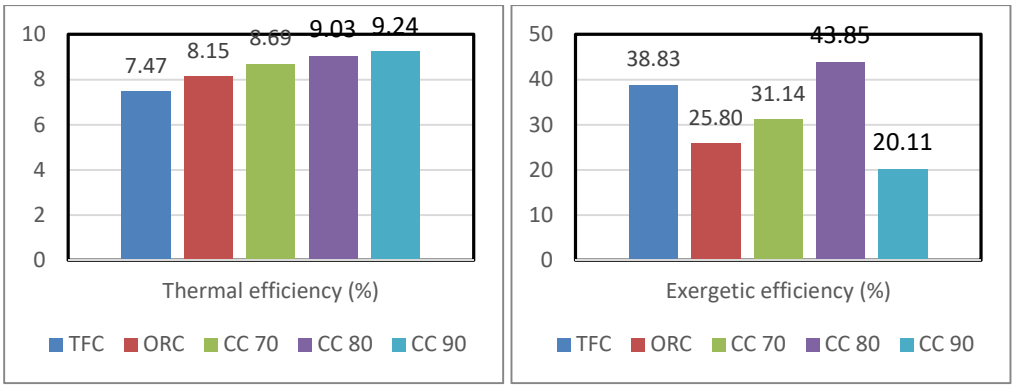

Figure 12.14. Comaprison of the and thermal efficiency and exergetic efficiency of the combined cycle with those of the simple TFC and ORC

An unconditional advantage of the combined cycle is revealed by Figure 12.14.a that shows that its thermal efficiency is higher than those of the TFC and ORC cycles at all three cascade temperatures and increases with the cascade temperature. Figure 12.14.b shows that the exergetic efficiency of the combined cycle at the cascade temperature of 80°C exceeds those for both the simple TFC and ORC cycles.

12.6. Analysis of the combined cycle with five low-GWP fluids

The evaluation of the combined cycle presented in the previous section did not take into consideration an important advantage of the combined cycle which is the allowance to use different working fluids in the TFC and ORC circuits. This section analyses the performance of the combined cycle for the medium-temperature source of 120°C with five fluids that have zero ozone-layer depletion potential (ODP) and low global-warming potential (GWP), which are R152a, R1234yf, R600, R600a, and R717. Table 12.3 shows their physical characteristics, GWP, and safety groups.

Table 12.3. Boiling point, ODP, GWP, and safety group of the five fluids [27]

Fluid	Normal boiling point (°C)	Critical temperature (°C)	Critical pressure (kPa)	GWP	Safety group
R1234yf	–29.4	94.7	3382.2	<1	A2L
R152a	–24	113.26	4516.8	138	A2
R600	0	151.98	3796.0	4	A3
R600a	–12	134.66	3629.0	−20	A3
R717	−33.33	132.25	11,333.0	0	B2L

Figures 12.5 and 12.6 show that R1234yf can achieve the highest power and exergetic efficiency in the lower-temperature range, but it has the lowest thermal efficency. By using R1234yf in the ORC circuit and R152a in the TFC circuit of the combined cycle, the model was used to calculate the power and thermal efficiency of the cycle at various temperatures in the cascade condenser. Figure 12.15 compares the values obtained by

this pair with those of the simple ORC shown on Figures 12.5 and 12.6 and those of the combined cycle with R152a in both circuits shown in Figure 12.11.

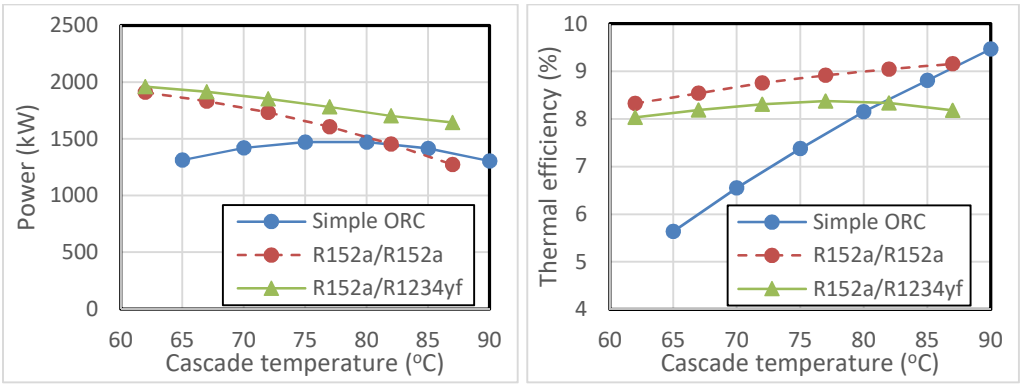

(a) (b)

Figure 12.15. Comparison of (a) the power and (b) thermal efficiency of the combined cycle with R152a/R1234yf with those with R152a/R152a and the simple ORC

Figure 12.15.a shows that both the power and thermal efficiency of the combined cycle with both fluid pairs are higher than those of the simple ORC at values of the cascade temperature below 80°C, i.e., when the contribution of the TFC circuit is dominant. The figure also shows that the power of the combined cycle with the R152a/R1234yf pair remains higher than that of the R152a/R152a pair over the whole range of cascade temperatures. However, Figure 12.15.b shows that the thermal efficiency of the combined cycle with the R152a/R1234yf pair remains lower than that of the R152a/R152a pair over the whole range of cascade temperatures. The model was also used to calculate the power and thermal efficiency of the combined cycle with the other three fluid pairs. The percentage deviations of the calculated values of the power and thermal efficiency from those of the R152a/R1234yf pair are shown on Figure 12.16.

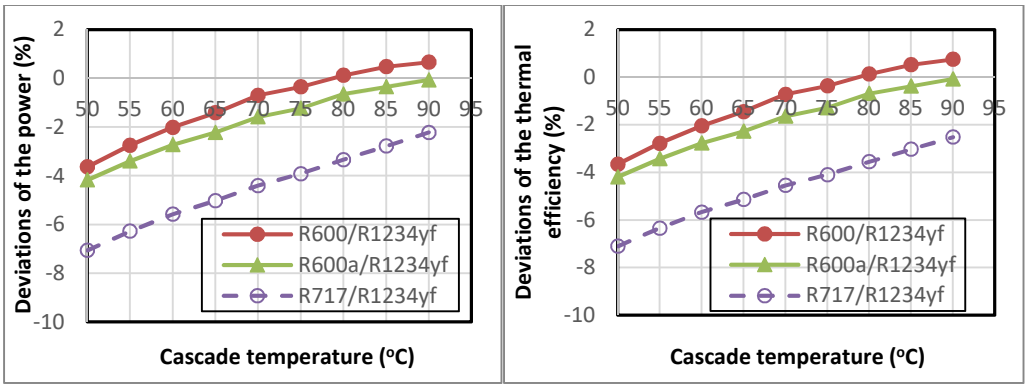

(a) (b)

Figure 12.16. Percentage deviations of (a) the power and (b) thermal efficiency of the combined cycle with R600, R600a, and R717 in the TFC circuit from those with R152a

Figure 12.16.a shows that all three pairs produce less power than R152a/R1234yf for cascade temperatures below 80°C, but the lowest values are those of the pair involving R717. For all three fluid pairs, the deficits from the R152a/R1234yf pair diminish steadily as the cascade temperature is increased, but only R600/R1234yf manges to produce more power than R152a/R1234yf at cascade temperatures above 80°C. Figure 12.16.b shows that the thermal efficiency for each fluid pair deviates from the corresponding values of the R152a/R1234yf pair by the same pecentage as the pair's power.

12.7. Tri-objective optimisation of the combined cycle

The previous analysis shows that the two most favourable pairs for the combined cycle are R152a/R152a and R152a/R1234yf, but the analysis did not take the exergetic efficiency into consideration. Comparing the cycle's performance with the two fluid pairs at the cascade temperature that gives the best trade-off between its power, thermal efficiency, and exergetic efficiency is a tri-objective optimisation (3OO) problem that requires the three cycle parameters to be simultaneously maximised. In general, multi-objective optimisation (MOO) analyses of energy-conversion systems involve other factors such as the economic and environmental factors. While single-objective optimisation analyses can easily be done by using Excel's Solver, MOO analyses require a suitable solver. Fortunately, the present analysis involves a single changing variable, which is the temperature in the cascade condenser and, therefore, it can be conducted by using the free version of the MIDACO solver [22] that allows up to four changing variables to be considered. The set-up for MIDACO is shown on Figure 12.17.

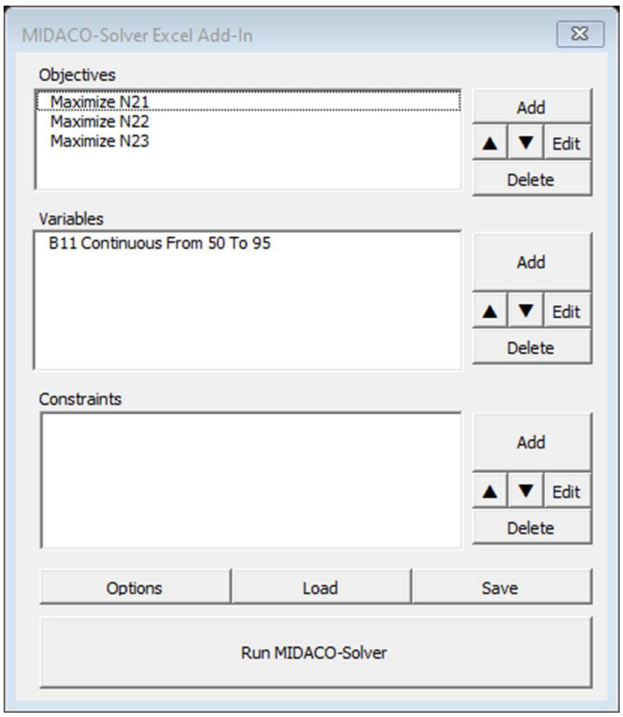

Figure 12.17. MIDACO's set-up for the 3OO analysis of the combined cycle

Figure 12.17 shows that three objective functions are involved in the analysis, which are the power, thermal efficiency, and exergetic efficiency of the combined cycle stored in cells N21, N22, and N23 of the model, respectively. All three objectives require the relevant performance parameter to be maximised by changing a single variable which is the cascade temperature of the fluid used in the TFC circuit stored in cell B10. The lower and upper limits imposed on the changing variable are 50°C and 95°C, respectively. In general, MIDACO allows constraints to be imposed on other cycle variables, such as the maximum allowable fluid pressure or flow rate, but this is not required in the present analysis.

As an MOO solver, MIDACO generates a Pareto front that contains a set of un-dominated solutions from which one solution is selected. Figure 12.18 shows the solution selected by MIDACO with R152a as the single working fluid. As the figure shows, the temperature of the cascade condenser determined by the 3OO solution is 72.74°C. Figures 12.19 and 12.20 compare the four cycle parameters of the 3OO optimised combined cycle with those of the ORC and TFC as shown on Table 12.2. Compared to the simple TFC, the optimised combined cycle reduces the power by 19.66%, but increases both the thermal efficiency and exergetic by 16.2%. and 13.54%, respectively. Compared to the simple ORC, the optimised cycle increases the power, thermal efficiency, and exergetic efficiency by 20.93%, 6.43%, and 70.92% respectively. The combined cycle has the highest thermal efficiency and exergetic efficiency.

Pevap_TFC | =RefPsat_T(Fluid_TFC,Tevap_TFC)

	A	B	C	D	E	F	G	H	I	J	K	L	M	N	O
1	**Working fluids**			**TFC cycle**									**TFC**		
2	Fluid_TFC	R152a		T_hsi	82.83		s6	1.446641		h8	432.53072		Workt_TFC	1071.495	kW
3	Fluid_ORC	R152a					h7	439.22		s8	1.7122446		Workp_TFC	558.5776	kW
4	**Heating source (hot water)**			Pevap_TFC	4243.2		s7	1.7058					Worknet_TFC	512.9178	kW
5	T_hs	120	oC	Pcc_TFC	2008.326								Q_TFC	15774.73	kW
6	mflow	100	kg/s	h5	337.25223		ss8	1.7058					η_TFC	3.252	%
7	ρ	943.10	kg/m3	s5	1.4368662		xss8	0.452576							
8	cp	4.24	kJ/kg.K	mf_TFC	160.18105		hss8	430.301		s_hs	1.5279		**ORC**		
9	**TFC**			v5	0.0013263	m3/kg				s_0	0.3672		Q_sensible	65.98475	kJ/kg
10	Tevap_TFC	110	oC	h6	340.7394					Exerg_hs	4041.24		Q_ORC	4760.691	kW
11	Tcc_TFC	72.830523	oC	T6	74.432907								Workt_ORC	1364.762	kW
12	ΔTcc	3	K	**ORC cycle**									Workp_ORC	95.784	kW
13	ΔT_hs2	10	K	Tcc_ORC	69.830523	oC	s4s	2.035337		h2	272.6776		Worknet_ORC	1268.978	kW
14	**ORC**			Pcc_ORC	1879.4091	kPa	h4s	520.0802		T2	40.702639		η_ORC	6.338	%
15	Tcond_ORC	40	oC	Pcond_ORC	909.27	kPa	h4	523.4184		s2	1.2452456				
16	ΔT_sc	0.00	K				T4	40					**Overall parameters**		
17	ηt_isen	0.85		h3	542.33441		s4	2.045996		h2b	264.81596		Q_total	20535.42	kW
18	ηp_isen	0.85		s3	2.0353373					T2b	36.508379	kJ/kg	T_hsout	71.61	oC
19	ηx_isen	0.75		h2c	330.80071		T1	40	oC	s2b	1.2203994	kg/s	Q_out	18753.52	kW
20	T_0	298.15	K	s2c	1.4185831		h1	271.35	kJ/kg						
21	P_0	101.325	kPa				v1	0.001163	m3/kg	Qevap_ORC	211.5337	kW	W_total	1781.895	kW
22				h4b	531.28		s1	1.2411		mf_ORC	72.15	kW	η_overall	8.677	%
23				s4b	2.0711								ε_overall	44.0928	%
24															

Figure 12.18. Performance of the combined cycle with the tri-objective optimised solution obtained by MIDACO

The 3OO solution for the combined cycle with the R152a/R1234yf pair was obtained following the procedure described above. Table 12.4 compares the performance of the cycle with this optimised solution to those of the 3OO solution with R152a/R152a.

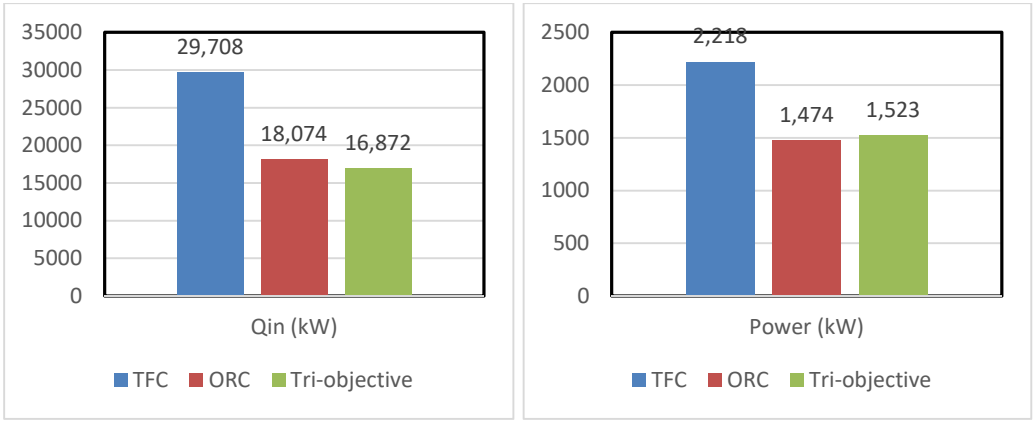

Figure 12.19. Comparison of the recovered heat and produced power by the optimised combined cycle with those of the simple TFC and ORC

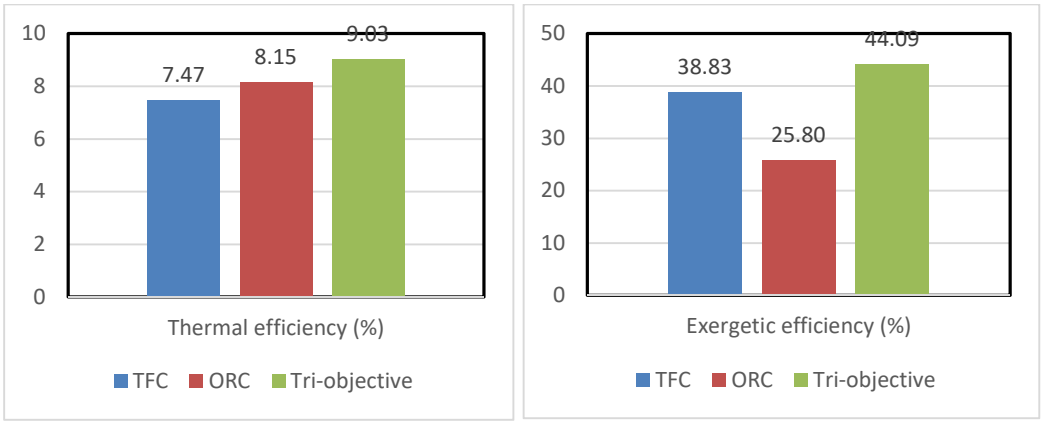

Figure 12.20. Comaprison of the thermal efficiency and exergetic efficiency of the optimised combined cycle with those of the simple TFC and ORC

Table 12.4. Thermodynamic parameters of the combined cycle at the two 3OO solutions using R152a/R152a and R152a/R1234yf

	3OO R152a/ R152a	3OO R152a/R1234yf
Ths,out (°C)	71.61	61.51
Qout (kW)	18753.52	22842.42
Qin (kW)	20535.42	24821.85
Power (kW)	1781.895	1979.427
Thermal efficiency (%)	8.677	7.975
Exergetic efficiency (%)	44.093	42.884

The table figures show that the 3OO solution with R152a/R1234yf lowered the exit temperature of the heat source to 61.51°C. The result is that the combined cycle produced more power, but with less thermal and exergetic efficiencies compared to the cycle with R152a/R15a. Therefore, the decision as to which of the two fluid pairs is favourable

should take into considerations other factors such as the economic, safety, and environmental factors.

12.8. Closure

This chapter presents a combined cycle for power generation from low-grade heat sources that utilises the TFC in the high-temperature circuit and the ORC in the low-temperature circuits. By connecting the two circuits via a casket condenser, the combined cycle allows different fluids to be used in the lower and the higher temperature ranges. The chapter first checks the accuracy of the functions used by the Excel-based model developed for analysing the cycle to determine the thermodynamic properties of the working fluids by comparing the estimations of the models developed of the ORC and TFC with relevant published data for a number of suitable working fluids. The performance of the combined cycle was then compared to those of the simple TFC and ORC by using R152a in both the HTC and LTC circuits. The comparison was made for a heat source available at 120^{o}C and cascade temperatures of 70^{o}C, 80^{o}C, and 90^{o}C. The results show that combined cycle gives more power and yields higher thermal and exergetic efficiencies than the simple ORC for cascade temperatures of 80^{o}C and below. Compared to the simple TFC, the cycle produces less power but achieves a higher thermal efficiency for all three cascade temperatures. The exergetic efficiency of the combined cycle is also higher than that of the simple TFC at a cascade temperature of 80^{o}C.

The performance of the combined cycle was also analysed at various values of the cascade temperature with four fluid pairs of low-GWP fluids that involve R1234yf in the ORC circuit and R152a, R600, R600a, or R717 in the TFC circuit. Comparing the cycle's performance with the R152a/R1234yf pair to its performance with R152a in both circuits shows that the cycle produces more power with the R152a/R1234yf pair over the entire range of cascade temperatures, but the cycle's thermal efficiency is higher when R152a is used in both circuits. The model results with the other three fluid pairs show that all three pairs produce less power than R152a over the range of cascade temperatures below 80^{o}C and only the R600/R1234yf pair manges to produce more power than the R152a/R1234yf pair at cascade temperatures above 80^{o}C. These results show that the most favourable fluids pairs for the combined cycle are those involving R152a, i.e., R152a/R152a and R152a/R1234yf.

Whether the same or different fluids are used in the two circuits of the combined cycle, the various analyses of the cycle show that its thermal efficiency steadily increases by increasing the cascade temperature, but the power decreases while the exergetic efficiency has an optimum cascade temperature. Therefore, selecting the appropriate cascade temperature for the combined cycle requires a trade-off between the power of the cycle on one side and its thermal and exergetic efficiencies on the other side. By using the MIDACO solver, tri-objective optimisation analyses of the cycle were conducted that simultaneously maximise the three performance parameters of the cycle with the two pairs R152a/R152a and R152a/R1234yf. In general, both 3OO solutions show that the cycle keeps its advantages over the simple ORC and TFC. However, it is difficult to

choose between R152a/R1234yf and R152a/R152a based on the thermodynamic performane alone because the first pair produces more power while the second pair gives a higher thermal efficiency. Therefore, determining the most suitable fluid pair among these two pairs for the cycle and the appropriate cascade temperature requires the economic, safety, and environmental factors be taken into consideration. In this respect, the Excel-based modelling platform allows multi-objective optimisation analyses to be conducted by using either the free version of the MIDACO solver or the Solver-TOPSIS technique described in [31].

References

[1] J.J. Fierro, C. Hern´andez-G´omez, C.A. Marenco-Porto, C. Nieto-Londo˜no, A. Escudero-Atehortua, M. Giraldo, H. Jouhara, L.C. Wrobel, Exergo-economic comparison of waste heat recovery cycles for a cement industry case study, Energy Conversion and Management: X 13 (2022) 100180

[2] A.A. Bidgoli and J.I. Yanagihar, Integration of the Compression Units of the Processing Plant with an Organic Rankin Cycle for Power Generation and Cooling Process, Proceedings of ECOS 2023 - the 36th International Conference on Efficiency, Cost, Optimization, Simulation and Environmental Impact of Energy Systems 25-30 June, 2023, Las Palmas De Gran Canaria, Spain

[3] C. Wolf, E. Rothuizen, T. Ommen, Exergoeconomic Analysis of a Solar Powered ORC using Zeotropic Mixtures for Combined Heat & Power Generation, Proceedings of ECOS 2023 - the 36th International Conference on Efficiency, Cost, Optimization, Simulation and Environmental Impact of Energy Systems 25-30 June, 2023, Las Palmas De Gran Canaria, Spain

[4] A. Skiadopoulos, C. Antonopoulou, K. Atsonios, P. Grammelis, A. Gkountas, P. Bakalis, G. Kosmadakis, and D. Manolakos, Trilateral Flash Cycle for efficient low temperature solar heat harvesting- A case study, Proceedings of ECOS 2023 - the 36th International Conference on Efficiency, Cost, Optimization, Simulation and Environmental Impact of Energy Systems 25-30 June, 2023, Las Palmas De Gran Canaria, Spain

[5] M. Yari, A.S. Mehr, V. Zare, S.M.S. Mahmoudi, M.A. Rosen, Exergoeconomic comparison of TLC (trilateral Rankine cycle), ORC (organic Rankine cycle) and Kalina cycle using a low grade heat source, Energy 83 (2015) 712-722

[6] K-Y. Lai, Y-T. Lee, M-R. Chen and Y-H. Liu, Comparison of the Trilateral Flash Cycle and Rankine Cycle with Organic Fluid Using the Pinch Point Temperature, Entropy (2019), 21, 1197

[7] P. Lykas, C. Antonopoulou, A. Gkountas, K. Atsonios, G. Itskos, N. Nikolopoulos, P. Grammelis, D. Manolakos and P. Bakalis, Thermodynamic and economic performance of novel organic cycle designs powered by low temperature waste heat, Proceedings of ECOS 2023 - the 36th International Conference on Efficiency, Cost, Optimization, Simulation and Environmental Impact of Energy Systems 25-30 June, 2023, Las Palmas De Gran Canaria, Spain

[8] Aspen HYSYS 2017, Aspen Technology Inc, https://www.aspentech.com/en/products/engineering/aspen-plus

[9] S.A. Klein, and F.L. Alvarado, EES: Engineering equation solver for the Microsoft Windows operating system. F-Chart software, 1992.
[10] E. Lemmon, M. McLinden, M. Huber, 2004, NIST Fluid Thermodynamic and Transport Properties-REFPROP, Version 7.0 User's Guide.
[11] CoolProp library wrapper, http://www.coolprop.org/coolprop/wrappers/MATLAB/index.html
[12] MATLAB R2012a. Available: www.mathworks.com/patents
[13] Aspen Plus, Aspen Technology Inc
[14] W. Sun, X. Yue, and Y. Wang. Exergy Efficiency Analysis of ORC (Organic Rankine Cycle) and ORC-Based Combined Cycles Driven by Low-Temperature Waste Heat. Energy Conversion and Management, 135, (2017), 63-73. https://doi.org/10.1016/j.enconman.2016.12.042
[15] N. Toujani, N. Bouaziz, M. Chrigui, L. Kairouani, Performance analysis of a new combined organic Rankine cycle and vapor compression cycle for power and refrigeration cogeneration, Transactions of the Institute of Fluid-flow Machinery, No. 140, 2018, 39–81
[16] C.O.C. Oko, M.M. Deebom, and, E.O. Diemuodeke, Exergoeconomic analysis of cascaded organic power plant for the Port Harcourt climatic zone, Nigeria, Cogent Engineering (2016), 3: 1227127, http://dx.doi.org/10.1080/23311916.2016.1227127
[17] Y.S.H. Najjar, A.E. Qatramez. Energy utilisation in a combined geothermal and organic Rankine power cycles. Int. J. Sustain. Energy 2019, 38, 831–848.
[18] N. Hassani Mokarram, A.H. Mosaffa. Investigation of the thermoeconomic improvement of integrating enhanced geothermal single flash with transcritical organic Rankine cycle. Energy Convers. Manag. 2020, 213, 112831.
[19] G. Liu, Q. Wang, J. Xu, Z. Miao. Exergy Analysis of Two-Stage Organic Rankine Cycle Power Generation System. Entropy 2021, 23, 43. https://doi.org/ 10.3390/e23010043
[20] J.C. Jiménez-García, A. Ruiz, A. Pacheco-Reyes, W.A. Rivera, Comprehensive Review of Organic Rankine Cycles. Processes 2023, 11, 1982. https://doi.org/10.3390/pr11071982
[21] S. Trædal, Analysis of the Trilateral Flash Cycle for Power Production from Low Temperature Heat Sources. Master's Thesis, Institutt for Energi-og Prosessteknikk, Kolbjørn Hejes v 1B, Trondheim, 2014.
[22] C.O.C. Oko and, E.O. Diemuodeke, MS Excel spreadsheet add-in for thermodynamic properties and process simulation of R152a, Energy Science and Technology, Vol. 5, No. 2, 2013, pp. 63-69.
[23] M. Schlueter, J. Rueckmann, M. Gerdts. A Numerical Study of MIDACO on 100 MINLP Benchmarks, Optimization: A Journal of Mathematical Programming and Operations Research, 61,2012,7, 873-900.
[24] M.M. El-Awad, A Solver-TOPSIS technique for multi-objective optimisation of innovative multi-stage VCR systems by using Microsoft Excel, Journal of Engineering Research. Faculty of Engineering-University of Tripoli, Issue (38), November 2024, 25-42, https://www.jer.ly/search_articles.php?f=38

[25] M.J, Moran and H.N. Shapiro, Fundamentals of Engineering Thermodynamics, 5th edition, John Wiley, & Sons. Inc. 2006

[26] M.M. El-Awad, A Multi-Subject Excel Add-In for Fluid Properties and its Use for analysing Cascade and Multi-Stage Compression Refrigeration Cycles, The Electronic Journal of Spreadsheets in Education (eJSiE) Vol. 12, Issue 1, April 18, 2019

[27] ASHRAE Handbook–Refrigeration, 2017, American Society of Heating, Refrigerating and Air-Conditioning Engineers, Inc., (SI Edition).

[28] M.M. El-Awad, M.S. Al Nabhani, K.S. Al Hinai, A. Younis. 2019. Development and Validation of an Excel Add-In for Determining the Properties of Various Refrigerants, Proceedings of First National Conference on Recent Trends in Applied Science, Engineering and Technology (CASET 2K19), Ipri College of Technology, June 11, 2019.

[29] H. Atalay, M.T. Coban, Modeling of Thermodynamic Properties for Pure Refrigerants and Refrigerant Mixtures by Using the Helmholtz Equation of State and Cubic Spline Curve Fitting Method , Universal Journal of Mechanical Engineering 3(6), 2015: 229-251, http://www.hrpub.org

[30] A. D. Parekh and P. R. Tailor, Thermodynamic Analysis of R507A-R23 Cascade Refrigeration System, World Academy of Science, Engineering and Technology International Journal of Mechanical and Mechatronics Engineering Vol:5, No:9, 2011